Data Assimilation Schemes in Colombian Geodynamics - Cooperative Research Plan for 2017 - 2020 Between Universidad EAFIT and TUDelft, With the Help of Universidad de Antioquia and universidad Nacional de Colombia Sede Medellin

Inicio: 1 de Enero de 2017
Final: 30 de Diciembre de 2020

Reporte de Procedimiento Análisis de Datos Satelitales 3D de Proyecto Copernicus

Medellin Air qUality Initiative MAUI

MAUI-RP-01

Entidad Ejecutora	Universidad EAFIT Cra 49 No 7sur - 50 Medellín, Colombia
	Grupo de investigación en modelado matemático – GRIMMAT Grupo reconocido por COLCIENCIAS Categoría A
Responsables	Prof. Olga Lucia Quintero Montoya Prof. Nicolás Pinel Peláez. Investigadores
Entidades Cooperadoras	Department of Applied Mathematics - Tu Delft, Delft The Netherlands TNO
Responsables	Arnold Heemink Arjo Segers

CONTROL DE EDICIÓN Y DISTRIBUCIÓN

Edición	Control*	Nombre y Cargo	Firma	Entidad	Fecha (Día/Mes/Año)
	Creación	O. Lucia Quintero		Universidad EAFIT	

* Especificar tipo de control: Creación - Revisión - Modificación - Distribución.

CONTENTS

LIST OF FIGURES

page

ABSTRACT

Four different analyses were carried out on twelve atmospheric composition variables, in order to provide a characterization of the main patterns, cycles and dependences of the substances of interest. The analyses were comprised of time and frequency plots, scatter plots for month of year and hour of day, and moving-time distribution plots.

INTRODUCTION

This report presents the characterization of the results provided by the MACC project, which is part of the Copernicus Atmosphere Monitoring Service initiative. The used model calculates atmospheric composition over 3D space and time. We are currently analyzing data spanning from March 2015 to April 2016 in the temporal dimension. The variables under consideration are:

1. GEMS Ozone
2. Nitrogen dioxide
3. Sulphur dioxide
4. Carbon monoxide
5. Formaldehyde
6. Sea Salt Aerosol (0.03 - 0.5 um) Mixing Ratio
7. Sea Salt Aerosol (0.5 - 5 um) Mixing Ratio
8. Sea Salt Aerosol (5 - 20 um) Mixing Ratio
9. Dust Aerosol (0.03 - 0.55 um) Mixing Ratio
10. Dust Aerosol (0.55 - 0.9 um) Mixing Ratio
11. Dust Aerosol (0.9 - 20 um) Mixing Ratio
12. Hydrophobic Organic Matter Aerosol Mixing Ratio
13. Hydrophilic Organic Matter Aerosol Mixing Ratio
14. Hydrophobic Black Carbon Aerosol Mixing Ratio
15. Hydrophilic Black Carbon Aerosol Mixing Ratio
16. Sulphate Aerosol Mixing Ratio

A detailed description of the database and model is presented in the technical report MAUI RT01. For each of these substances, it is desired to characterize the principal characteristics and trends in both time and vertical dimensions. For this purpose, four different analyses are used:

- **Time-height plot:** this analysis presents a two-dimensional plot, where the concentration of a given substance is presented for each time and altitude. This allows to identify regions of both time and space where higher values of the chemical are found.

- **Frequency plot:** the concatenated spectrum for each of the altitude layers are presented here. This allows to identify the principal cycles the describes the variable under analysis. These periodicities are important for the characterization of the variables as they can be related to the different production mechanisms.

- **Day cycle scatter plot**: the day cycle scatter plot shows the data dispersion of the substance concentration according to the specific time of day and month of emission. This analysis is performed over four different altitude layers.

- **Moving histogram plot:** for four different altitude layers, a moving window of approximately one month worth of data is taken, with an overlap of one data point. The histogram is taken for each window to estimate the probability density function of the concentration dispersion as a function of time. This process is repeated for each hour of day to evidence possible day-night dependences.

The presented analyses are described thoroughly in the technical report MAUI RT001.

The spatial resolution of the data is presented in Figure 1. The characterization of the atmospheric over the Aburra valley is of special interest, which is represented by four data points as showing in the right part of the figure. The presented results correspond to the characterization of the longitude-latitude of point 1 in the figure.

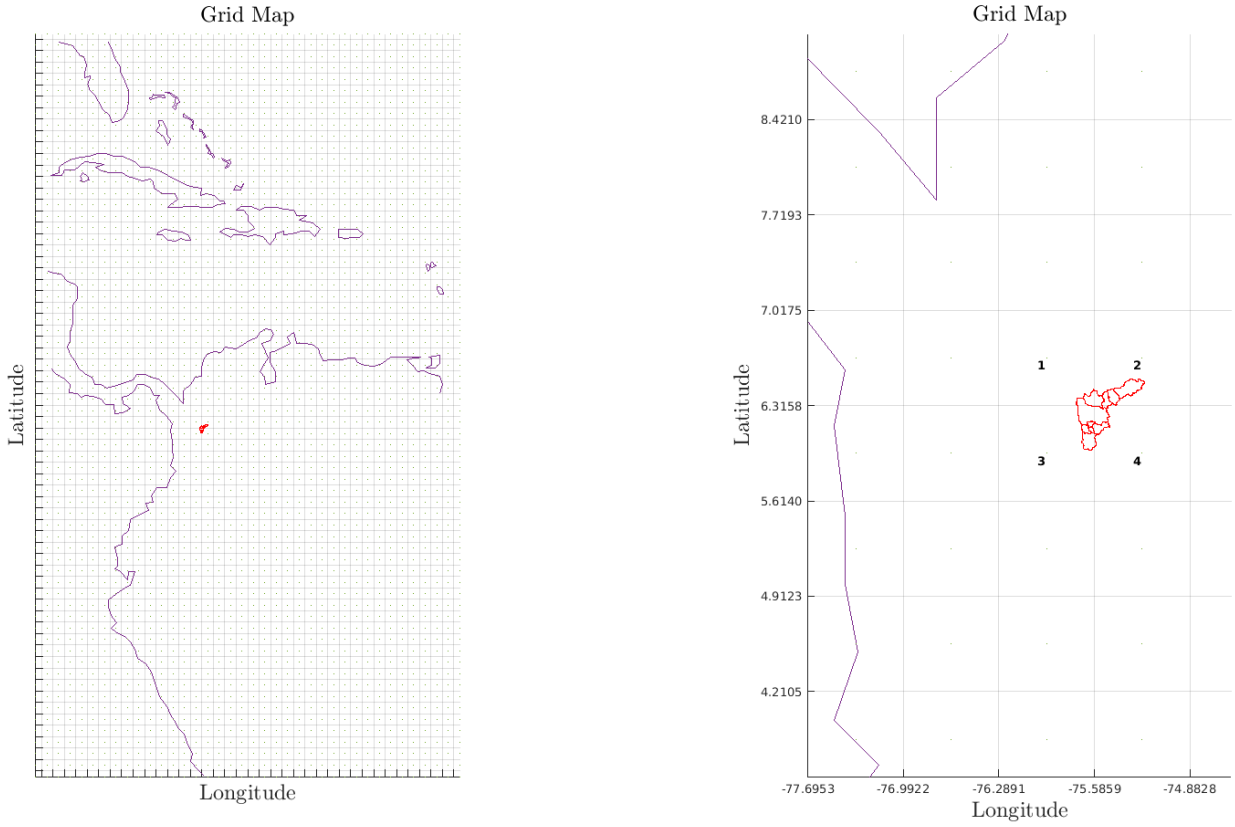

Figure 1: Spatial resolution of the current data

1. GEMS OZONE

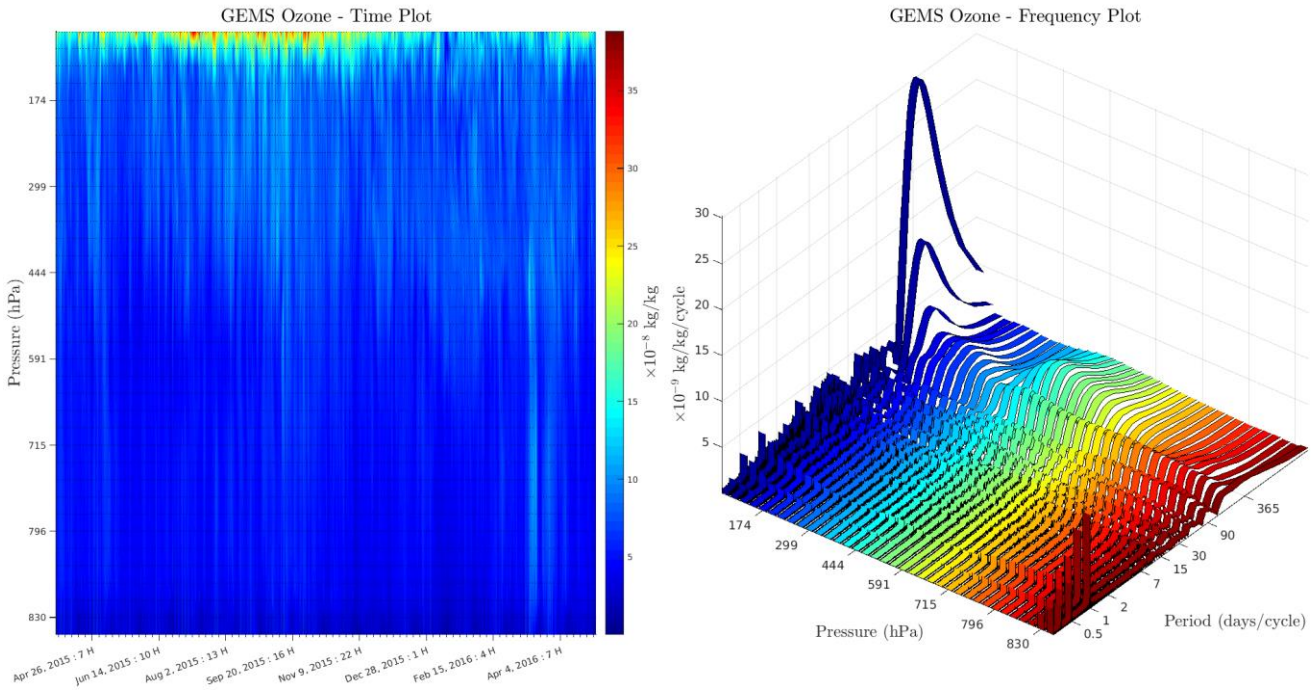

Figure 2: Time and frequency plot for ozone.

Figure 2 shows the time and frequency plots for ozone. It can be seen that this substance presents the highest concentrations at high altitudes (low pressures). The time plot shows that there is an important period of high concentrations from July 2015 to December 2015 for pressure values lower than 174 hPa.

The frequency plot shows relevant information about the behavior of ozone. At high altitudes, the predominant frequency of concentration values is the yearly cycle. However, at surface level the predominant cycles correspond to the day cycle. This could suggest that at surface level, ozone chemical reactions to other substances are influenced by the presence of sun radiation.

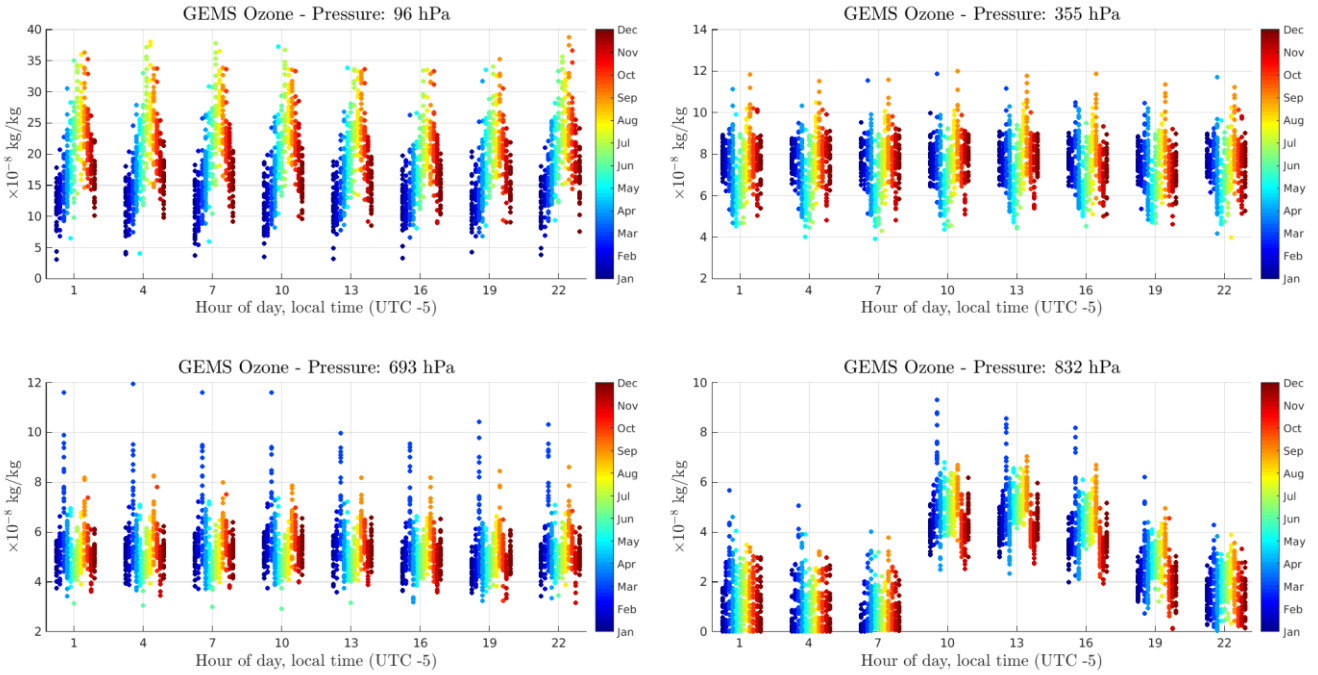

Figure 3: Day cycle plot - Ozone.

Figure 3 shows how the behavior of ozone's day cycle depends on the pressure (layer height). At pressures close to 100 hPa, the concentration of ozone does not depends on the hour of day, but depends heavily on the month of year, having maximum values between June and August. At mid pressure levels (300 hPa,700 hPa), it can be seen that the behavior is still independent on the hour of day. However, the monthly cycle is different, as the period of June-August now presents the minimum values. Finally, the surface layers show a clear cycle day, with maximum values during periods of sunlight (10 am to 4 pm). The monthly cycles are similar to those of medium pressure levels.

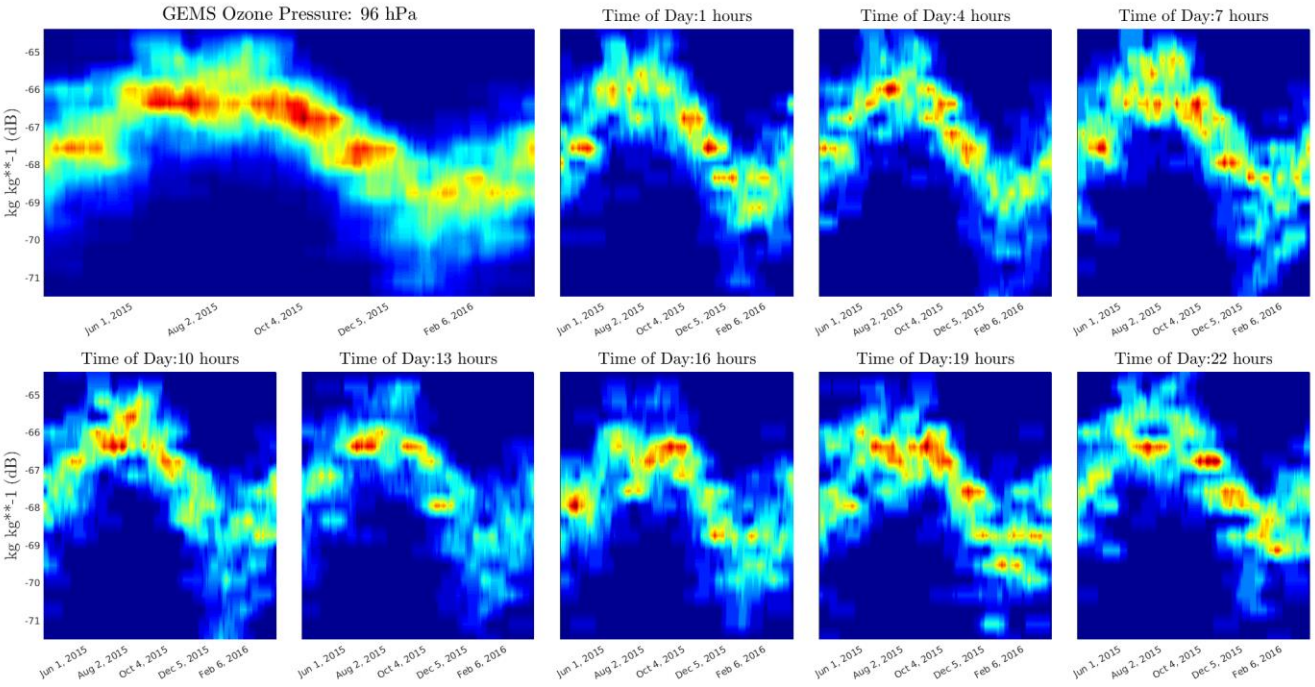

Figure 4: Moving distribution, high layers – Ozone

The moving distribution for ozone is shown in Figure 4 for high altitudes. It can be seen that the yearly distribution resembles a sine wave and is independent of the hour of day. This is in congruence with the results shown in the frequency and day cycle plots.

Figure 5 shows the moving distribution for the mid-high and mid-ow layers. It is seen that the distribution of the data does not depend on the hour of day. A yearly cycle can be seen; however, the maximum values are shifted with respect to the peaks of Figure 4.

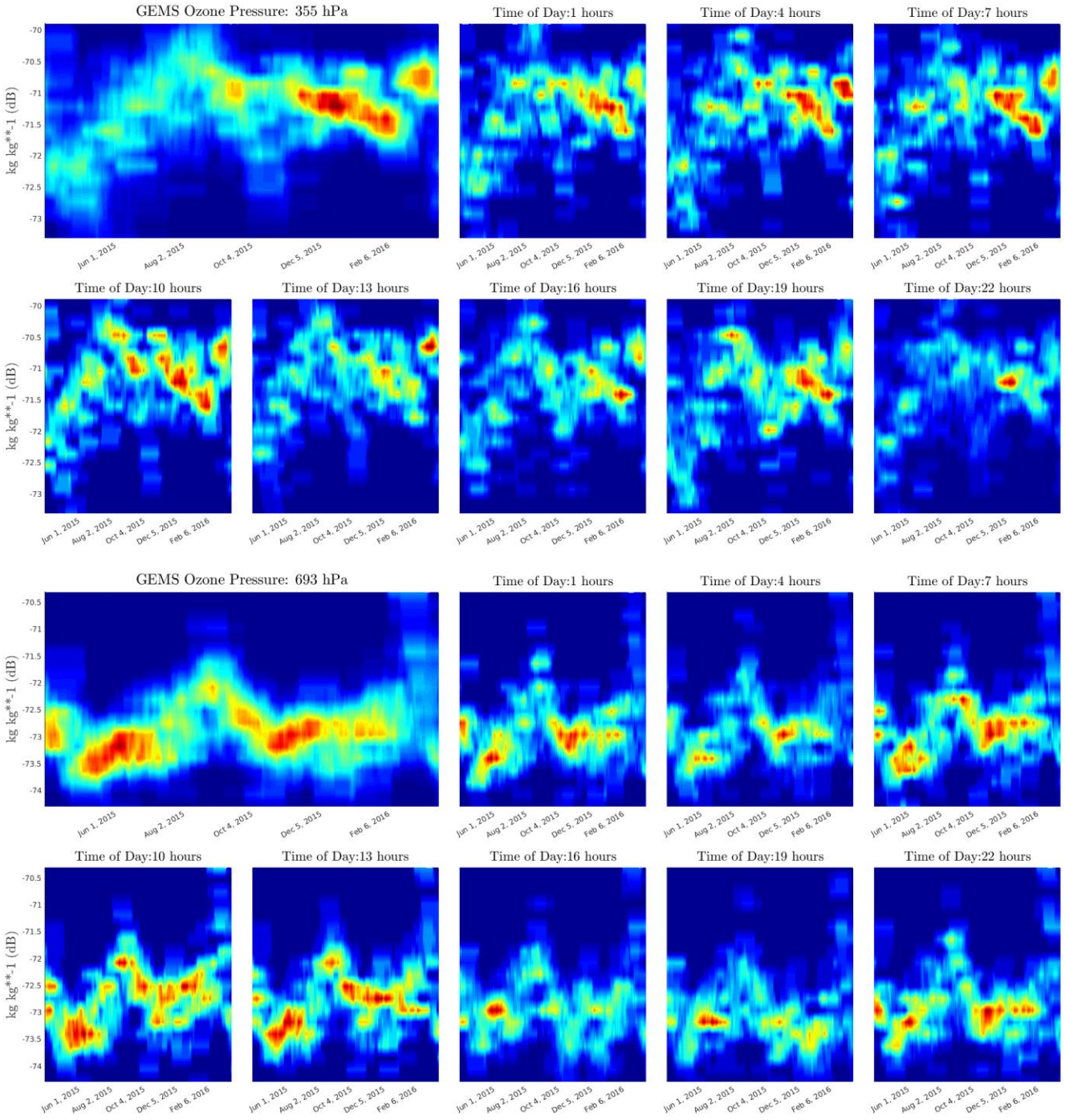

Figure 5: Moving distribution, mid-high and mid-low layers - Ozone

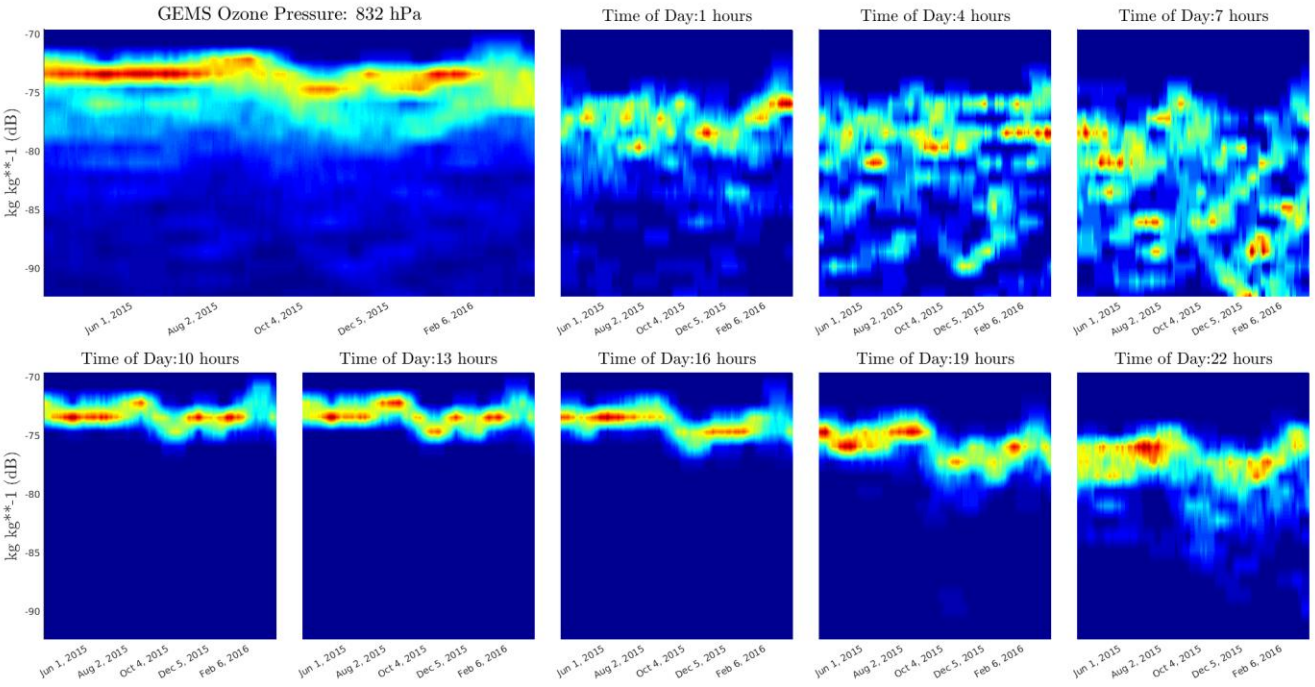

Figure 6: Moving distribution, low layers - Ozone

Figure 6 shows that for surface levels, the ozone moving distribution depends greatly on the hour of day: between 10 am and 4 pm, the concentration values are almost constant throughout the year. Between 7 pm and 10 pm, the mean values are considerable smaller, and the data are dispersed, as evidenced by a widening of the distribution lines. Between 1 am and 7 am the distribution of the data is dispersed in a range up to 20 dB lower than the values obtained during sunlight.

2. NITROGEN DIOXIDE

Figure 7 shows the time and frequency plots for nitrogen dioxide concentration at different height levels. It is clear that most of the data is contained at surface level. Also, the principal frequency component of the signal is the daily cycle, and there is little dependence on lower frequency values.

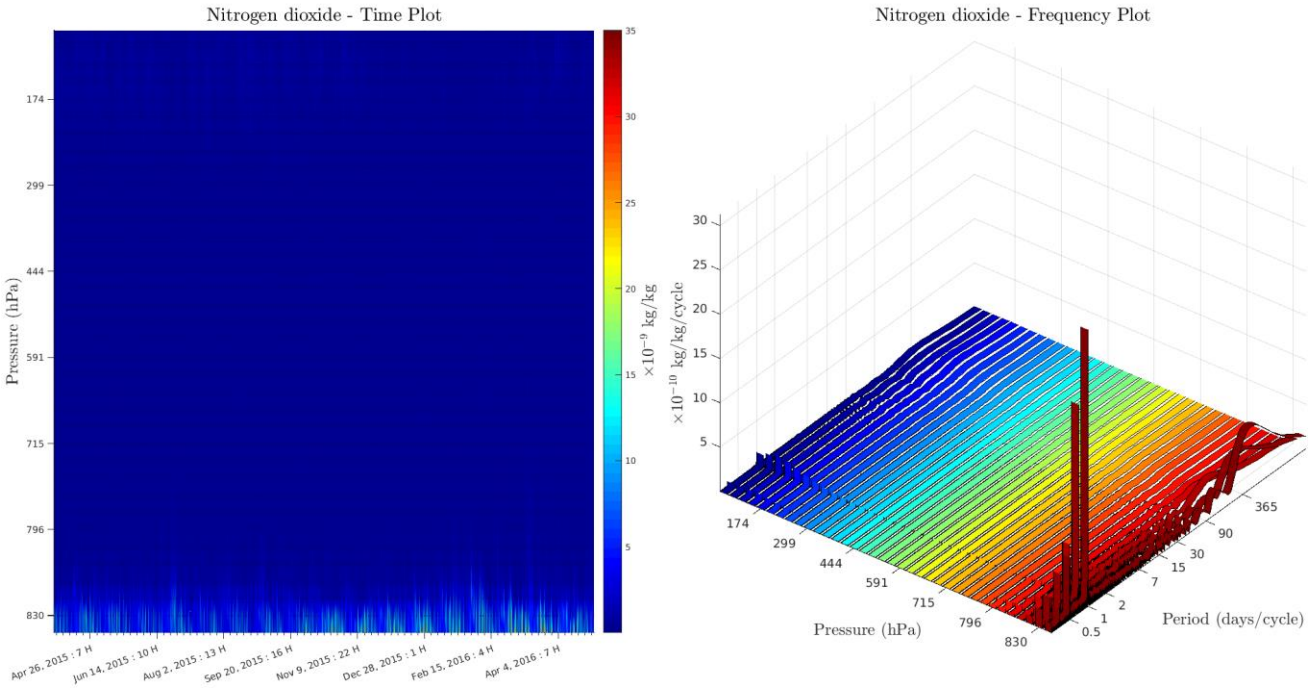

Figure 7: Time and frequency plot for nitrogen dioxide

The day cycle plot shown in Figure 8 shows that for every altitude layer, the concentration values are very influenced by the time of day. However, the monthly behavior changes depending on pressure: at high and mid-high layers, peak values are evidenced from May to September; whilst at low and mid-low layers, the highest values are found between October and April. The difference between the high values of October-April and the low values of May-September is clearer at surface level. For all cases, the concentration values are higher during night time.

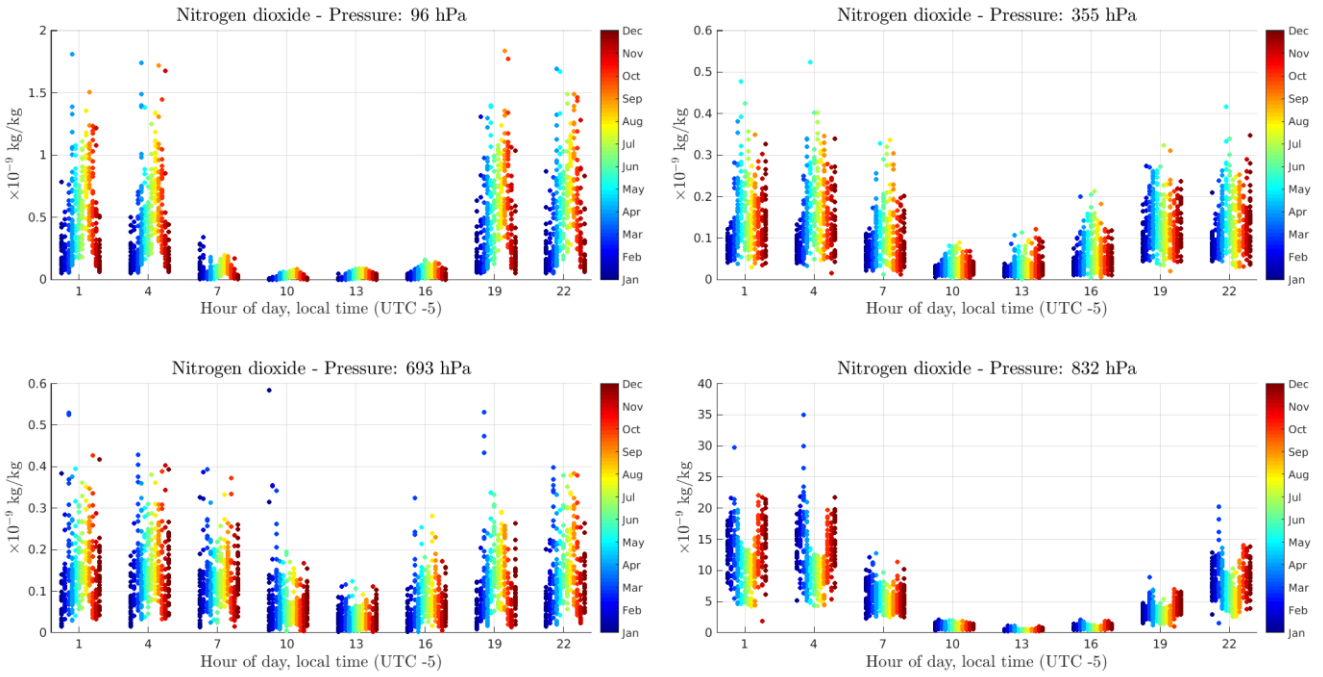

Figure 8: Day cycle plot - nitrogen dioxide

The moving distribution plots for high and low altitude layers show a clear time of day dependence of the concentration values. For each hour, data is contained in clear strips that barely overlap with the rest of the frames. At low pressures (around 100 hPa), there are high fluctuations during time, with a maximum found at August, and a minimum found at December. In contrast, at surface levels, the data are distributed almost uniformly during the year in clear strips, with some peak values during November/December.

For mid pressure levels, the mean values of the data distributions are seen to depend heavily on the time of day. Nevertheless, the data are highly dispersed over a wide range of values. Also, there is not a clear monthly dependence on the month of the year.

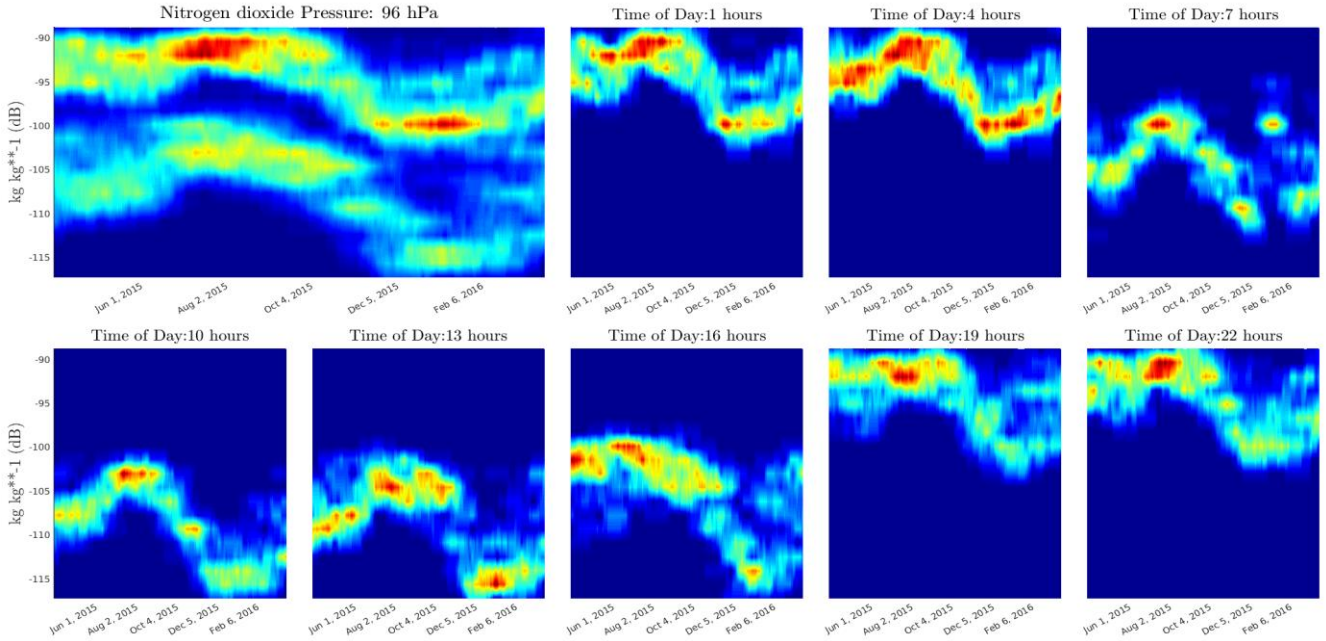

Figure 9: Moving distribution, high layers - Nitrogen Dioxide

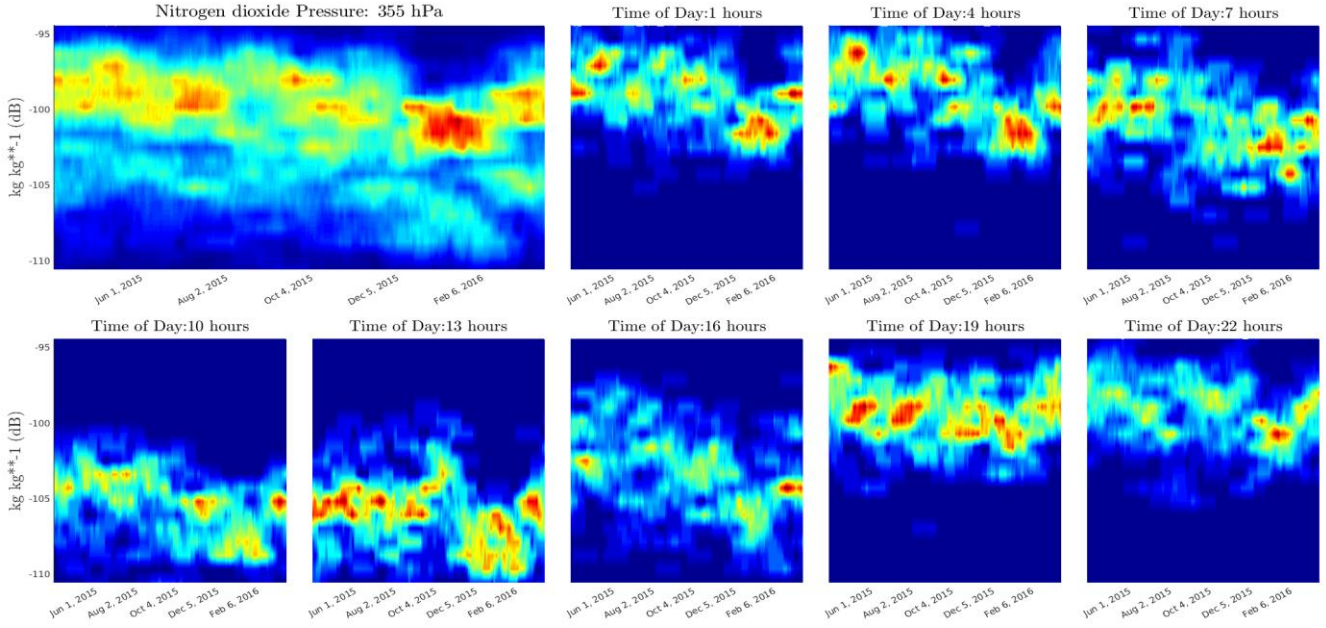

Figure 10: Moving distribution, mid-high layers - Nitrogen dioxide

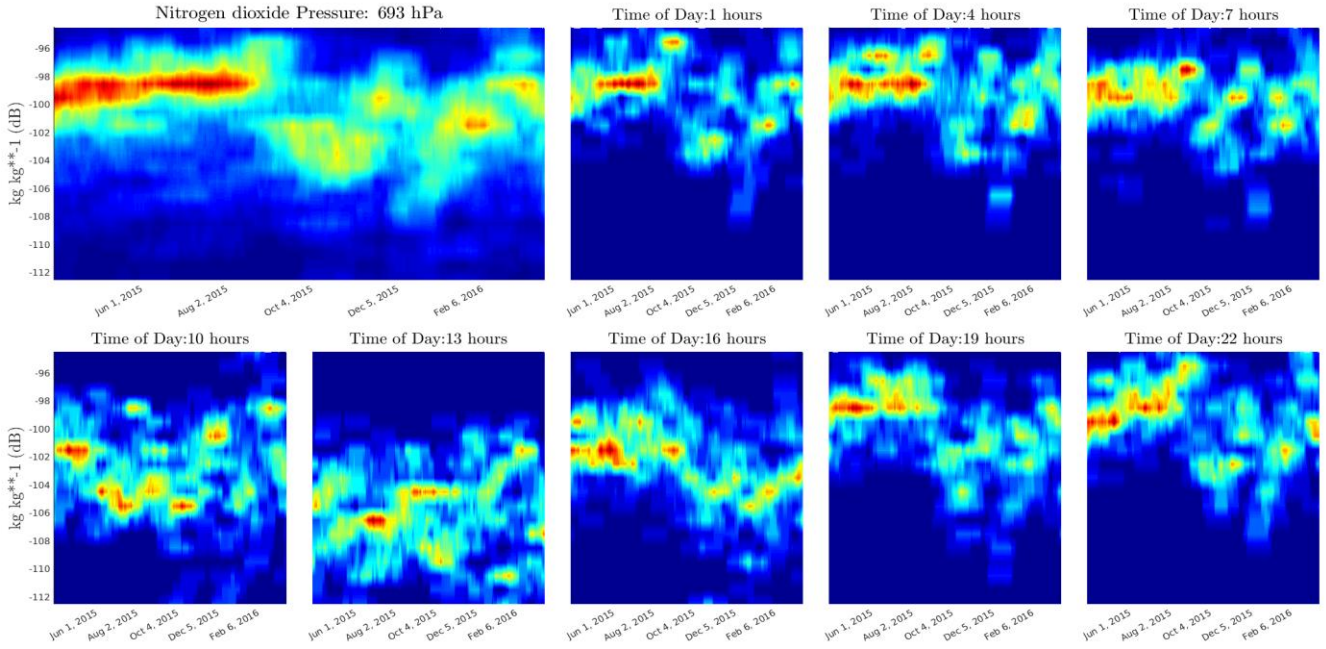

Figure 11: Moving distribution, mid-low layers - Nitrogen dioxide

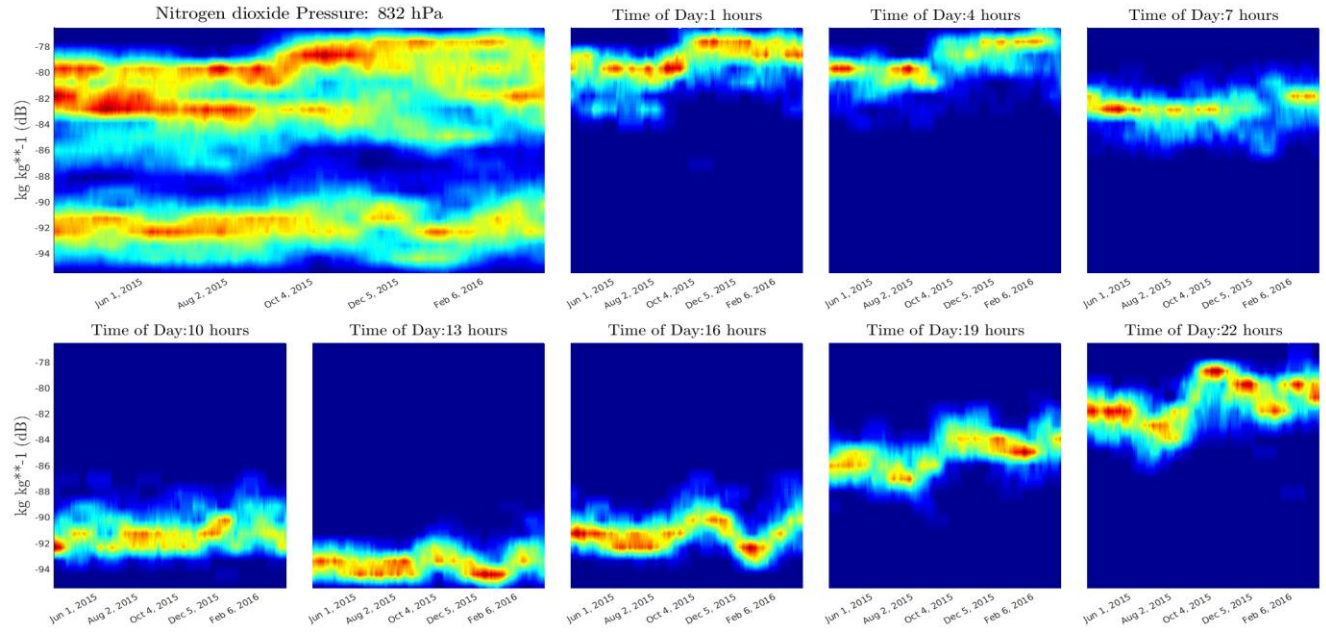

Figure 12: Moving distribution, low layers - Nitrogen dioxide

3. SULPHUR DIOXIDE

As seen in Figure 13, sulphur dioxide concentration shows a rich frequency representation: there is considerable information in many layers that go from 400 hPa to 850 hPa. Surface layers are represented mainly by daily frequencies, whilst mid-low layers present lower frequency values, with a high peak at the yearly period, and minor peaks at bi-annual, quarterly and monthly frequencies. Mid pressure levels present a lower dependence on the yearly cycle, and instead contain frequencies related to a weekly basis. High and mid-high layers contain little information in comparison with the rest of the vertical dimension.

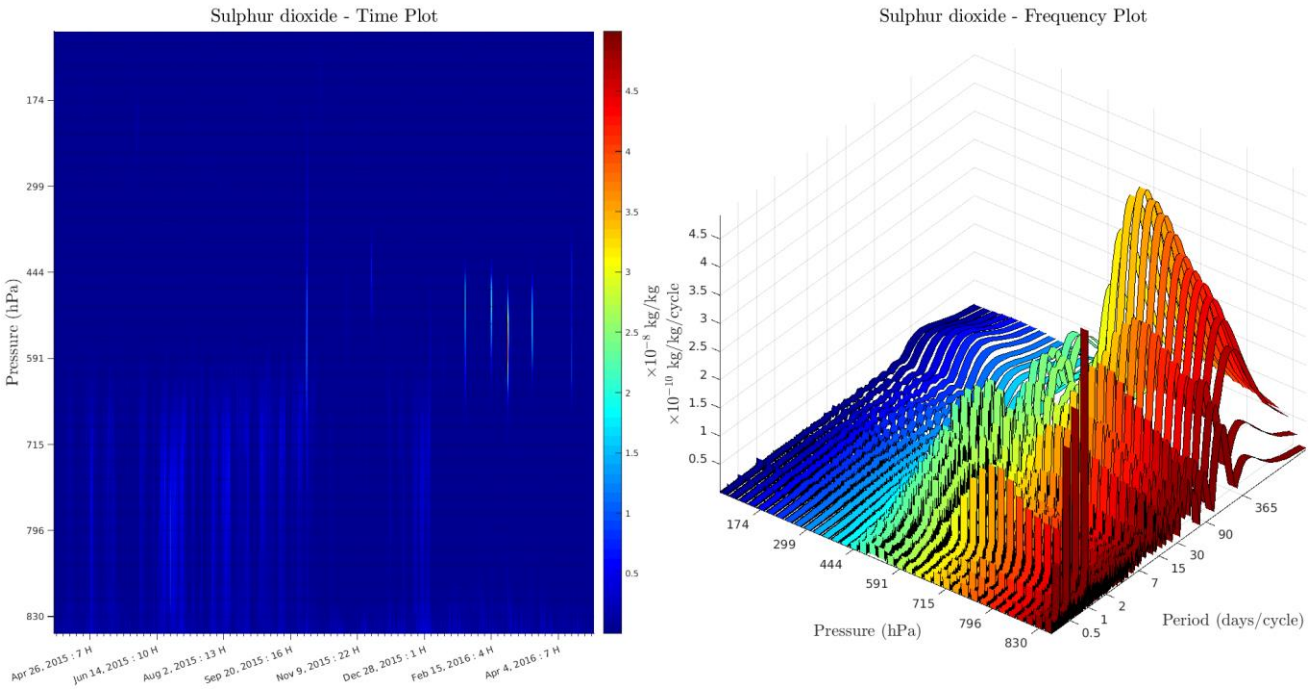

Figure 13: Time and frequency plot for sulphur dioxide

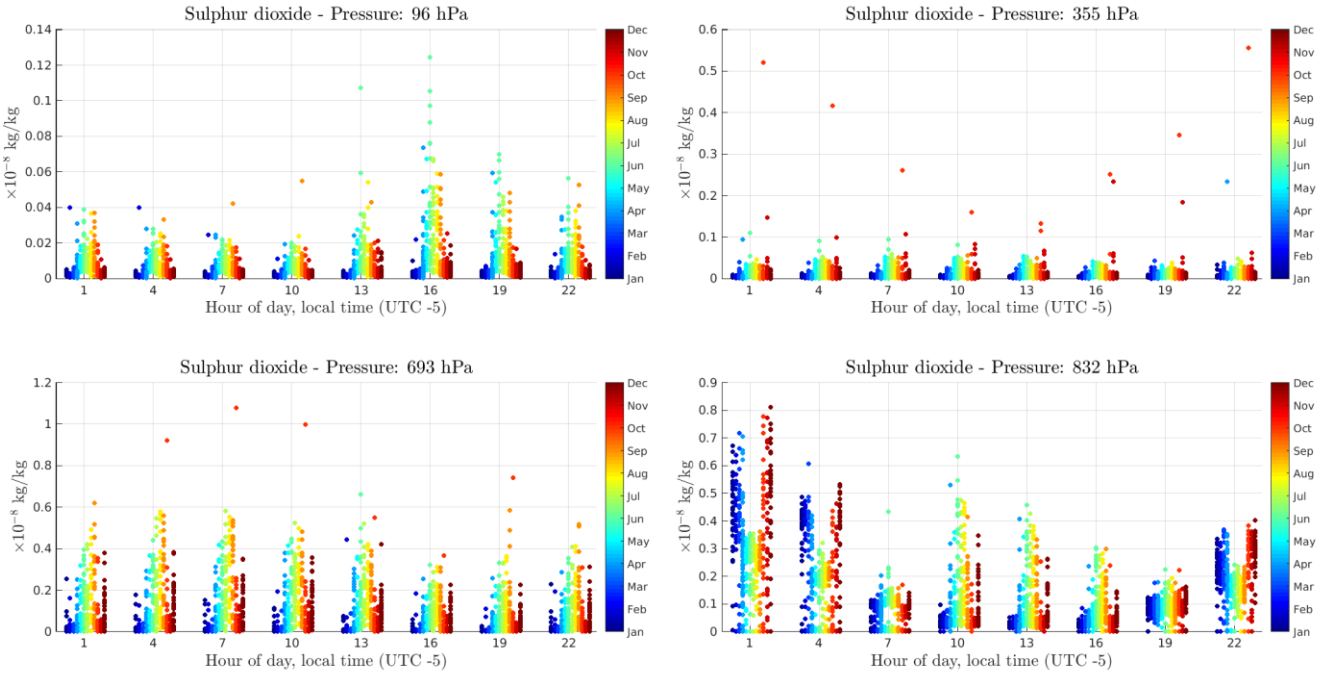

Figure 14: Day cycle plot - sulphur dioxide.

The cycle day scatter plot for sulphur dioxide is presented in Figure 14. For pressure levels between 100 and 700 hPa, it can be seen that there is little dependence on the hour of the day, and that the three cases present a similar yearly structure: the higher peak is found between June and August, and minimum values are found at the beginning of the year. In contrast, the surface layer has both dependence on the hour of day and month of the year: during night time (10 pm to 4 am), higher concentration values are found between October and April, whereas between 7 am and 4 pm, the higher values are found between May and September.

The moving histogram plots in Figures 15 and 16 for high and mid-high altitudes present a similar structure: the mean distribution value increases from April 2015 until it reaches an absolute maximum at June/July 2015. From there on wards, the concentration values decrease monotonically until April 2016.

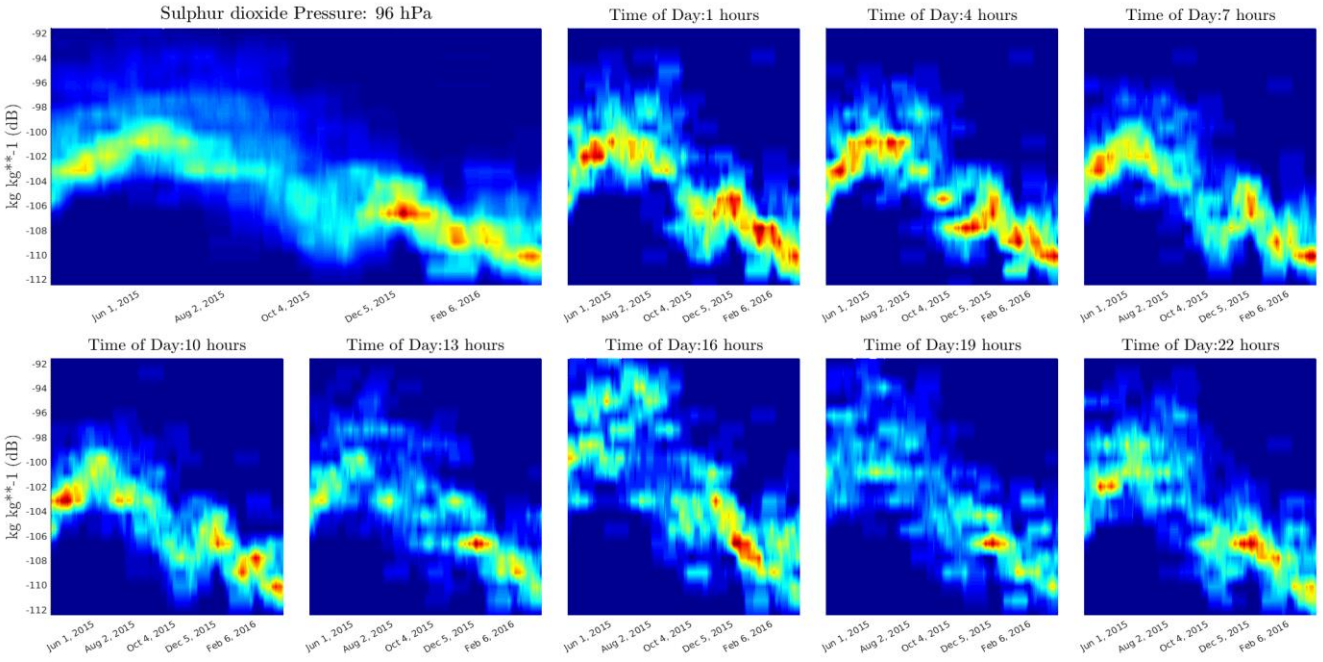

Figure 15: Moving distribution, high layers - Sulphur dioxide

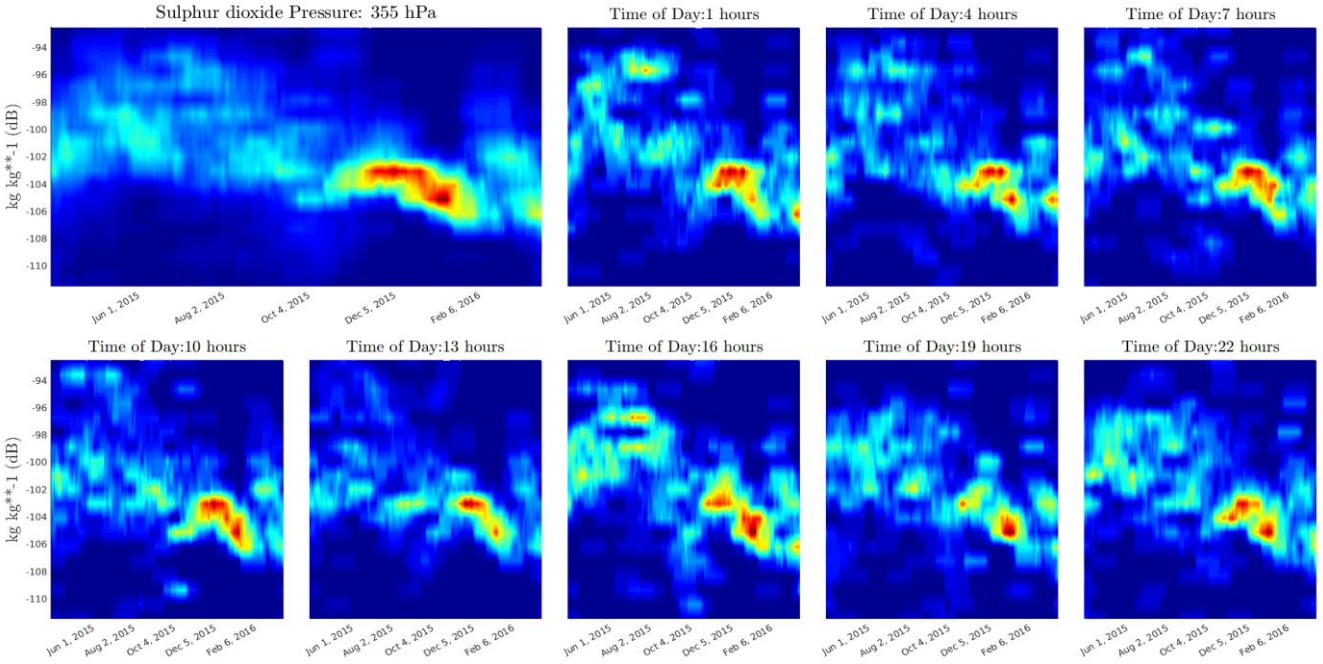

Figure 16: Moving distribution, mid-high layers - Sulphur dioxide

The distribution behavior for mid-low altitudes is shown in Figure 17. From April 2015 until December 2015, there is an almost stationary distribution of high values, with the exception of a sudden drop during November. From January 2016, the distribution takes significant lower values, which are maintained until April 2016.

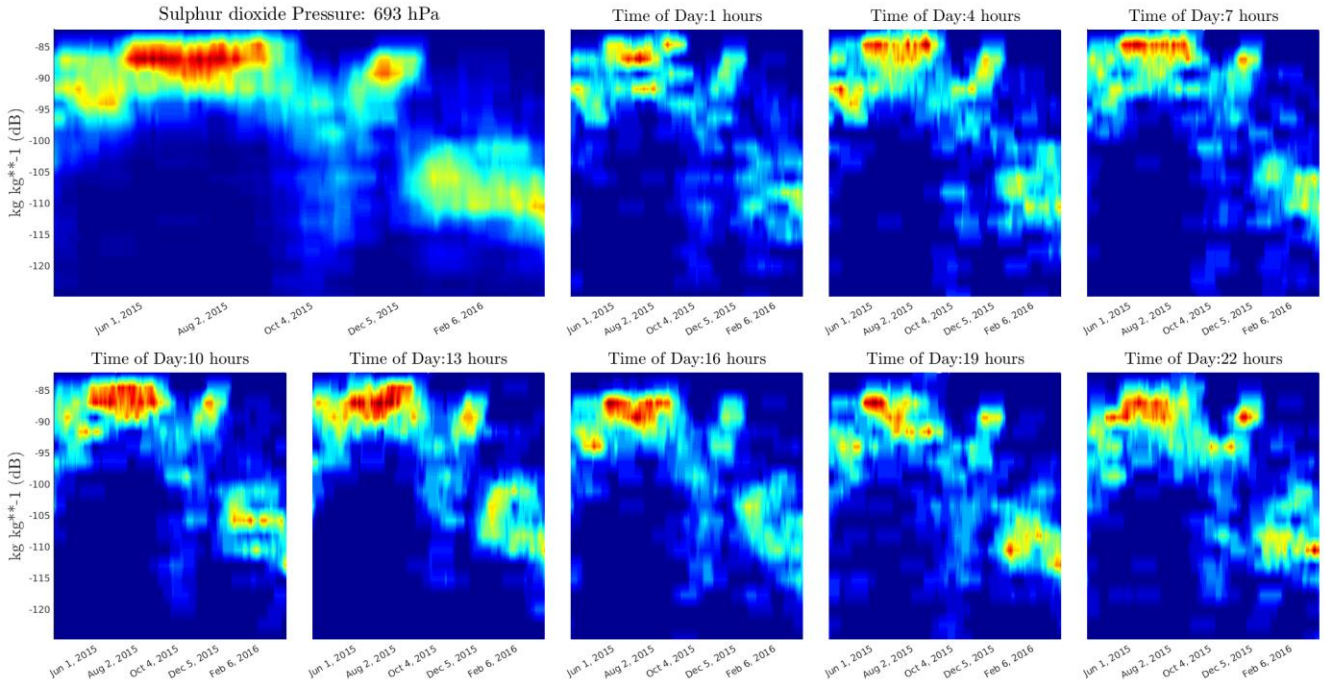

Figure 17: Moving distribution, mid-low layers - Sulphur dioxide

For surface levels, concentration values moving distribution is shown in Figure 18. This case clearly presents an hour of day dependence. Night time data (10 pm to 4 am) have a similar structure, presenting higher values in the period between October 2015 and April 2016. Transition hours (7 am and 7 pm) have an almost stationary distribution throughout the year. Day time data (10 am to 4 pm) present the same behavior: from April 2015 to September 2015, high concentration are registered with high dispersion; whereas from October 2015 to April 2016 the distribution is characterized by low concentrations with little dispersion.

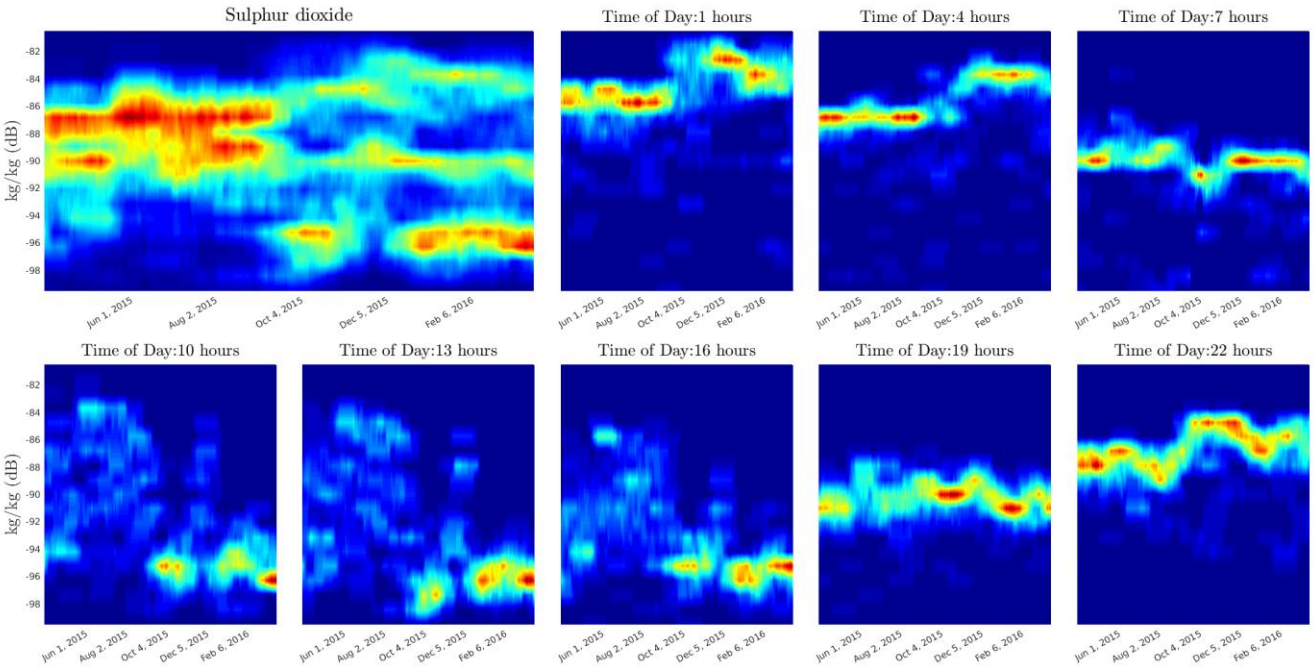

Figure 18: Moving distribution, low layers - Sulphur dioxide

4. CARBON MONOXIDE

Figure 19 shows the time and frequency plot for the different height layers for carbon monoxide. It can be seen that the annual cycle is present throughout all the pressure levels. Additionally, the surface level presents an equally important daily cycle which decreases as pressure is reduced. Note that the time plot shows a singular concentration event during March 2016.

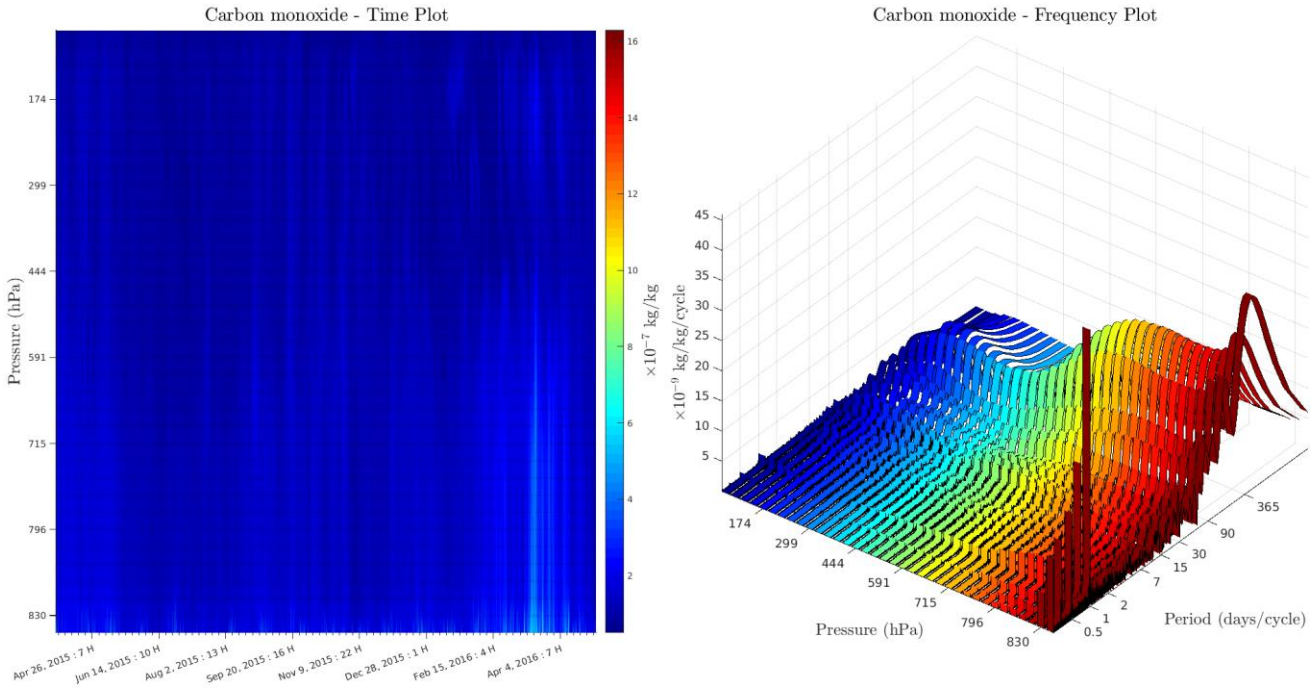

Figure 19: Time and frequency plot for carbon monoxide.

The day cycle plot in Figure 20 shows that for all pressure levels, there is a maximum peak between April and May, and a minimum between June and July. However, the higher altitude layers also present a secondary peak between September and November, which is absent at low and mid-low layers. Only the surface level presents the daily cycle behavior, showing higher concentrations during night time.

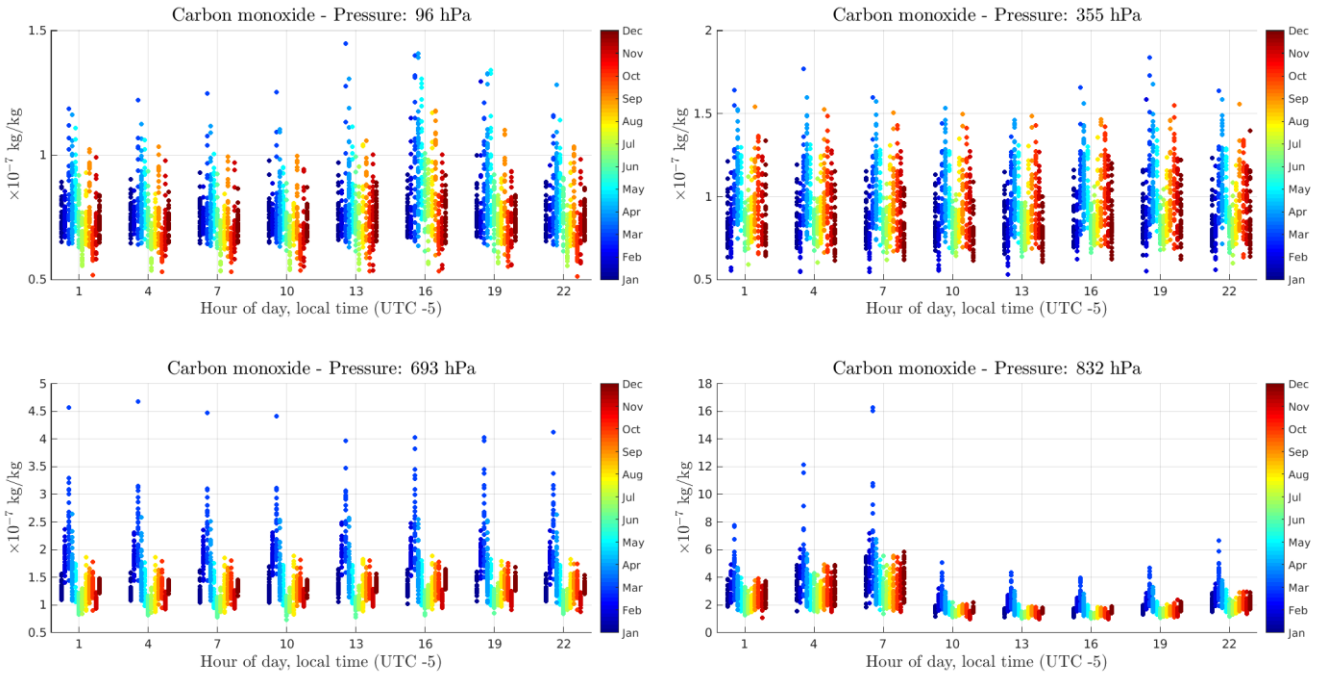

Figure 20: Day cycle plot - carbon monoxide

The results shown in Figures 21-24 agree with the analysis extracted from the day cycle plot. Initially, Figures 21-23 show that the data is independent on the time of day, which is not the case of Figure 24. Figures 22 and 23 (mid pressure layers) show the clear yearly variation of the concentration values, with a series of local minimums (present during at and December) and local maximums (present at October and March).

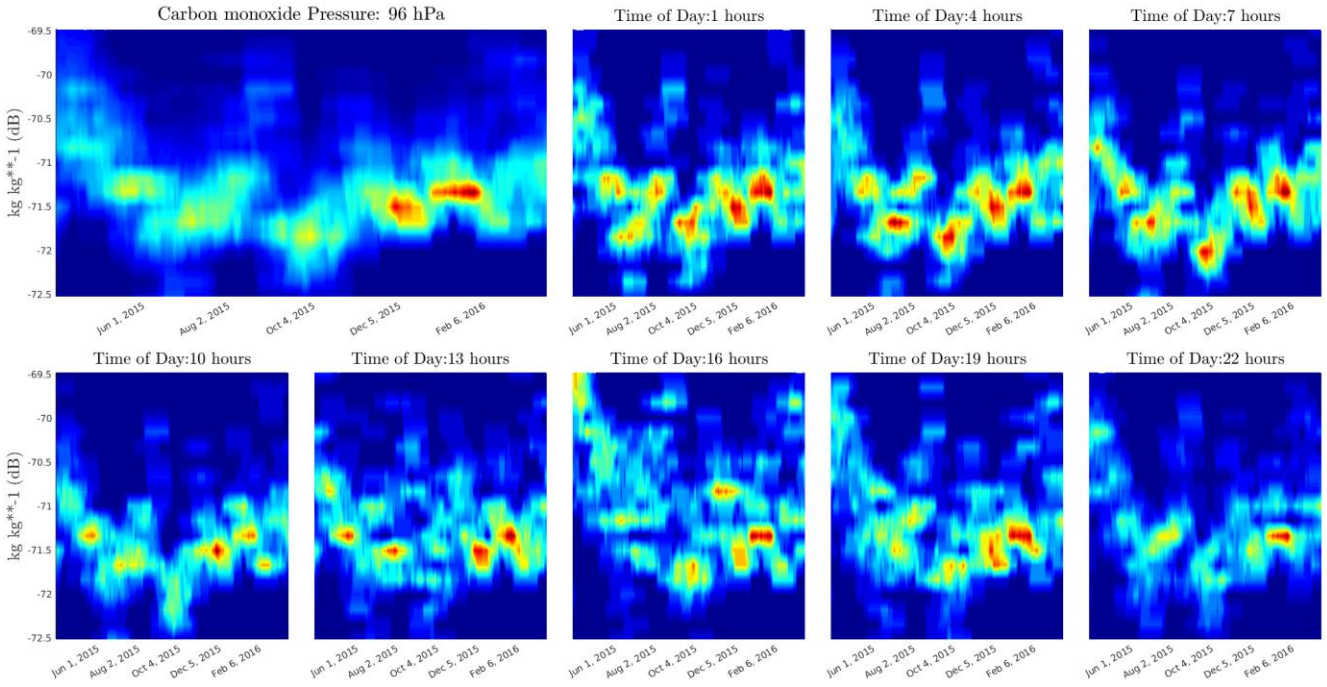

Figure 21: Moving distribution, high layers - Carbon monoxide

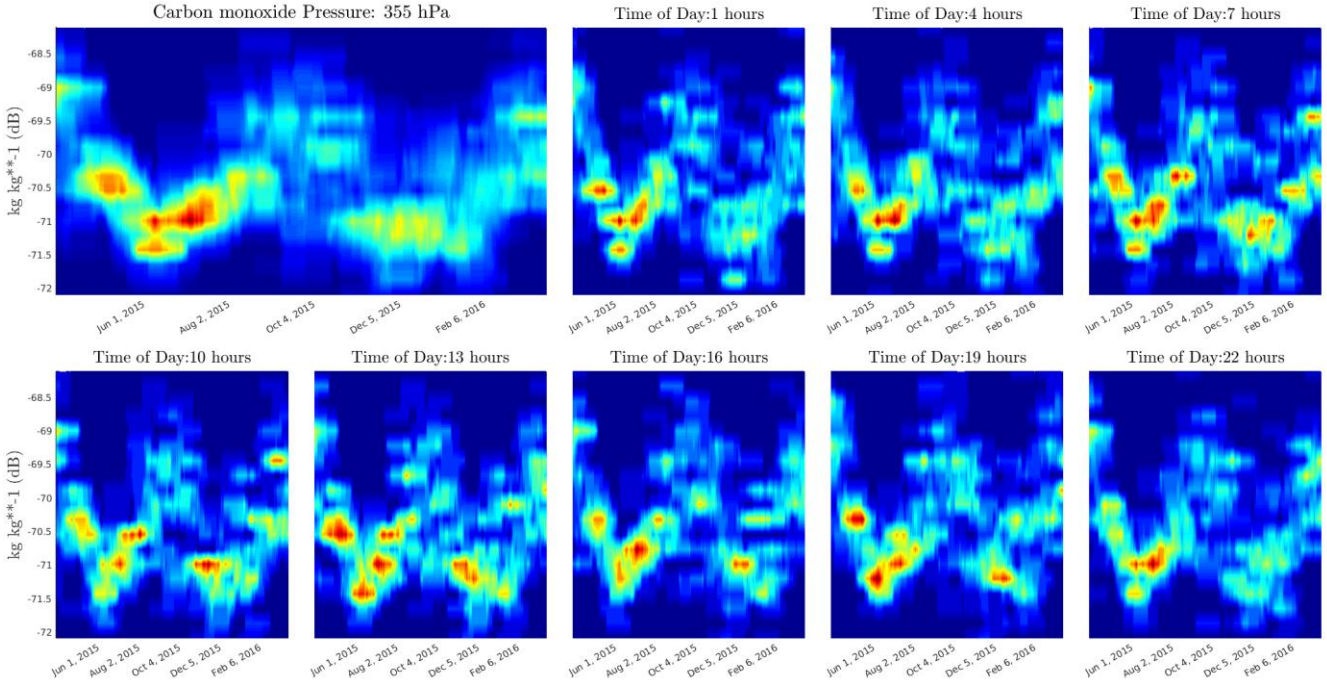

Figure 22: Moving distribution, mid-high layers - Carbon monoxide

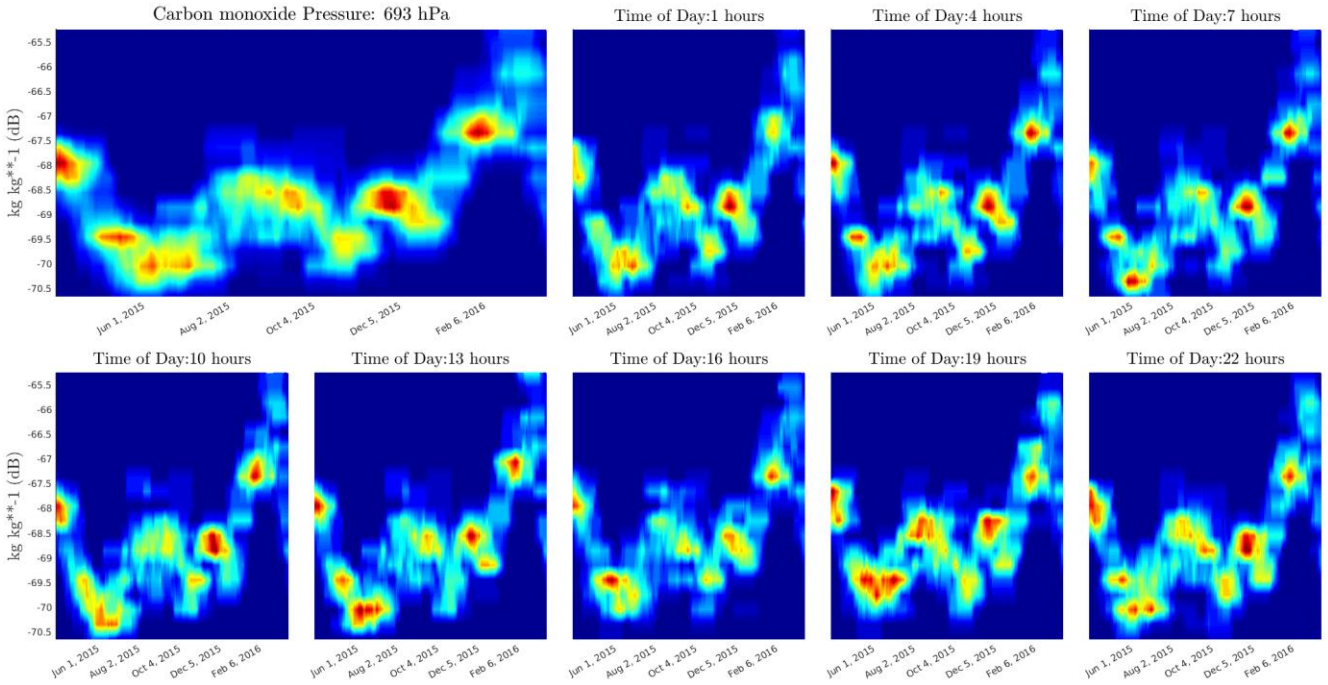

Figure 23: Moving distribution, mid-low layers - Carbon monoxide

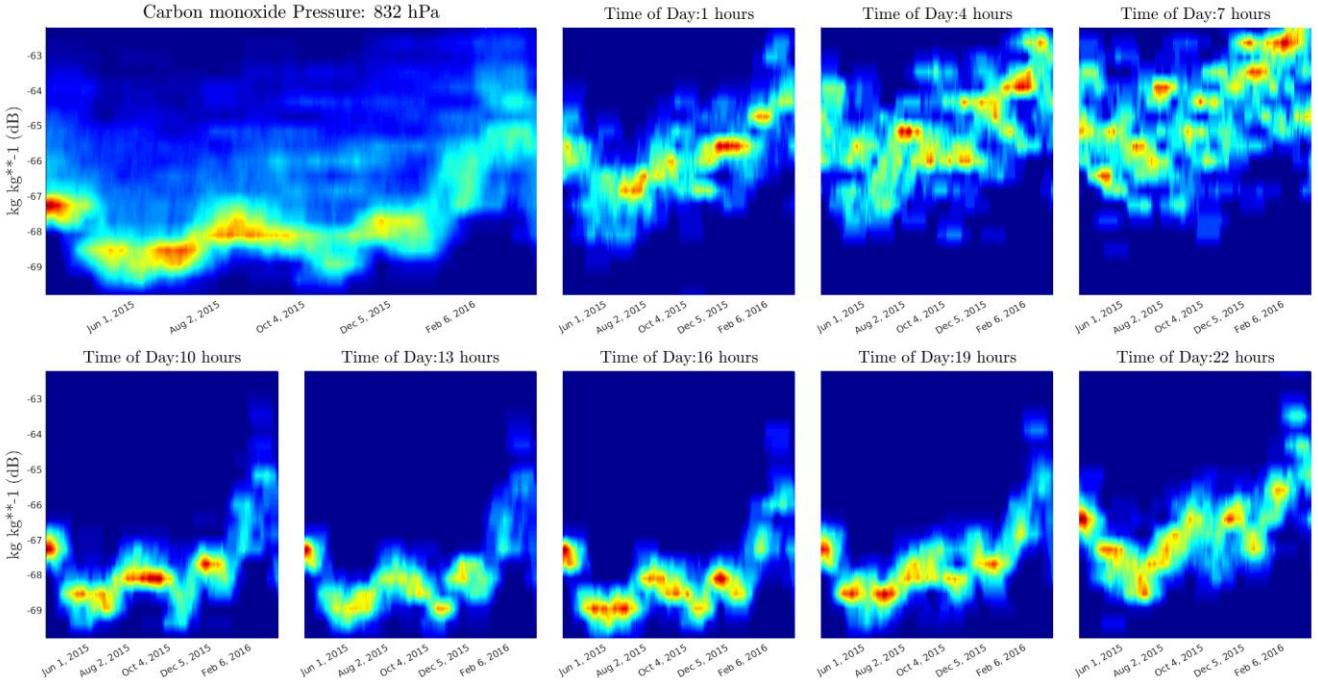

Figure 24: Moving distribution, low layers - Carbon monoxide

5. FORMALDEHYDE

Figure 25 shows that the concentration values of Formaldehyde are higher at surface levels, which a primary peak at daily cycle and a secondary peak at yearly cycle.

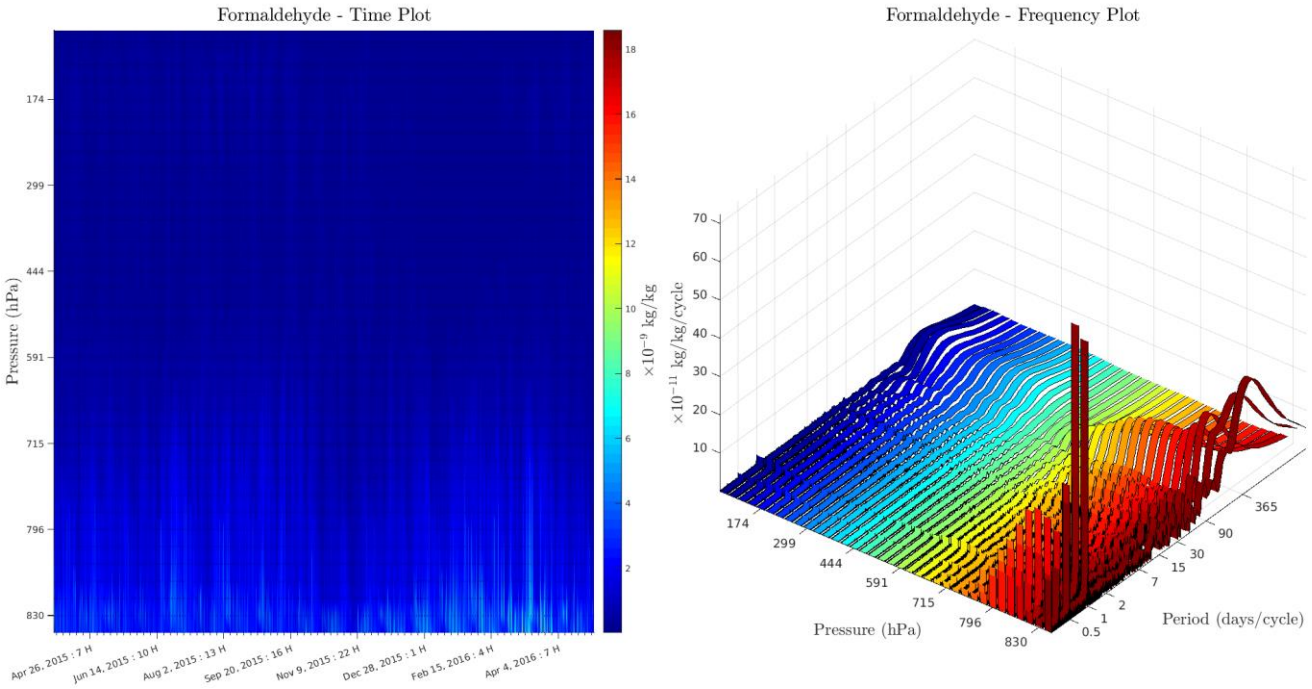

Figure 25: Time and frequency plot for formaldehyde.

The behavior of formaldehyde is shown to be dependent on altitude in Figure 26. For high and mid-high layers, higher concentration values are present between June and August. However, at surface level the highest values are present during March, especially during night time.

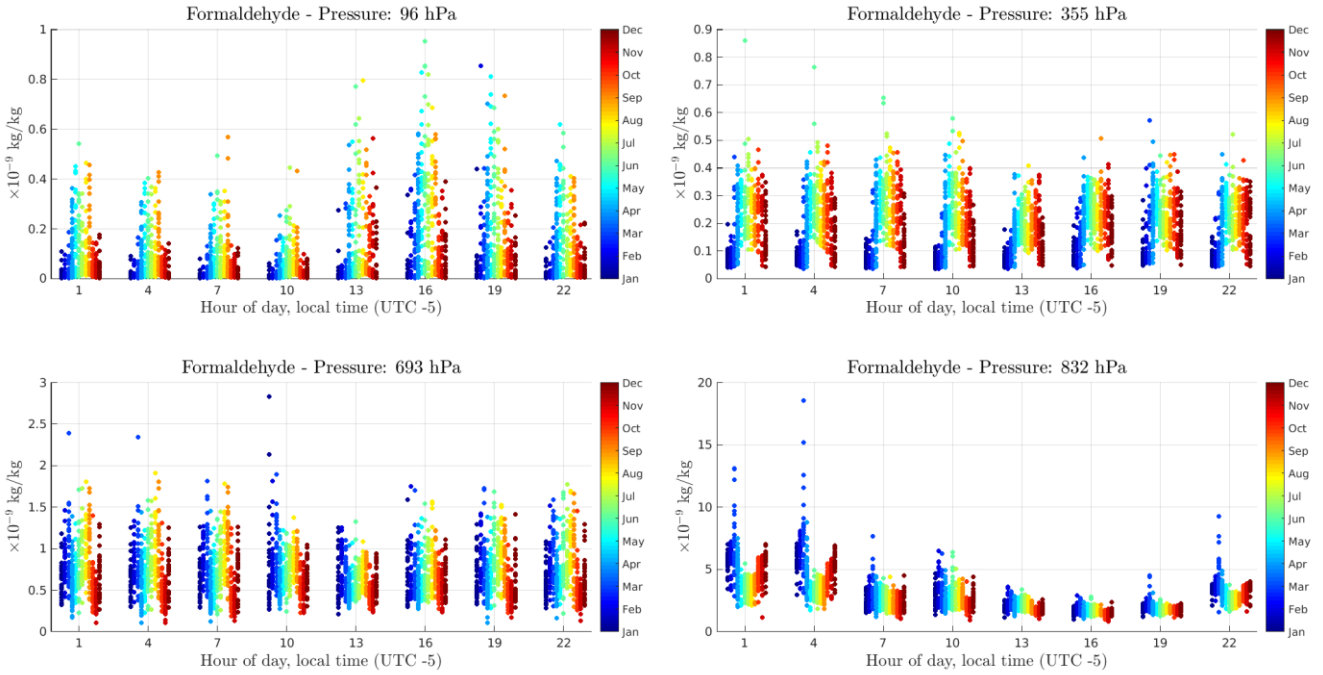

Figure 26: Day cycle plot – formaldehyde.

Figures 27 and 28 for high and mid-high altitude layers of formaldehyde, show that the concentration value distribution is approximately constant throughout the year, except for a significant minimum present between December and March 2016. In contrast, Figure 29 shows that for mid-low layers, there are two maximum peaks during August and February, and a minimum peak during November.

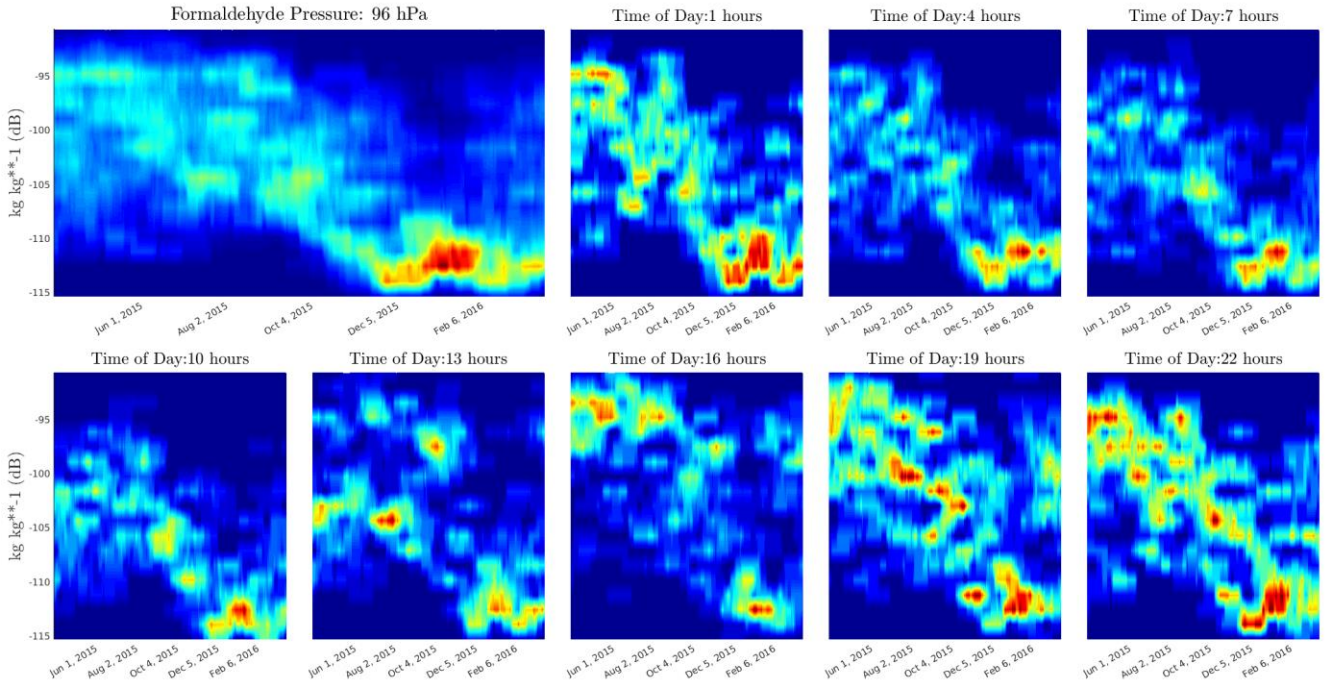

Figure 27: Moving distribution, high layers – Formaldehyde

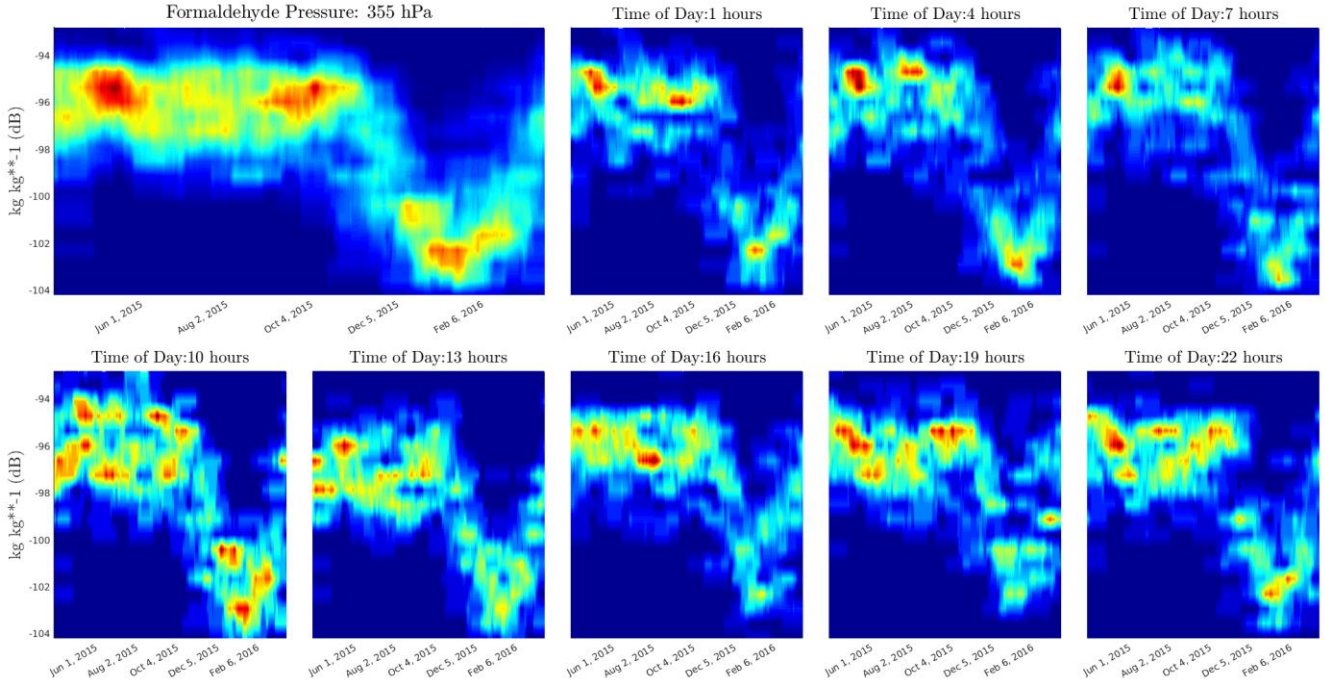

Figure 28: Moving distribution, mid-high layers - Formaldehyde

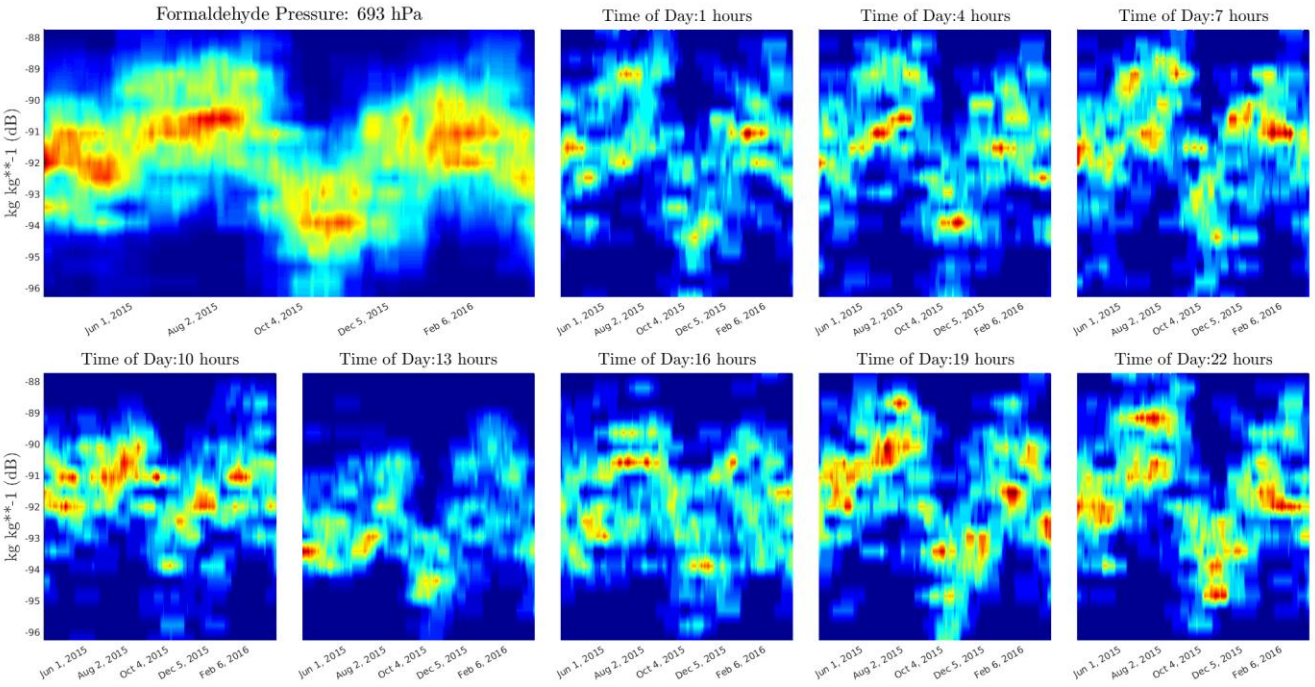

Figure 29: Moving distribution, mid-low layers - Formaldehyde

Lastly, Figure 30 shows the behavior of formaldehyde at surface level. There is a strong daily cycle dependence, as higher concentrations are observed during night time. Maximum peaks are recorded during February 2016 between 10 pm and 4 am.

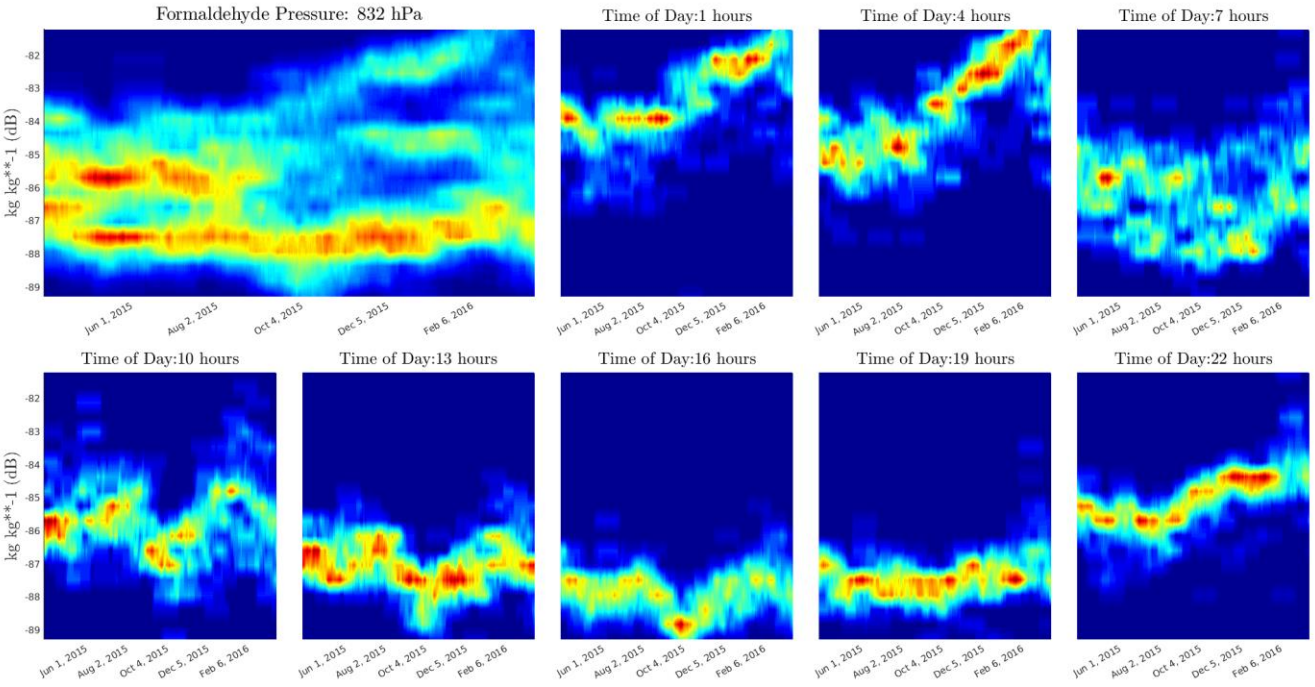

Figure 30: Moving distribution, low layers - Formaldehyde

6. SEA SALT (0.03 – 0.5 um) MXING RATIO

Figure 31 shows the time and frequency plots for sea salt (small particle size) mixing ratio. It can be seen that most of the information is contained between mid and surface levels, approximately between 500 and 900 hPa. The time plot shows that there was a significant event of high concentrations between January and May 2016. The frequency plot presents that this variable is primarily represented by the yearly cycle. However, there are relevant secondary frequency components, with periods of 3 months, 1 month, and the daily cycle.

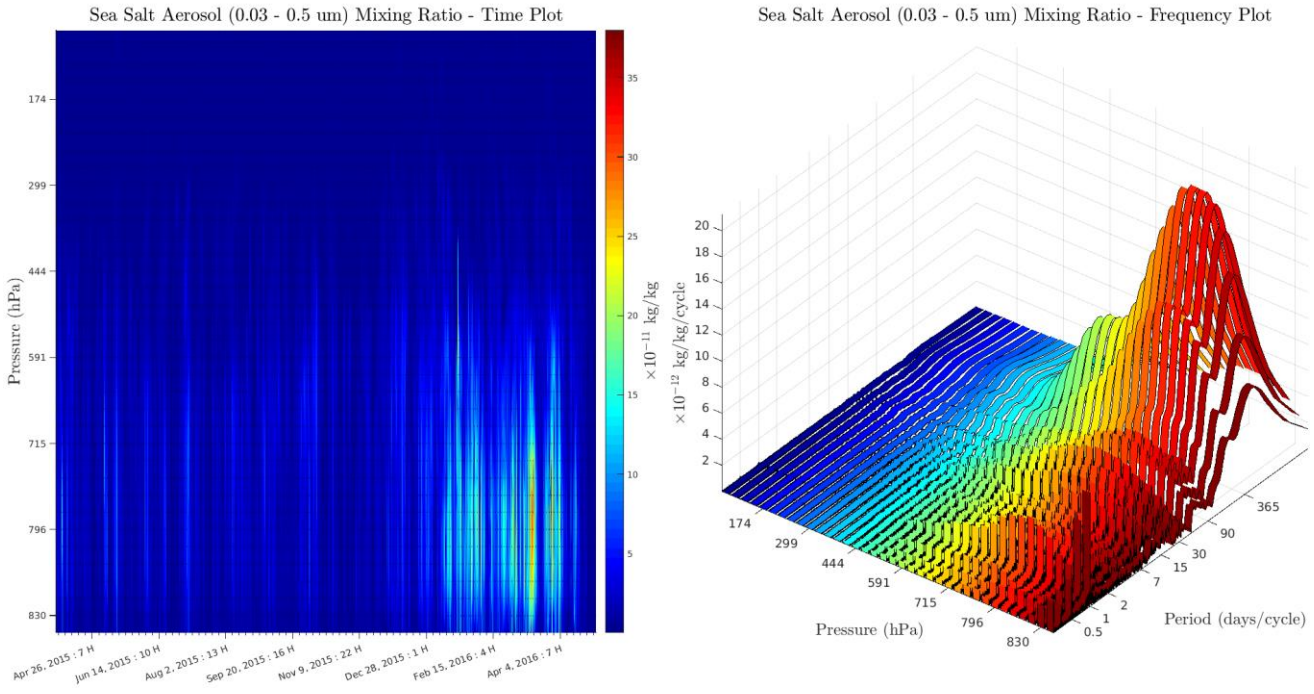

Figure 31: Time and frequency plot for sea salt aerosol (small)

The daily cycle scatter plot in Figure 32 presents the behavior of small sea salt mixing ratio at different pressure layers. For high altitudes, data values are higher during and after day time (between 1 pm and 7 pm), and are approximately constant throughout the year. For mid high altitude, the data distribution appears to be constant independently of time of day and month of year. Both mid-low and low altitude layers presented the highest values between January and April. However, surface level presented a strong dependence on the hour of day (higher values between 10 am and 4 pm), whilst for mid-low altitudes there is no evident dependence on time of day.

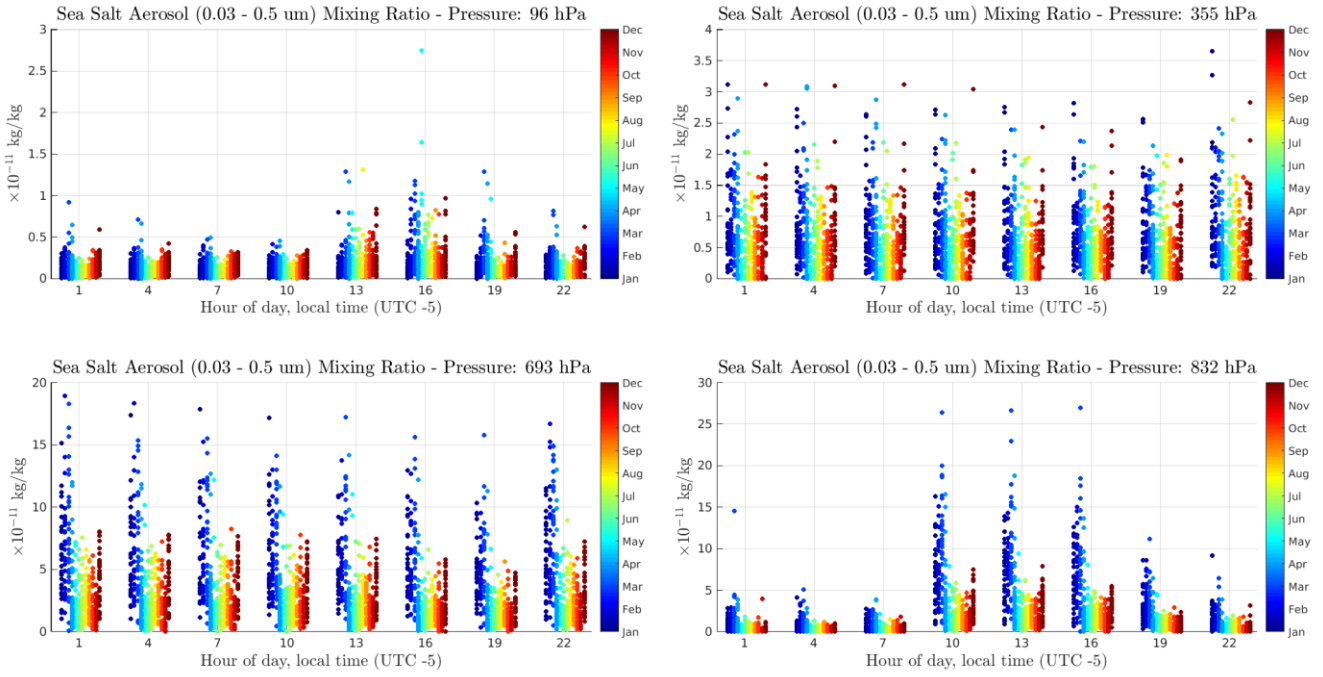

Figure 32: Day cycle plot - sea salt aerosol (small).

The moving distribution plot for high altitude sea salt mixing ratio in Figure 33 shows that there is little change in the data distribution along the year. However, between 1 pm and 4 pm there is an increase in the probability of higher concentration values in comparison with the rest of the plots.

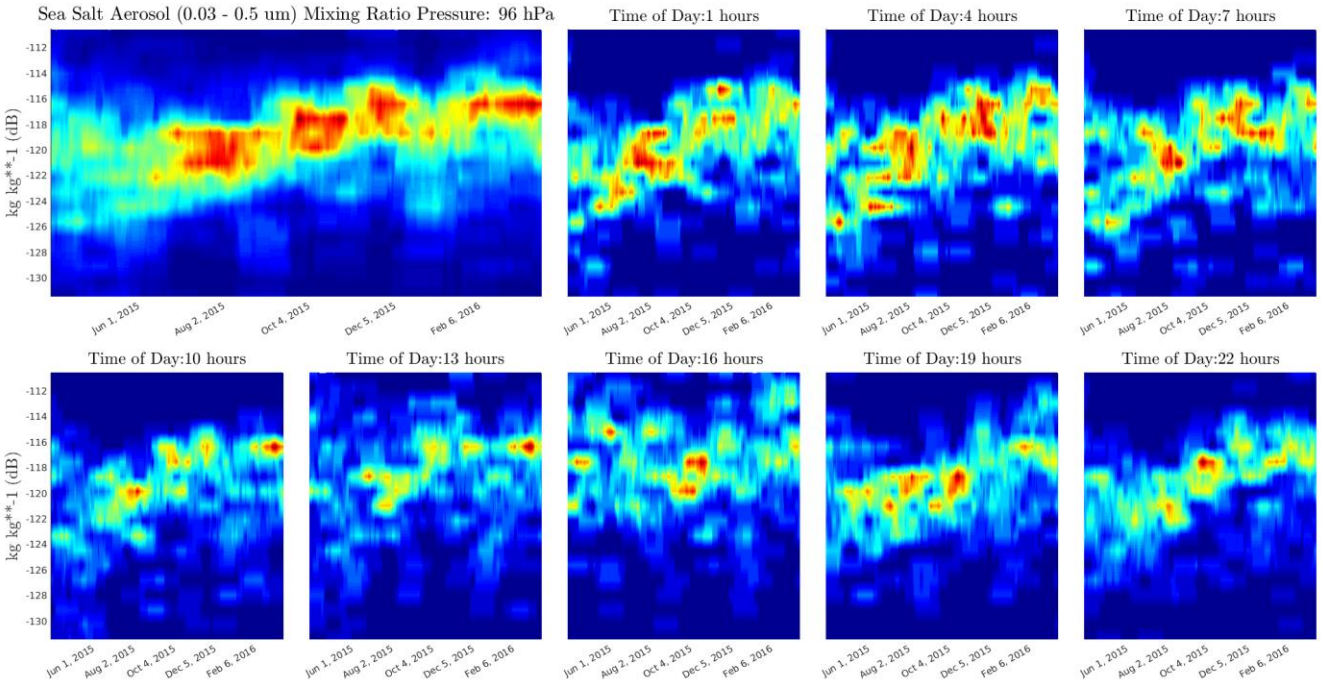

Figure 33: Moving distribution, high layers - Sea salt aerosol (small)

Figure 34 shows that the distribution of sea salt mixing ratio for mid-high altitude layers is approximately constant for all times.

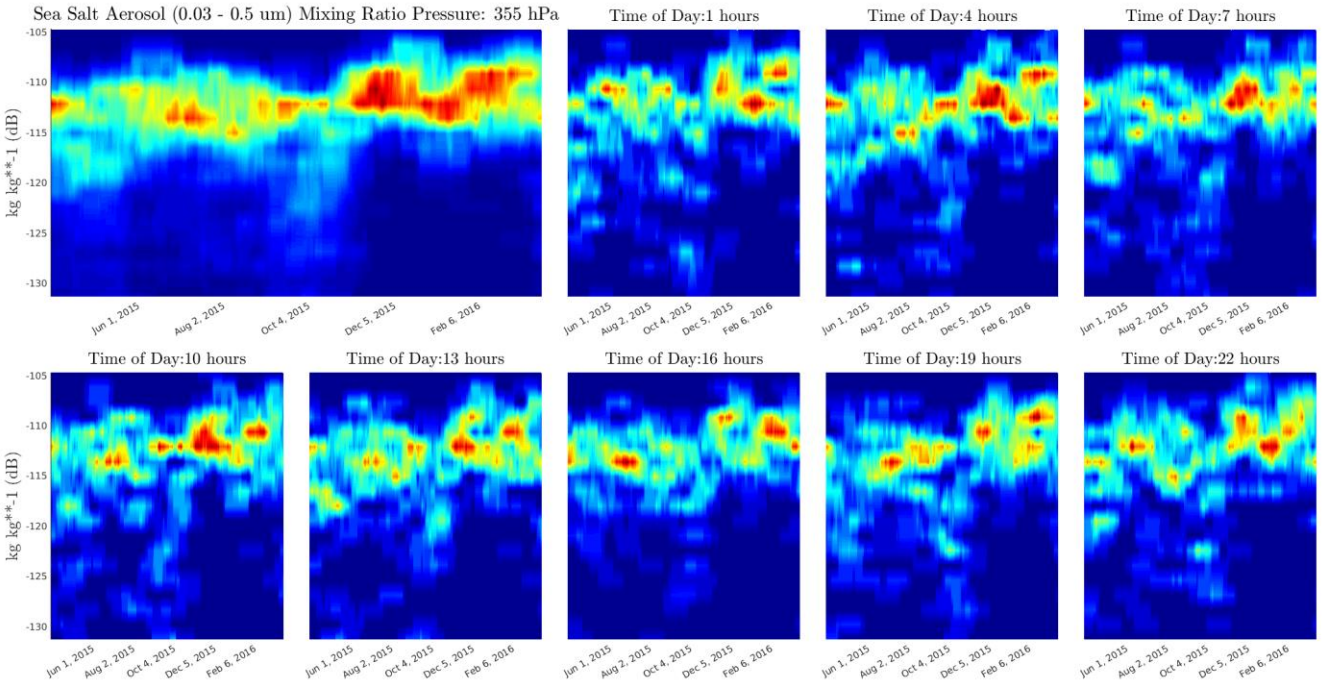

Figure 34: Moving distribution, mid-high layers - Sea salt aerosol (small)

For mid-low altitude layers, Figure 35 shows that there is a concentration peak after February 2016. The distribution is shown to be independent on the hour of day.

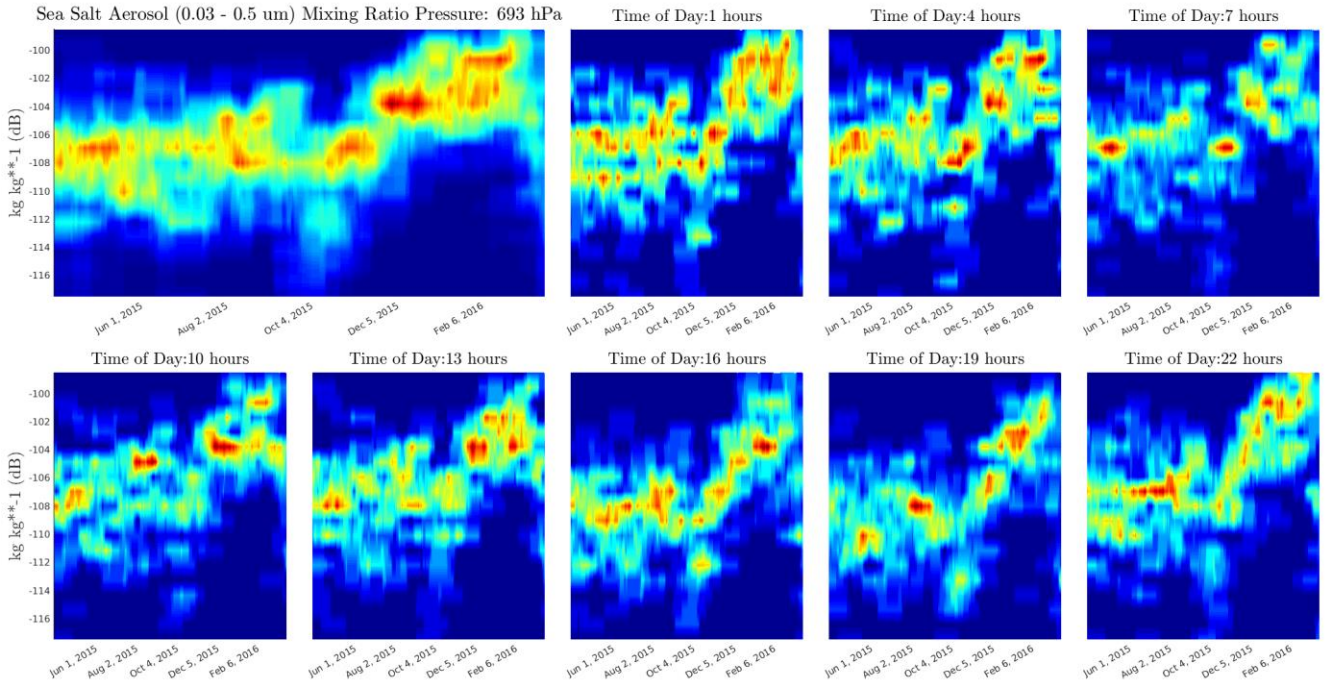

Figure 35: Moving distribution, mid-low layers - Sea salt aerosol (small)

Lastly, Figure 36 shows the results for surface level. The daily cycle dependence is evident, as higher distributions are shown between 10 am and 4 pm. Additionally, between 10 am and 10 pm, the shape of the plots is similar: the distributions are constant from June to December, and then a maximum peak begins from January through February. The plots for hours of day from 1 am through 7 am present low, highly dispersed distributions, with no evident trend.

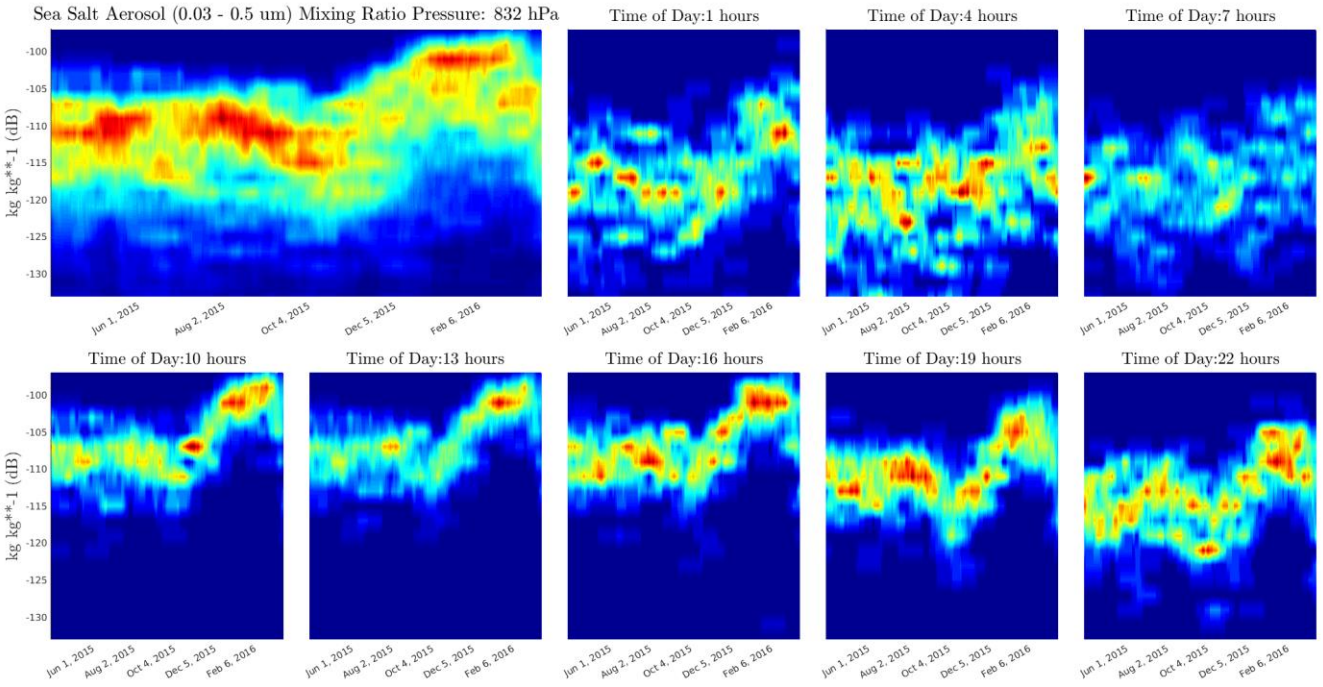

Figure 36: Moving distribution, low layers - Sea salt aerosol (small)

7. SEA SALT (0.5 – 5 um) MIXING RATIO

The results for sea salt medium size particle are very similar for those described in section 6 for the small sized particles. For the analysis description, read the discussion in the previous section.

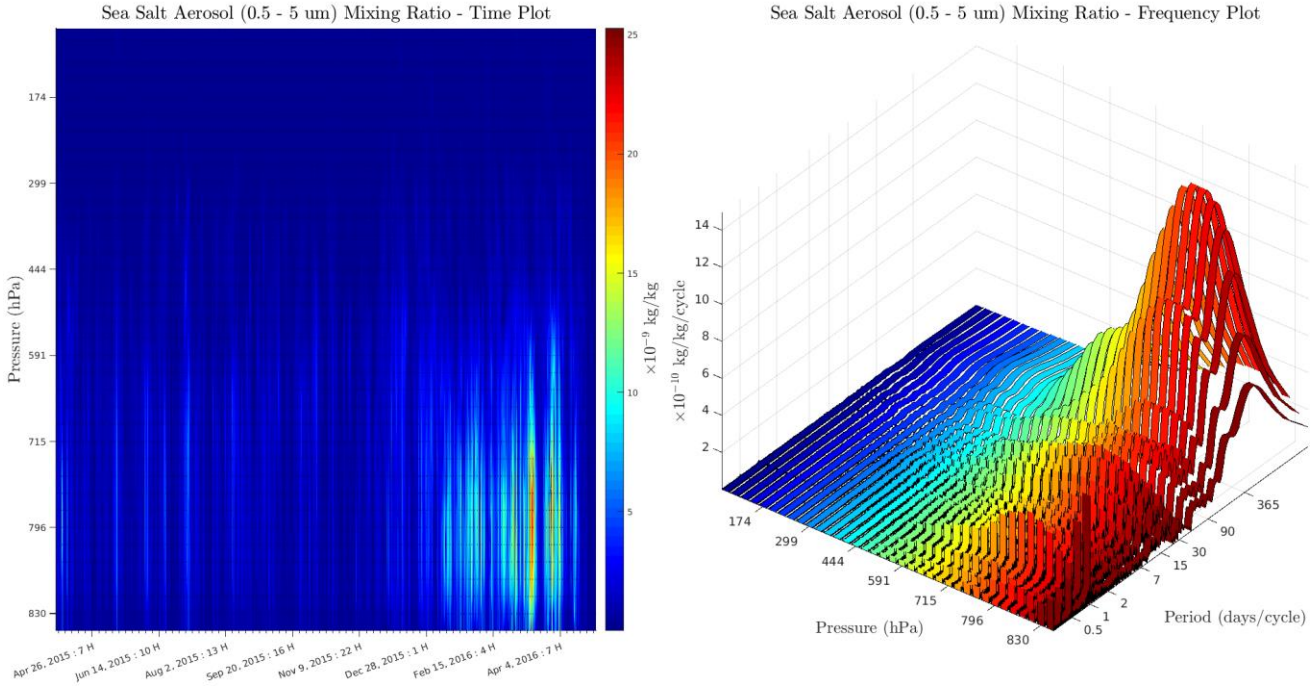

Figure 37: Time and frequency plot for sea salt mixing ratio (medium).

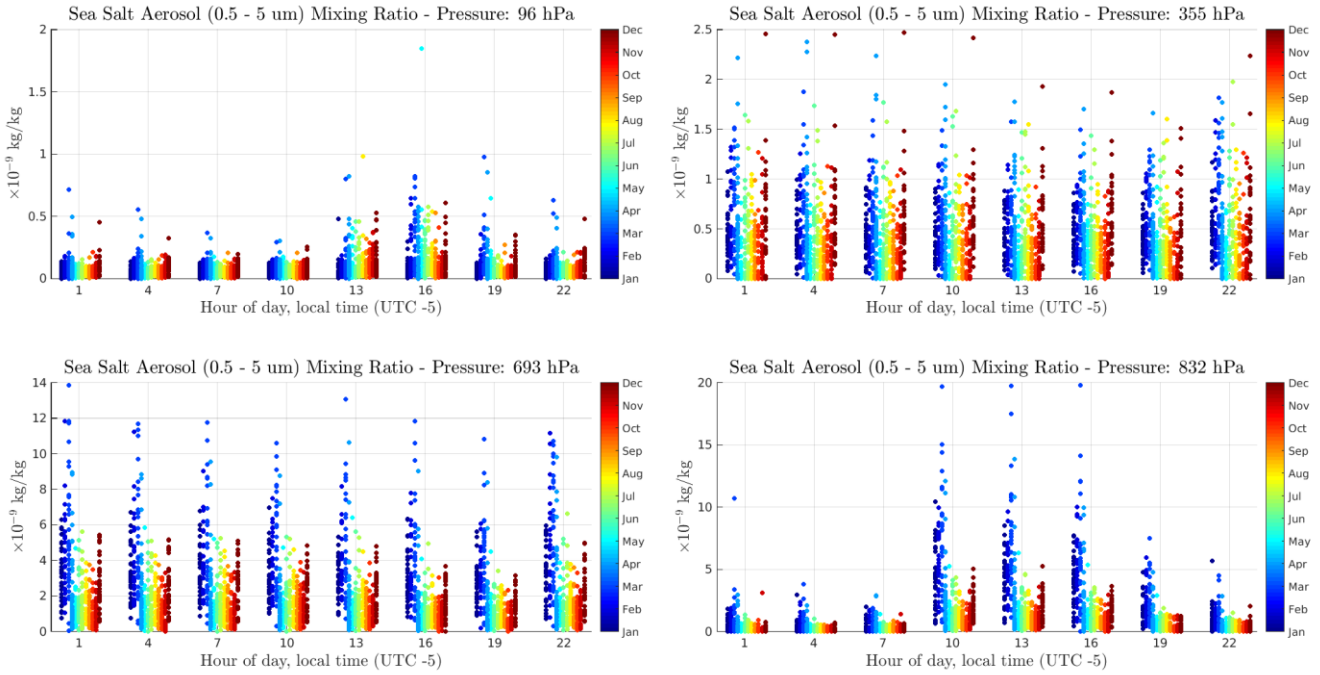

Figure 38: Day cycle plot - sea salt aerosol (medium)

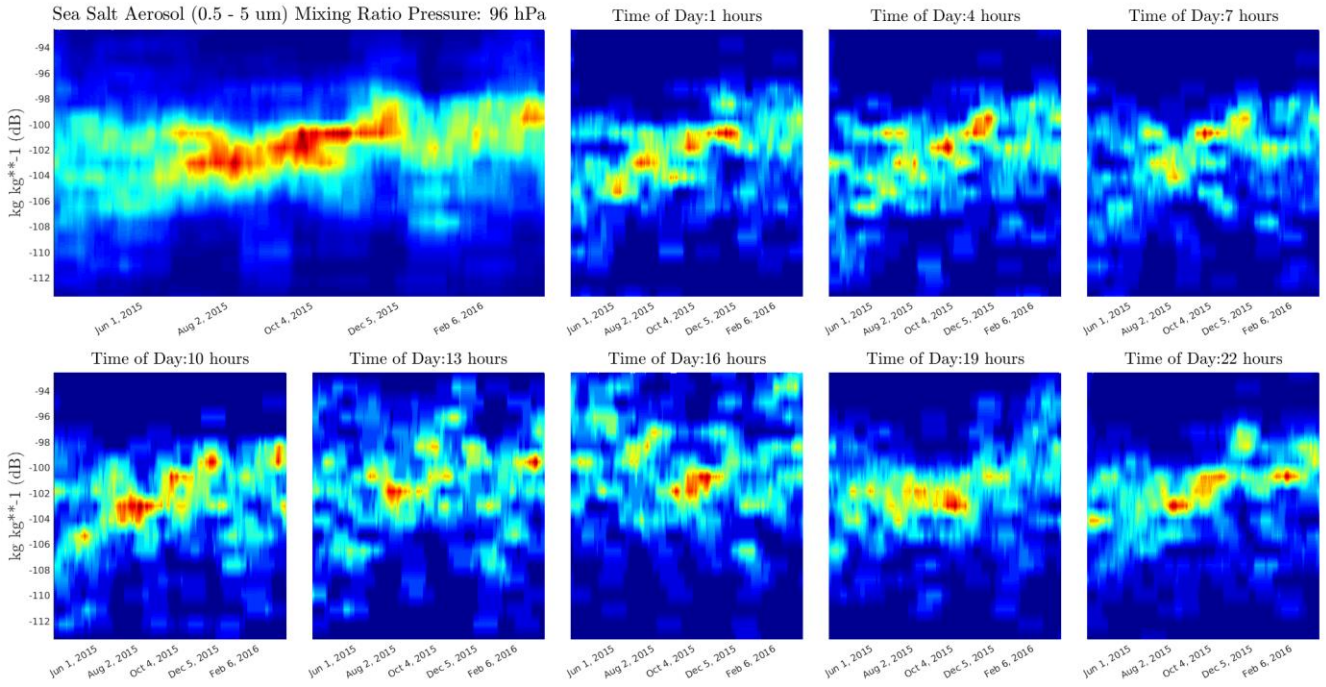

Figure 39: Moving distribution, high layers - Sea salt aersol (medium)

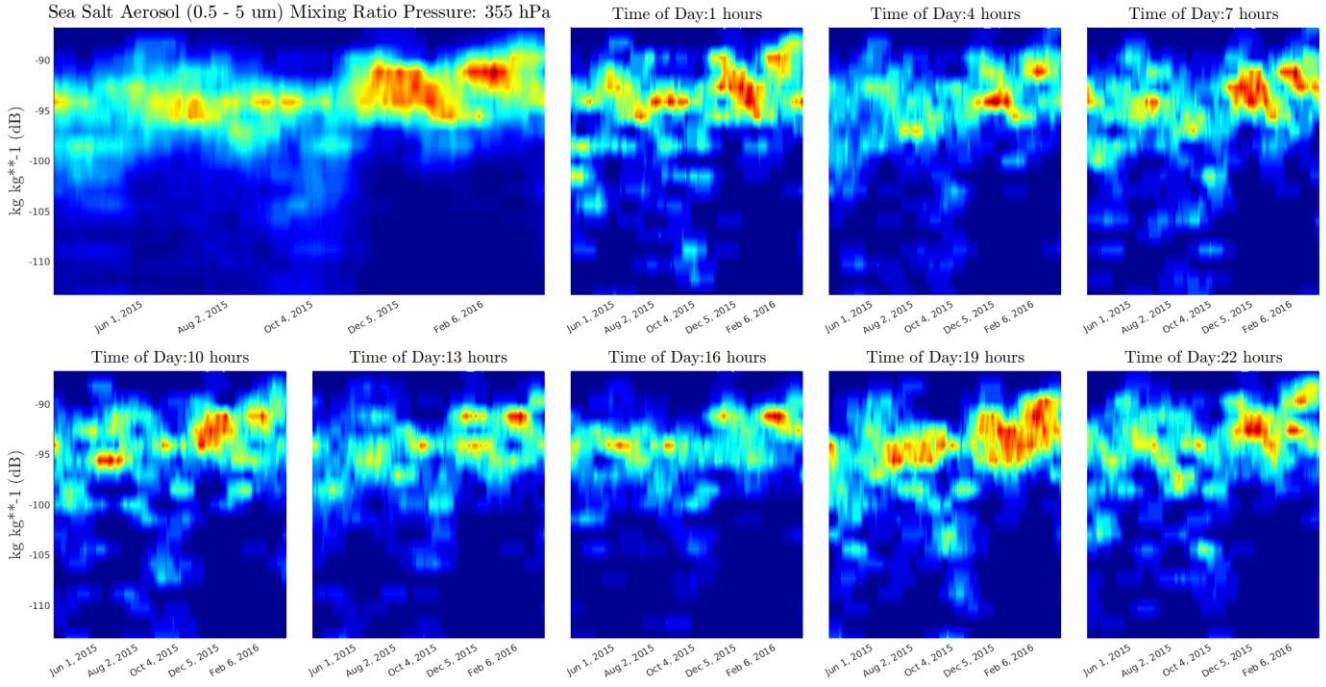

Figure 40: Moving distribution, mid-high layers - Sea salt aerosol (medium)

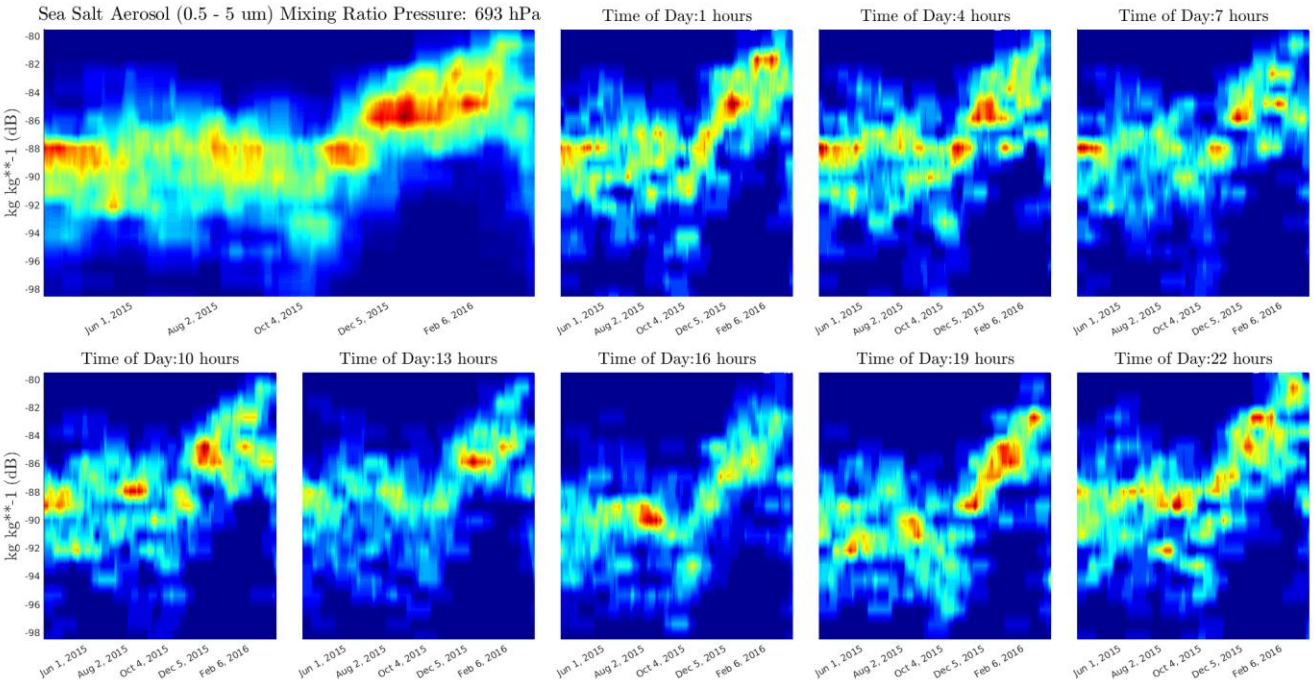

Figure 41: Moving distribution, mid-low layers - Sea salt aerosol (medium)

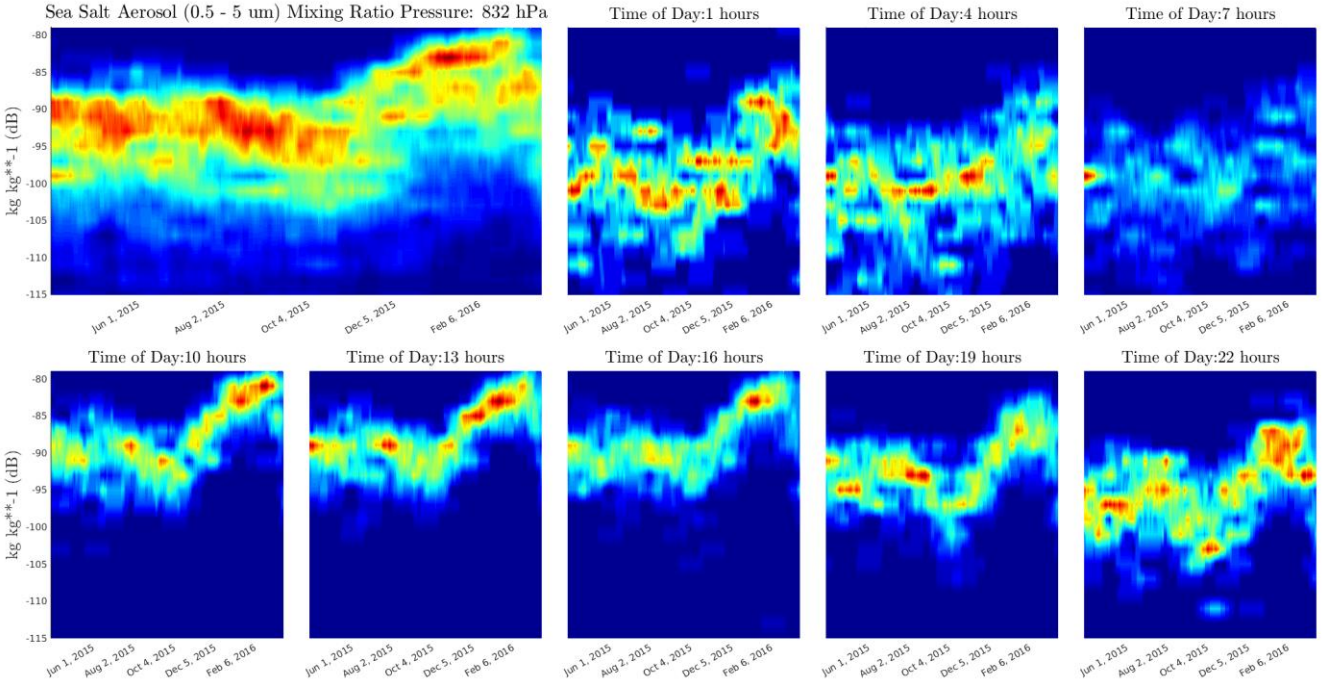

Figure 42: Moving distribution, low layers - Sea salt aerosol (medium)

8. SEA SALTA AEROSOL (5 – 20 um) MIXING RATIO

The results for sea salt (large-size particle) are very similar for those described in section 6 for the small sized particles. For the analysis description, read the discussion in the mentioned section.

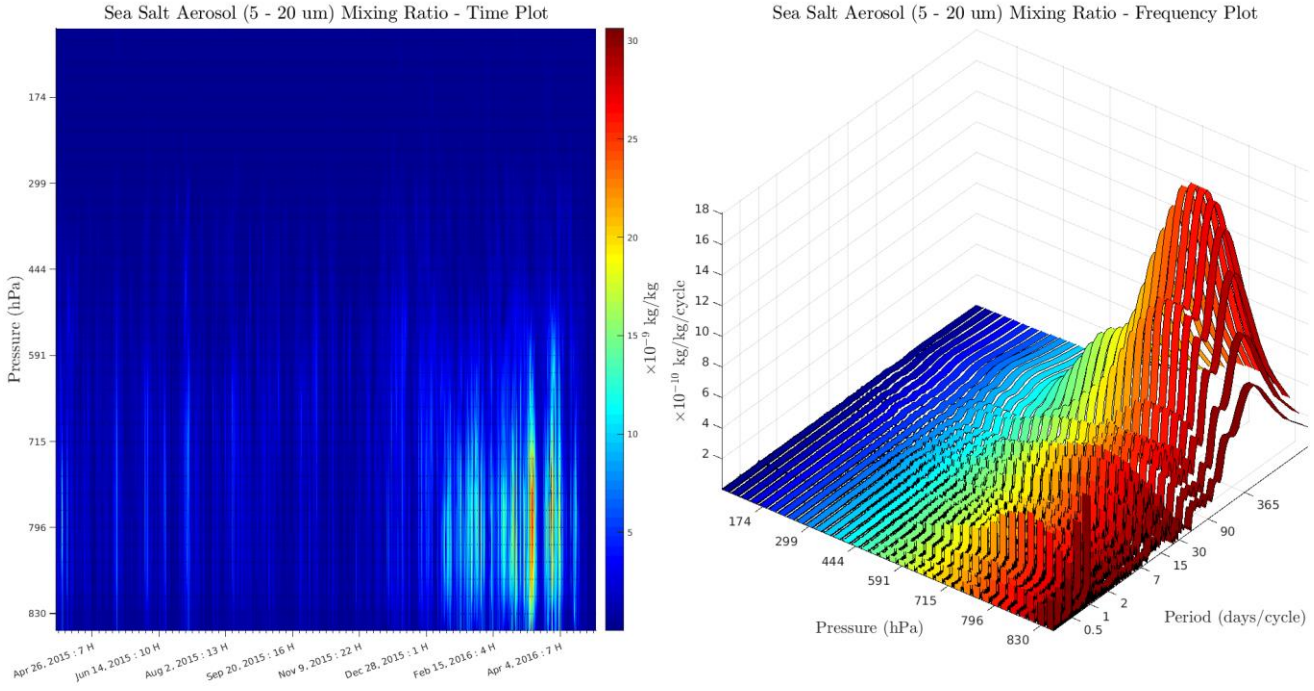

Figure 43: Time and frequency plot for sea salt aerosol (large)

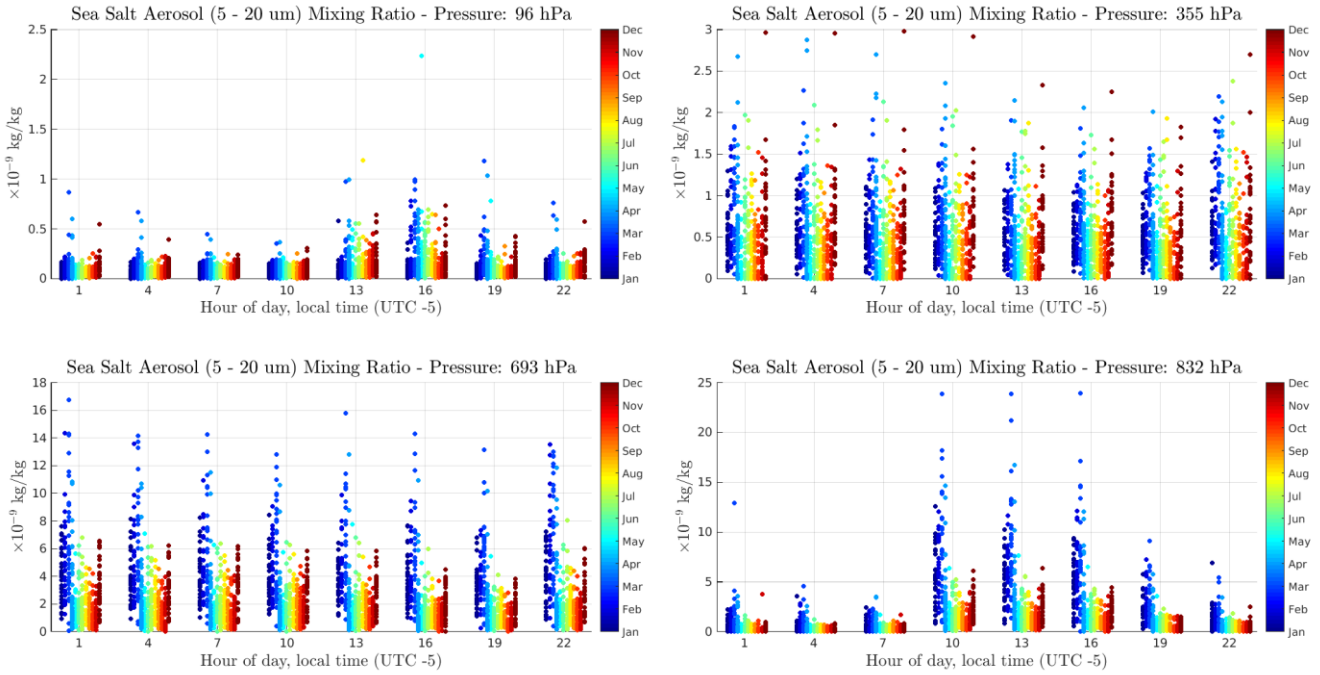

Figure 44: Day cycle plot - sea salt aerosol (large)

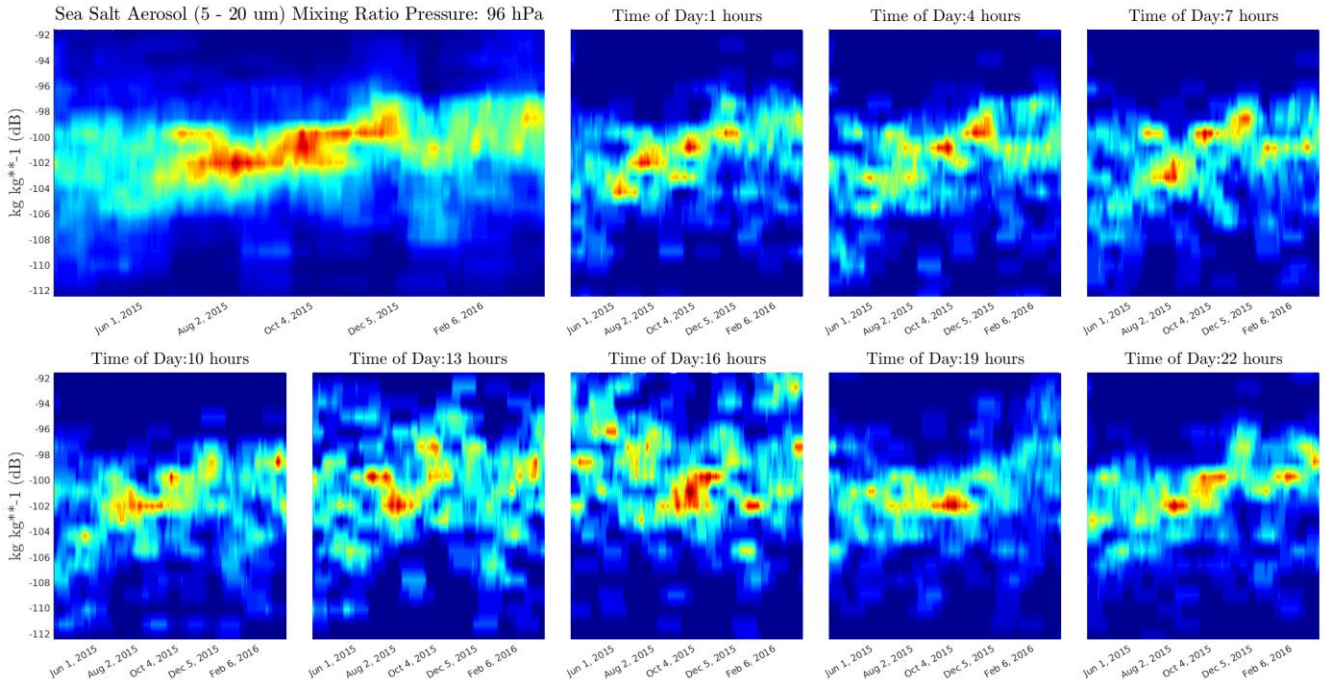

Figure 45: Moving distribution, high layers - Sea salt aerosol (large)

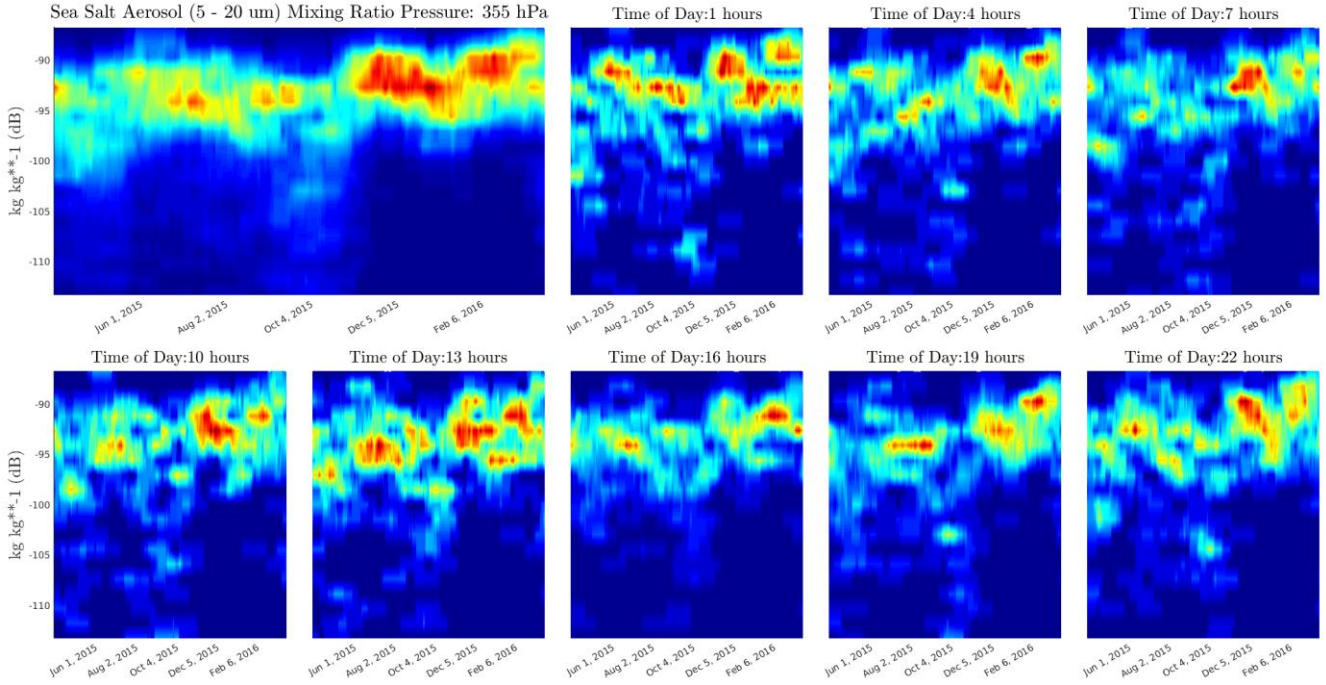

Figure 46: Moving distribution, mid-high layers - Sea salt aerosol (large)

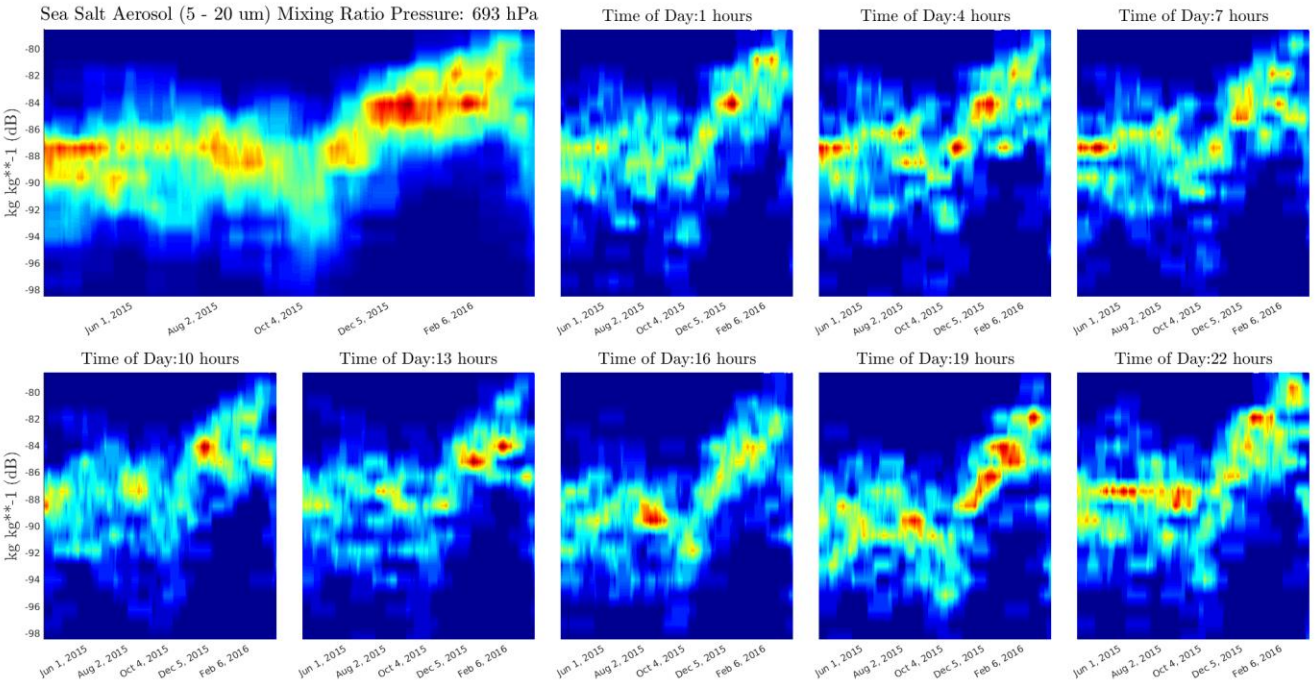

Figure 47: Moving distribution, mid-low layers - Sea salt aerosol (large)

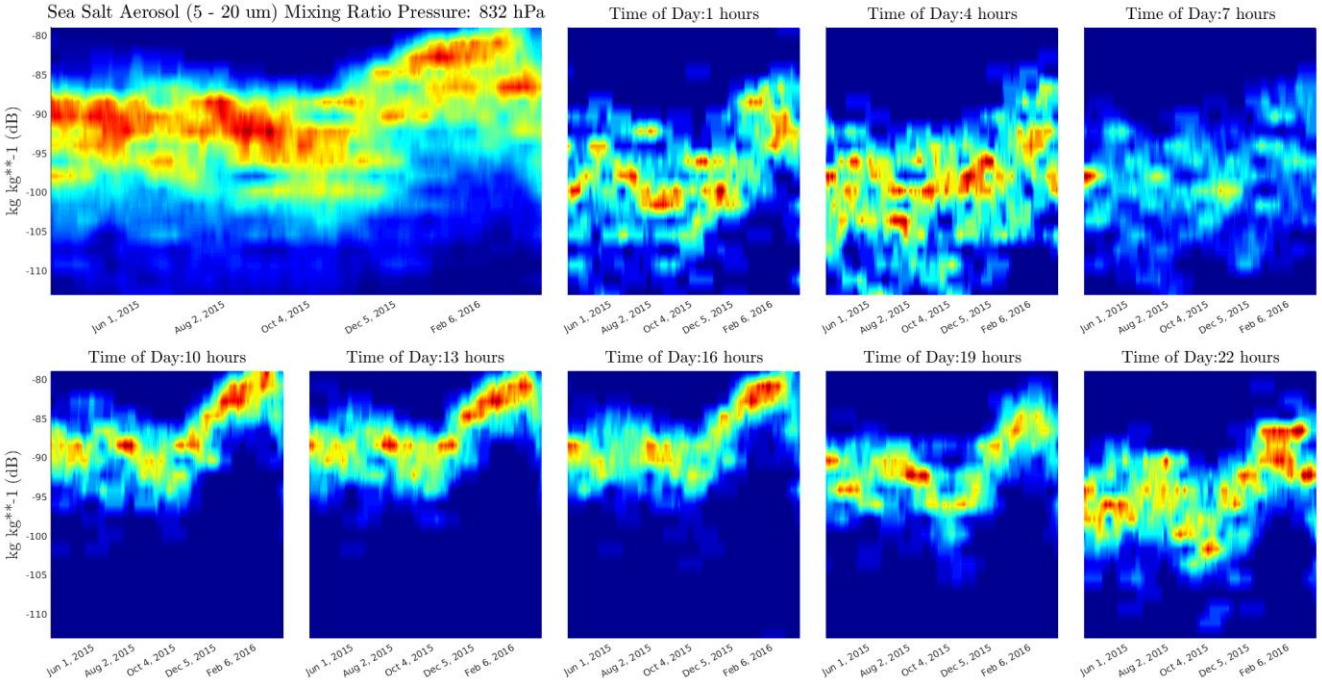

Figure 48: Moving distribution, low layers - Sea salt aerosol (large)

9. DUST AEROSOL (0.03 – 0.55 um) MIXING RATIO

The time and frequency plots for dust aerosol mixing ratio (small particle size) is shown in Figure 49. Information is contained mostly between the low and mid altitude layers (approximately between 400 and 900 hPa). It can be seen in the time that there are two high-concentration events, one between April and August 2015, and the other between January and April 2016. The frequency plot shows that this variable is characterized mainly by the yearly cycle.

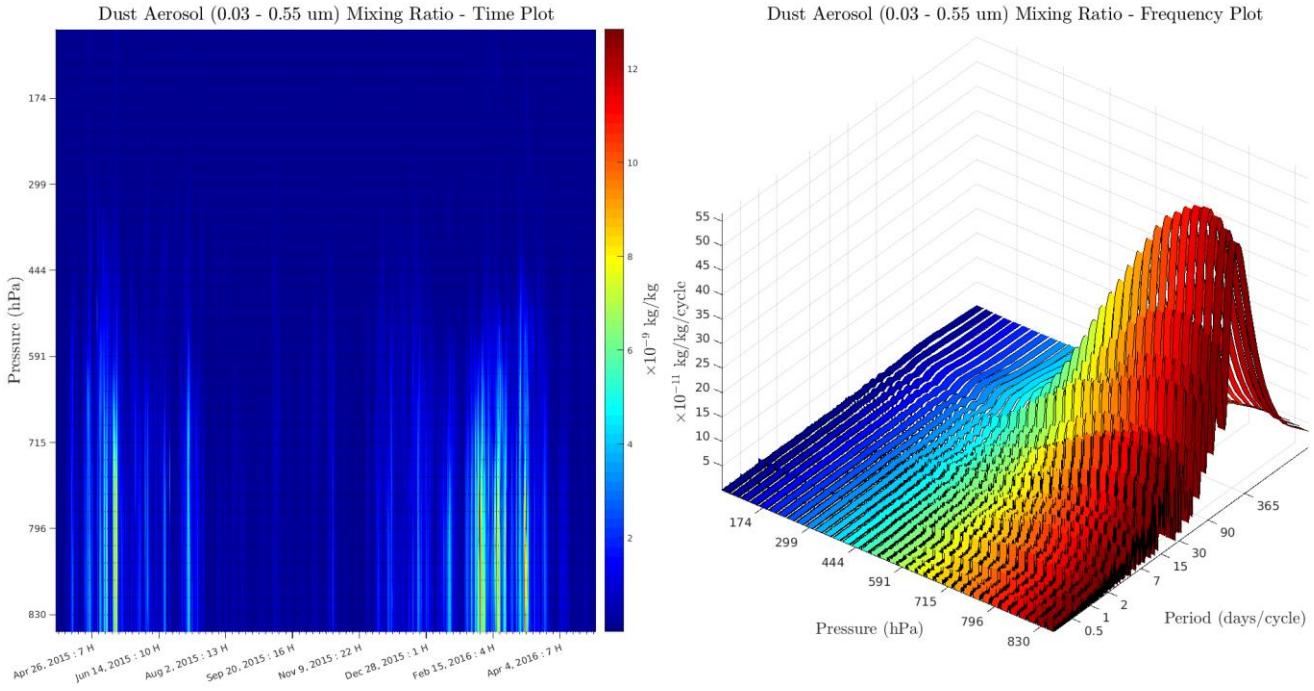

Figure 49: Time and frequency plot for dust aerosol (small).

Figure 50 shows the daily cycle plot for different pressure levels. At low pressures (high altitudes), the dust aerosol mixing ratio presents a daily cycle behavior, with high values between 1 pm and 7 pm, with a maximum at 4 pm. Additionally, June exhibits the highest concentrations. The rest of the pressure layers (from 300 to 900 hPa) are not influenced by the hour of day. Low and mid-low altitudes show peak values from December to June, with maximum values at February and May. Mid-high altitudes show a similar behavior, as the lower concentrations are registered from July to September, but it lacks the extreme values of February seen in lower altitudes.

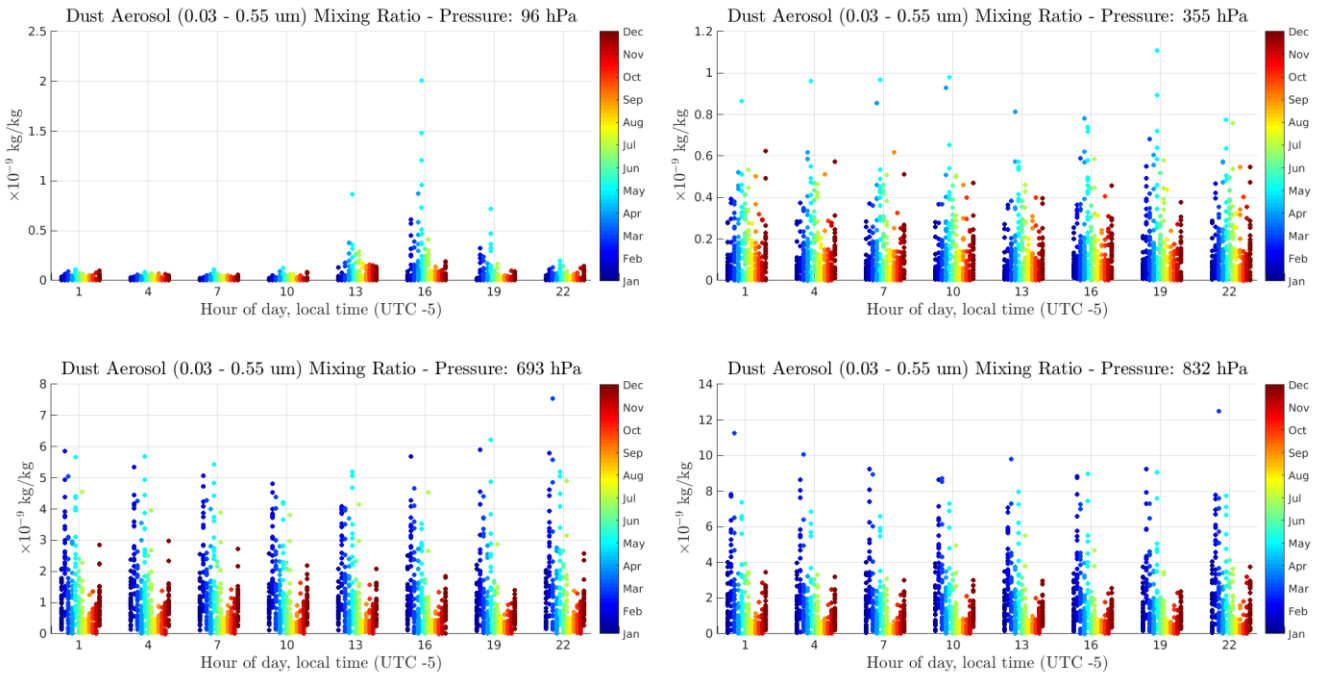

Figure 50: Day cycle plot - dust aerosol (small)

The moving histogram for high altitude layers in Figure 51 shows a peak of concentration from April to June, specially during 1 pm to 7 pm. However, between December and February (lower values), all hours of day present approximately the same distribution.

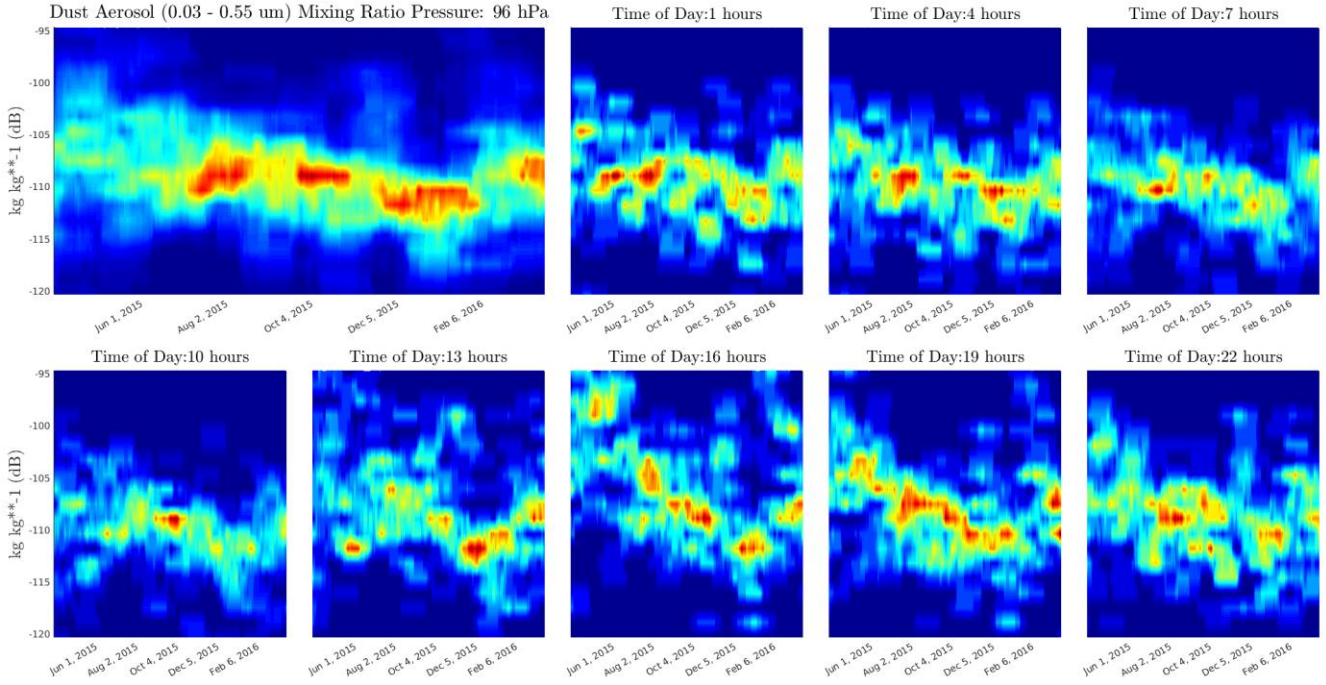

Figure 51: Moving distribution, high layers - Dust aerosol (small)

For mid-high altitudes (Figure 52), it is seen that the concentration values are independent of the hour of day. A significant minimum is found during October, whereas the higher values are found at May.

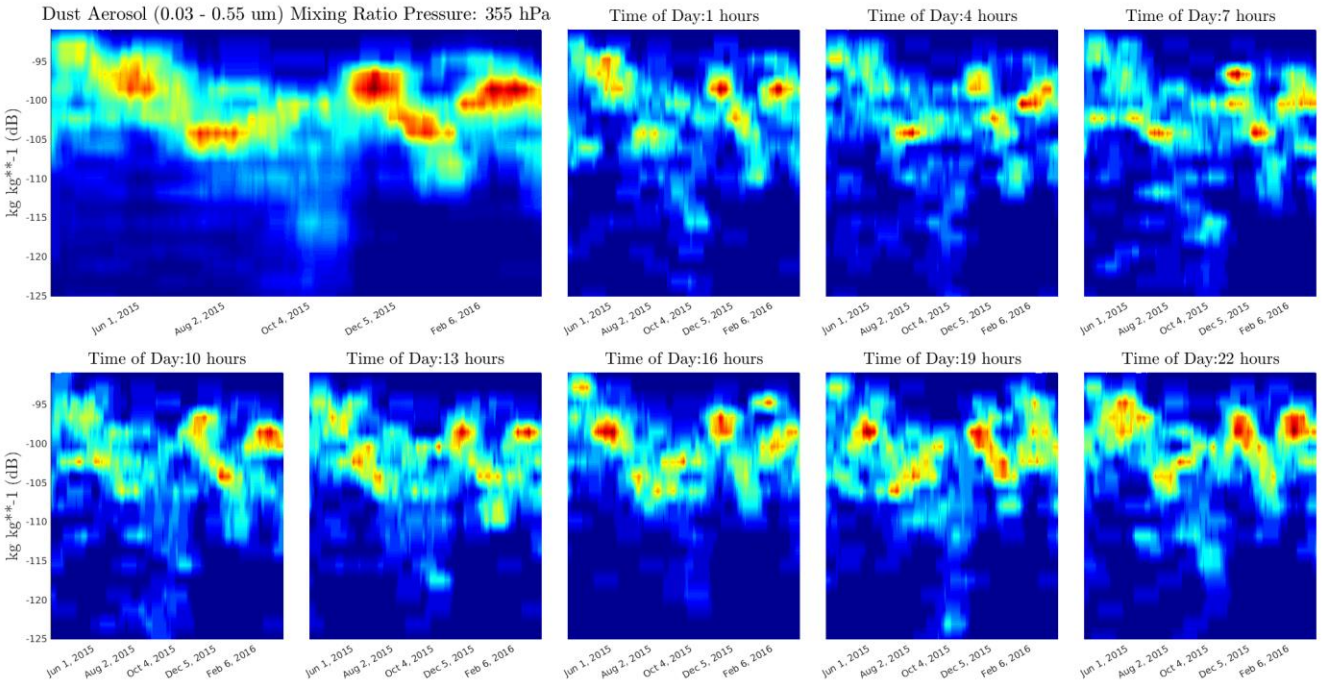

Figure 52: Moving distribution, mid-high layers - Dust aerosol (small)

The histogram plots for mid-low and surface levels (Figures 53 and 54) follow the same structure: both resemble a sinusoid, with local maxima located at February and May, and local minima located at August and April. These data points are independent of the hour of day.

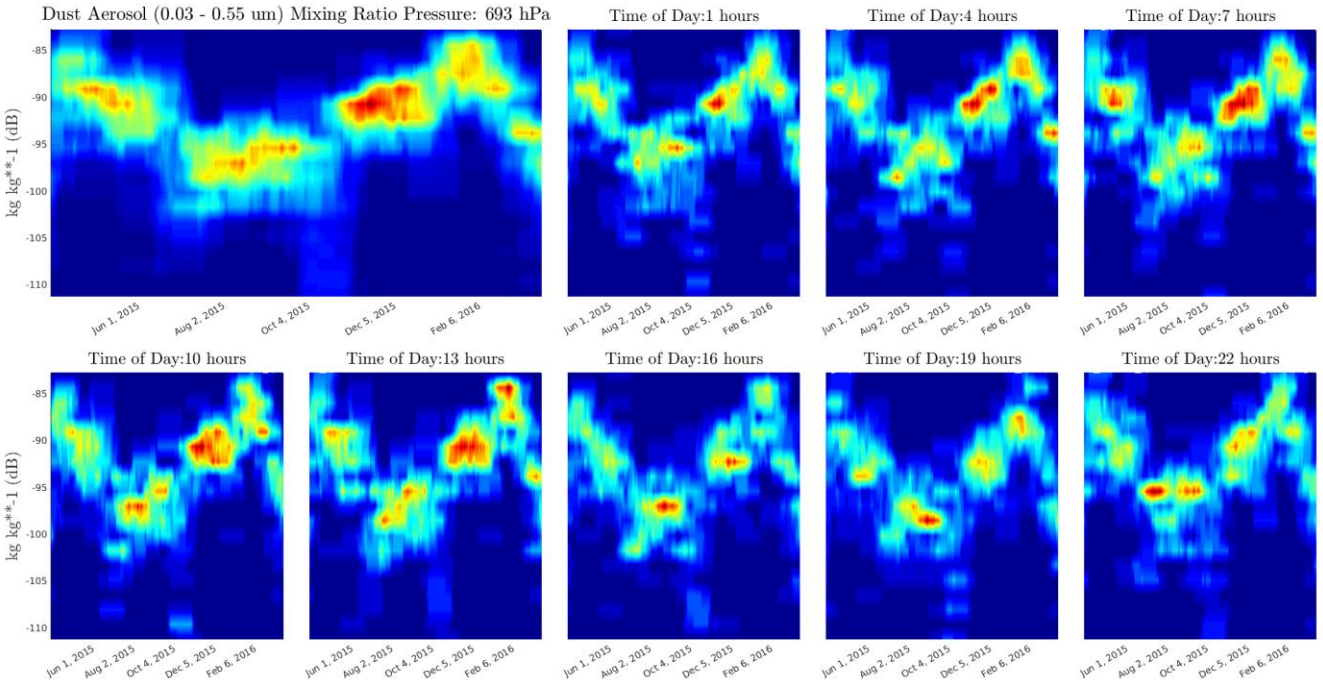

Figure 53: Moving distribution, mid-low layers - Dust aerosol (small)

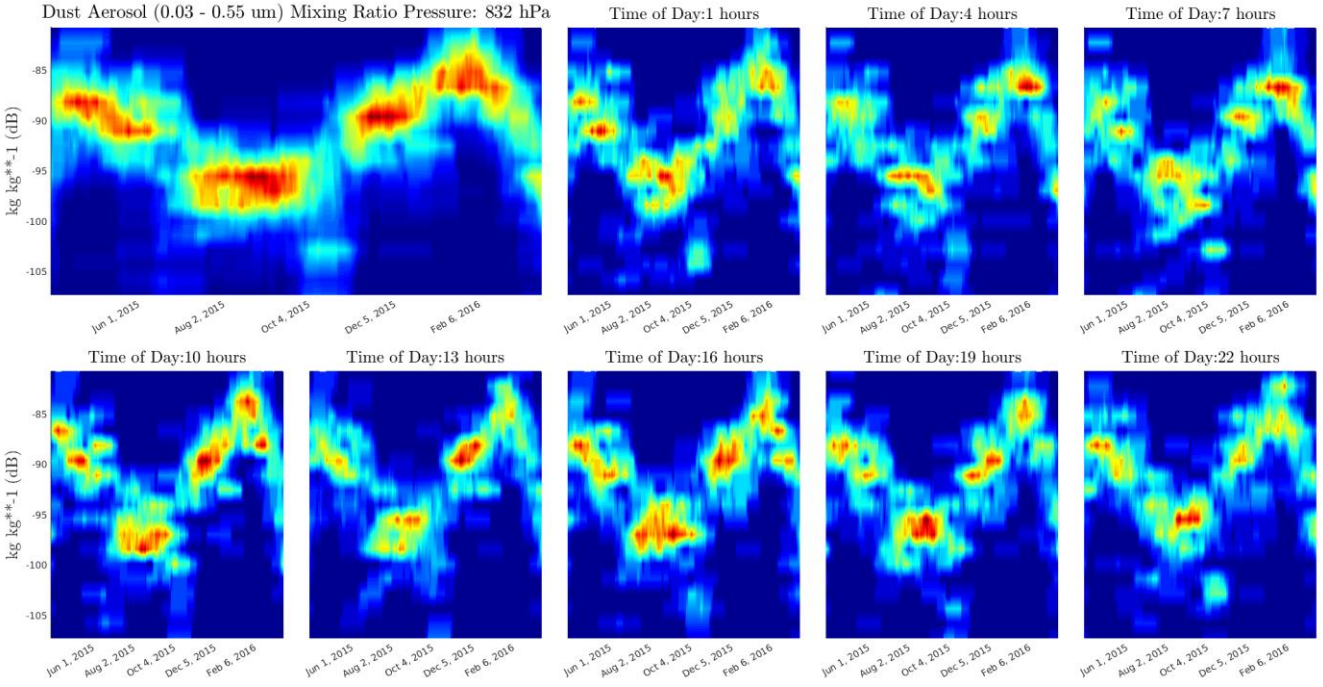

Figure 54: Moving distribution, low layers - Dust aerosol (small)

10. DUST AEROSOL (0.55 – 9 um) MIXING RATIO

The results for dust aerosol (medium-size particles) are very similar for those described in section 9 for the small sized case. For the analysis description, read the discussion in the mentioned section.

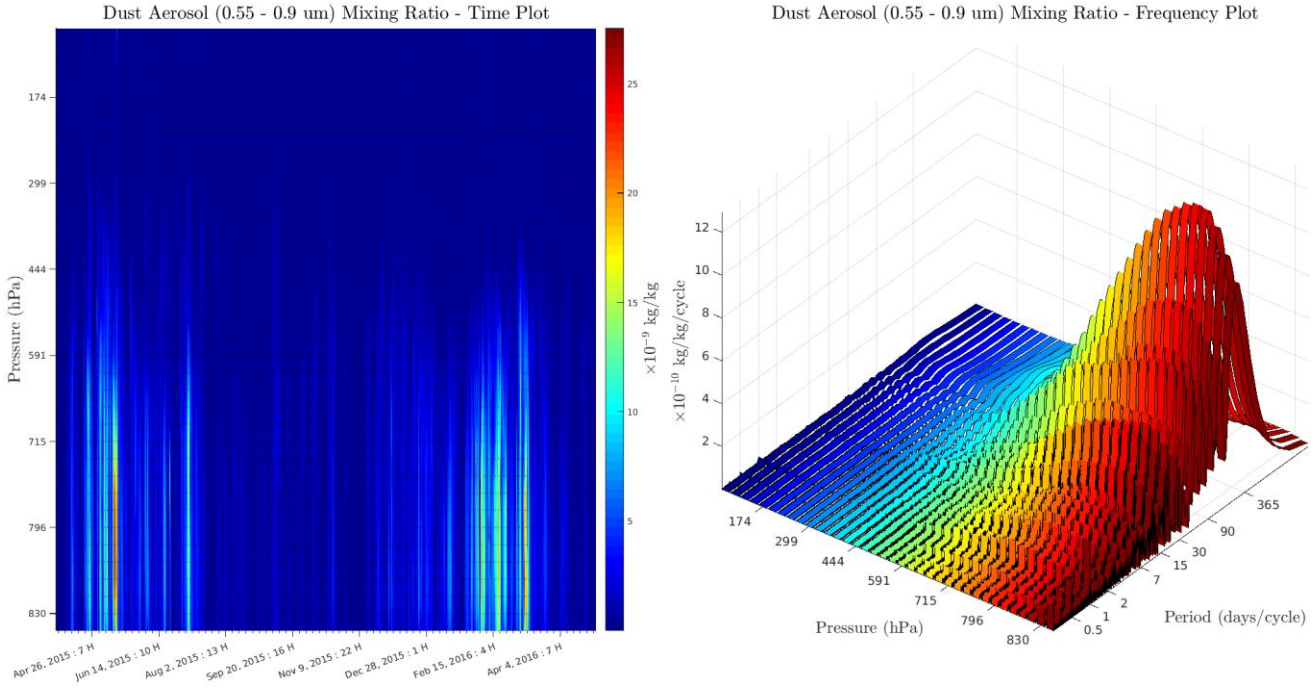

Figure 55: Time and frequency plot for dust aerosol (medium)

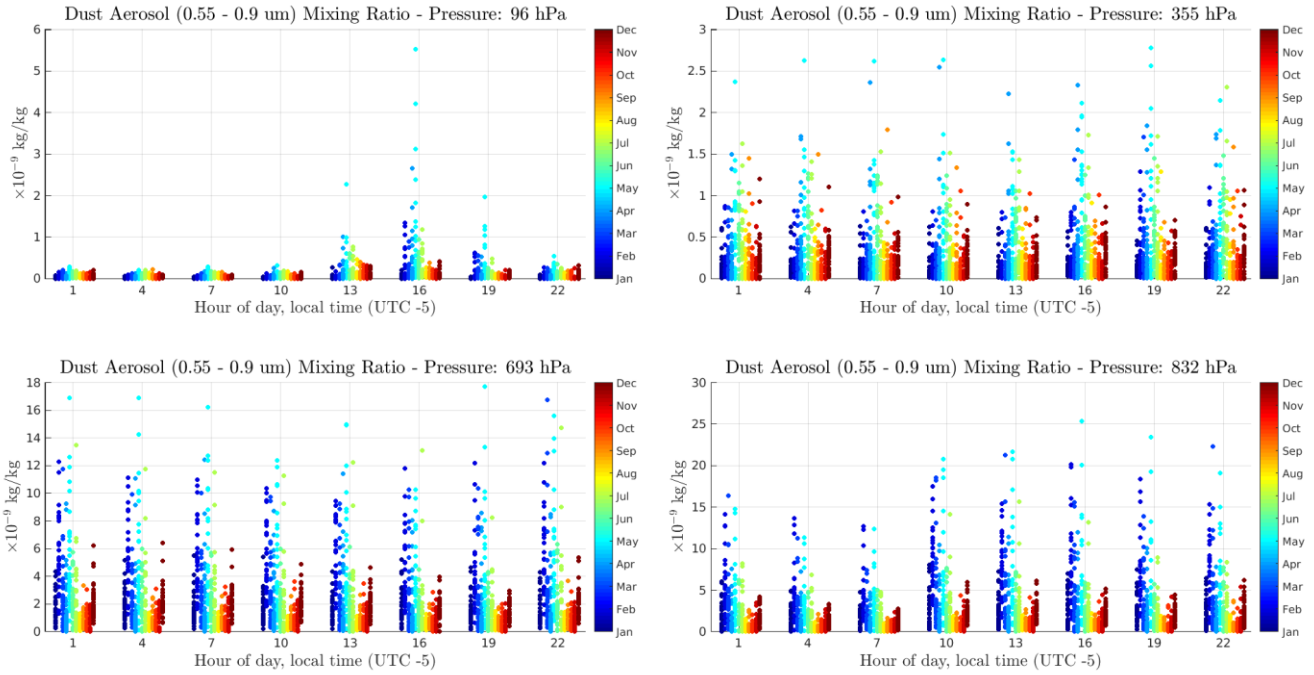

Figure 56: Day cycle plot - dust aerosol (medium)

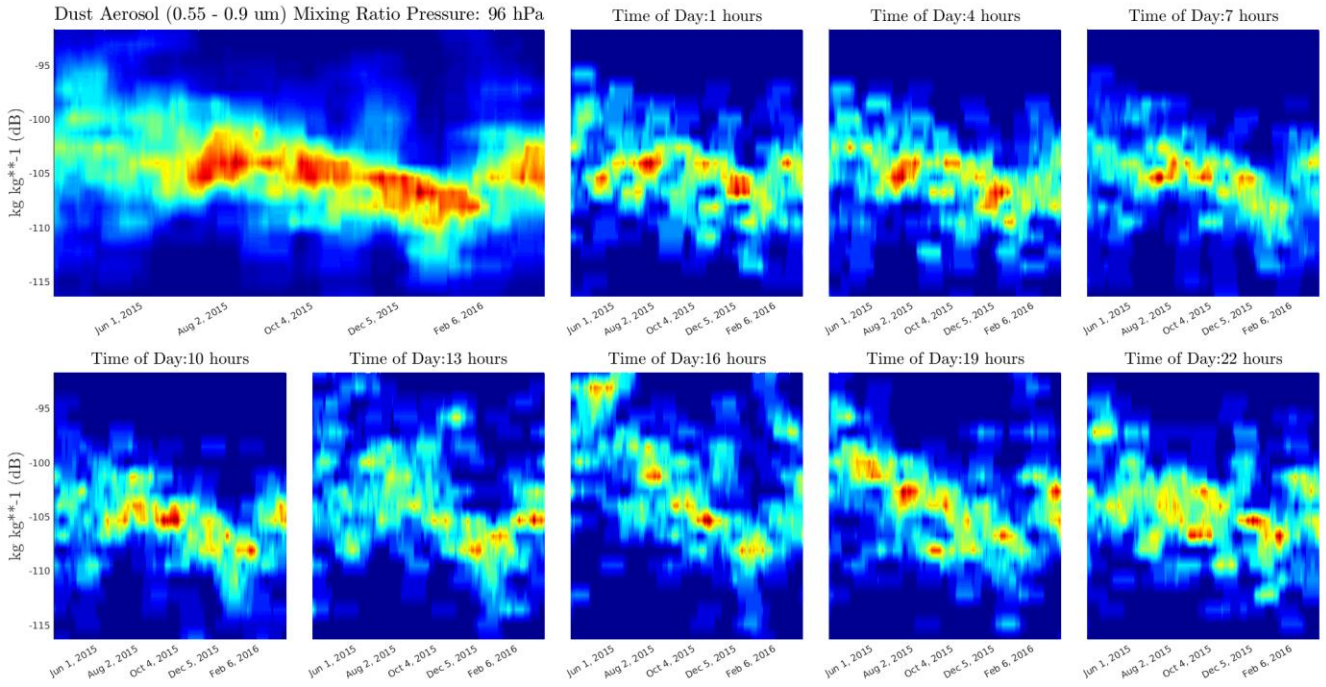

Figure 57: Moving distribution, high layers - Dust aerosol (medium)

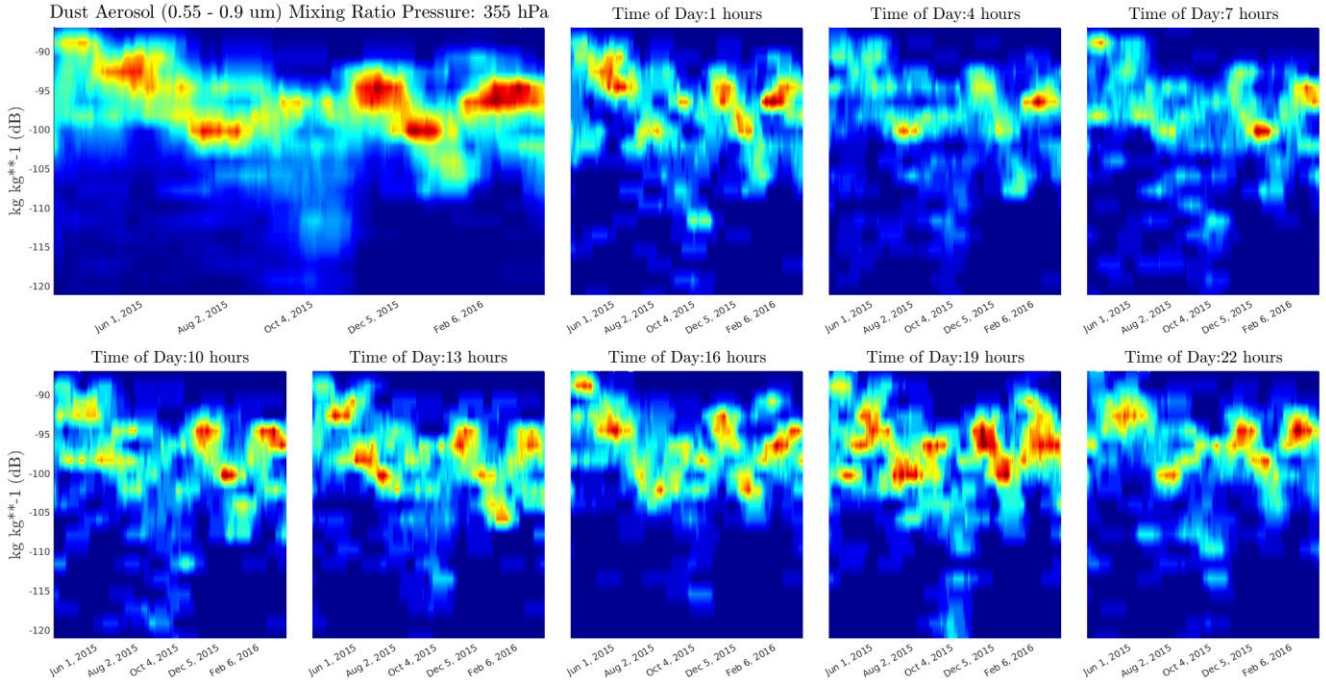

Figure 58: Moving distribution, mid-high layers - Dust aerosol (medium)

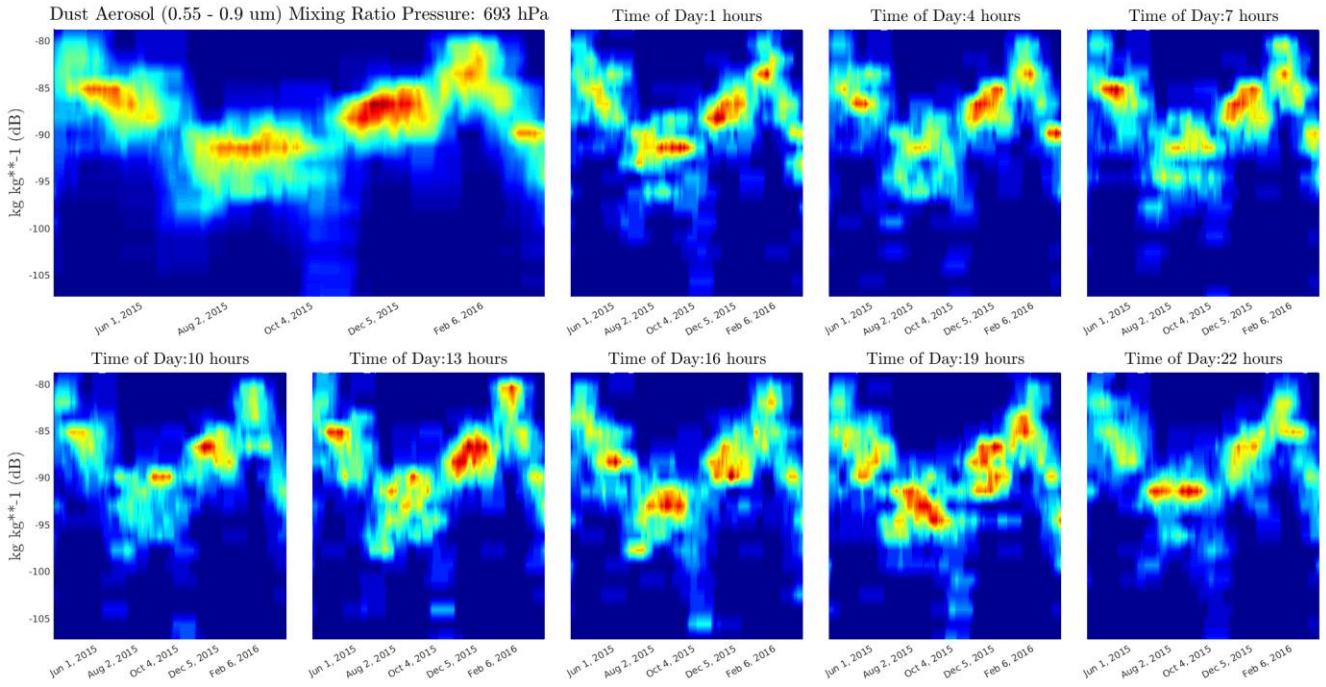

Figure 59: Moving distribution, mid-low layers - Dust aerosol (medium)

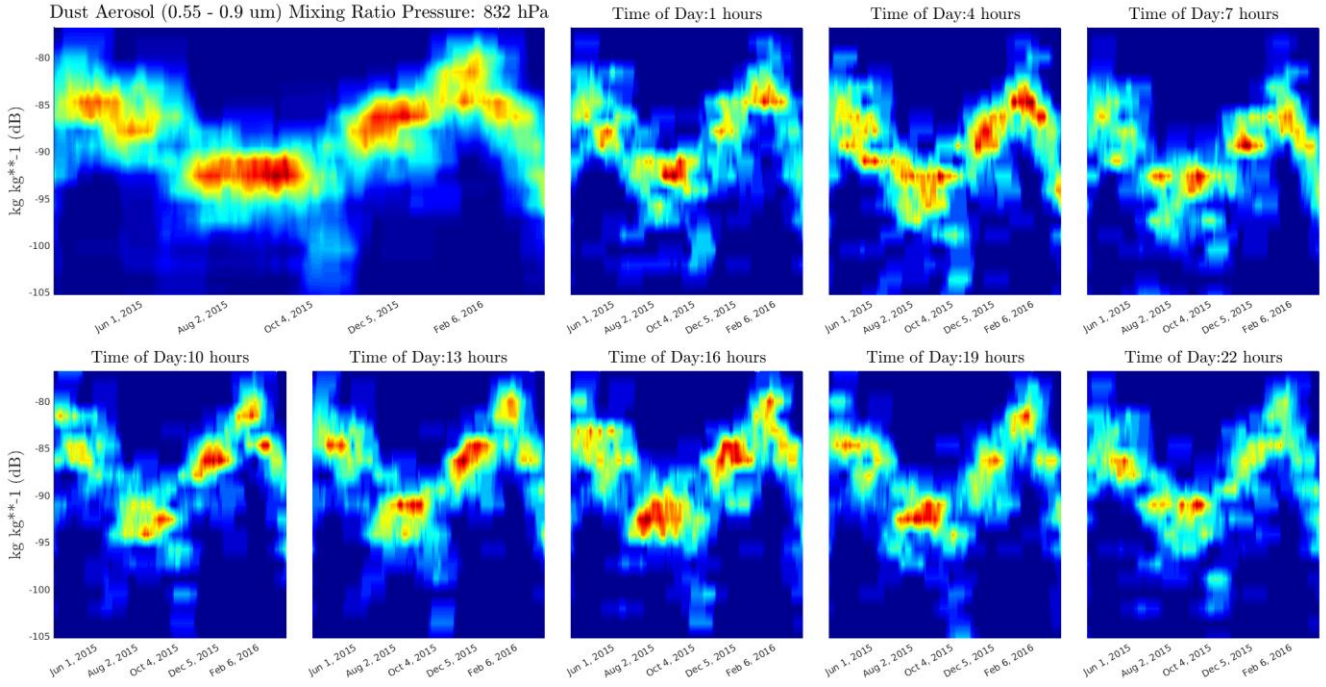

Figure 60: Moving distribution, low layers - Dust aerosol (medium)

11. DUST AEROSOL (0.9 – 20 um) MIXING RATIO

The results of the analyses for large particle size of dust aerosol mixing ratio differs from the results obtained for small and medium particle sizes. The time plot in Figure 61 shows only one event of high concentrations, which occurred between April and August 2015. Additionally, the spectrum plot shows that the main frequency component for surface level is the daily cycle for medium-low altitude layers, it is shown that the main frequency peak corresponds to a lower frequency than the yearly cycle, with important secondary amplitudes for the quarterly and monthly cycles. However, the most of the information is contained in the same pressure range (400 to 900 hPa) as the previous particle sizes.

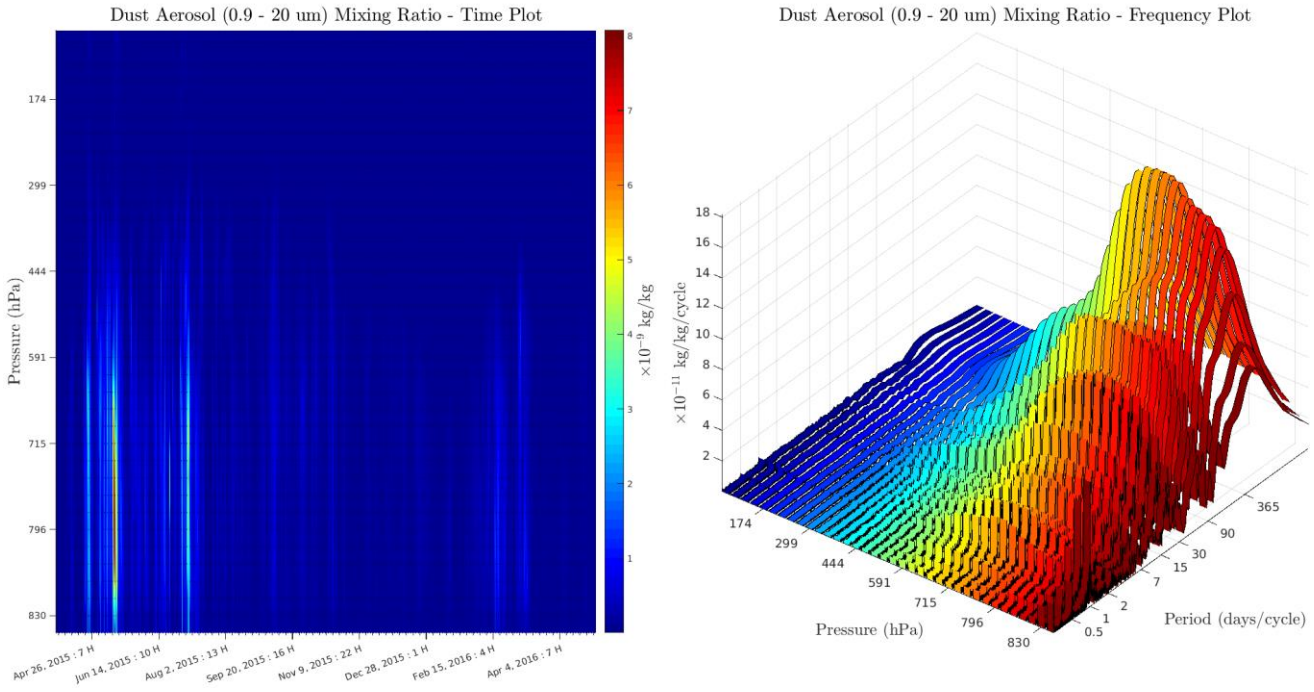

Figure 61: Time and frequency plot for dust aerosol (large).

Figure 62 shows that the daily cycle scatter plots for all pressure levels present a similar yearly distribution: higher values are observed from April to August, whereas the period from October to January exhibits significant lower amplitudes. Mid-high and mid-low layers show independence from the hour of day. High altitude layers present higher concentrations from 1 pm to 7 pm (maximum at 4 pm). Surface level presents higher values from 10 am to 7 pm.

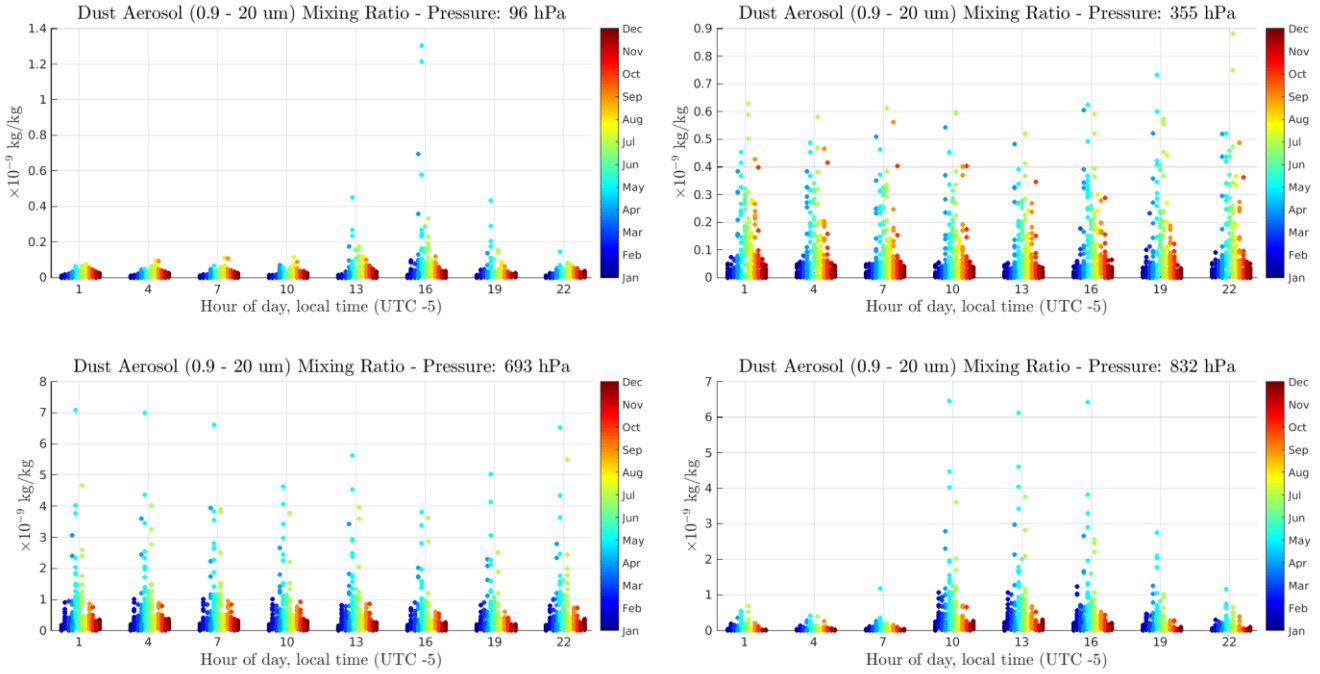

Figure 62: Day cycle plot - dust aerosol (large)

The moving histogram plots for high and mid-high layers (Figures 63 and 64) have a similar structure. Both cases present a reduction of the concentration values around January 2016. However, for mid-high layers (Figure 64), values around June 2015 are slightly higher than the rest.

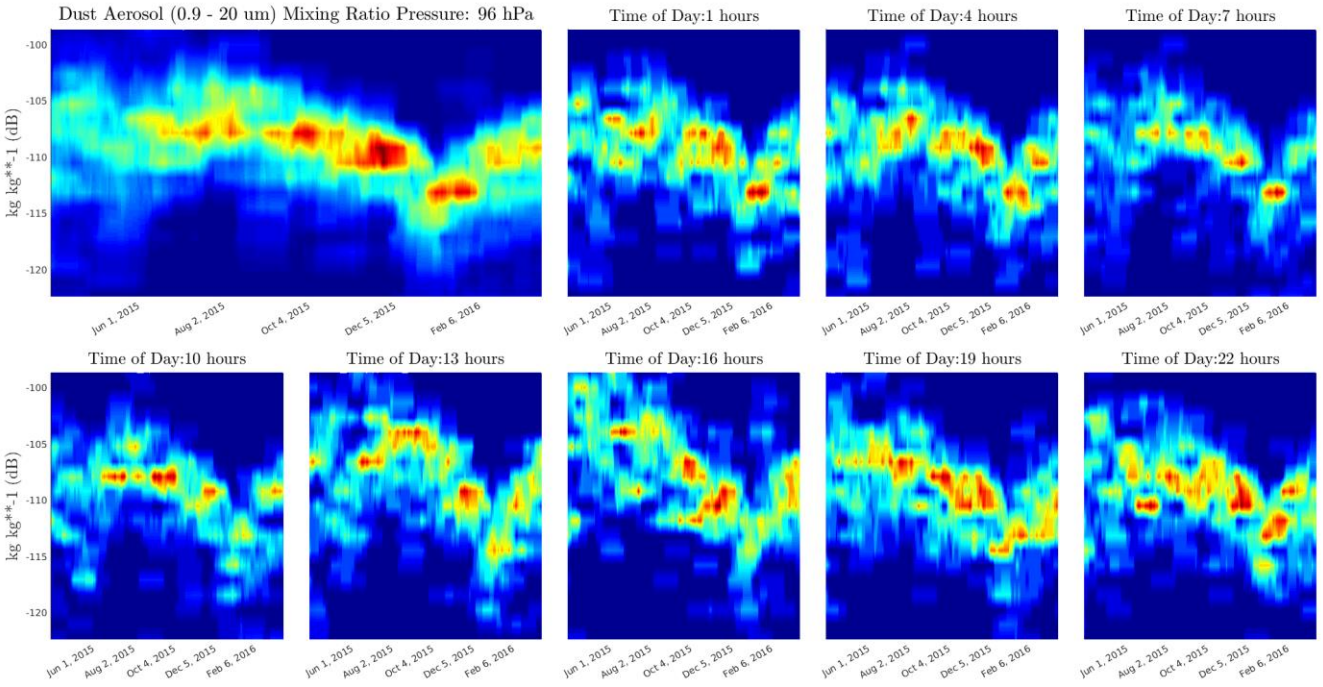

Figure 63: Moving distribution, high layers - Dust aerosol (large)

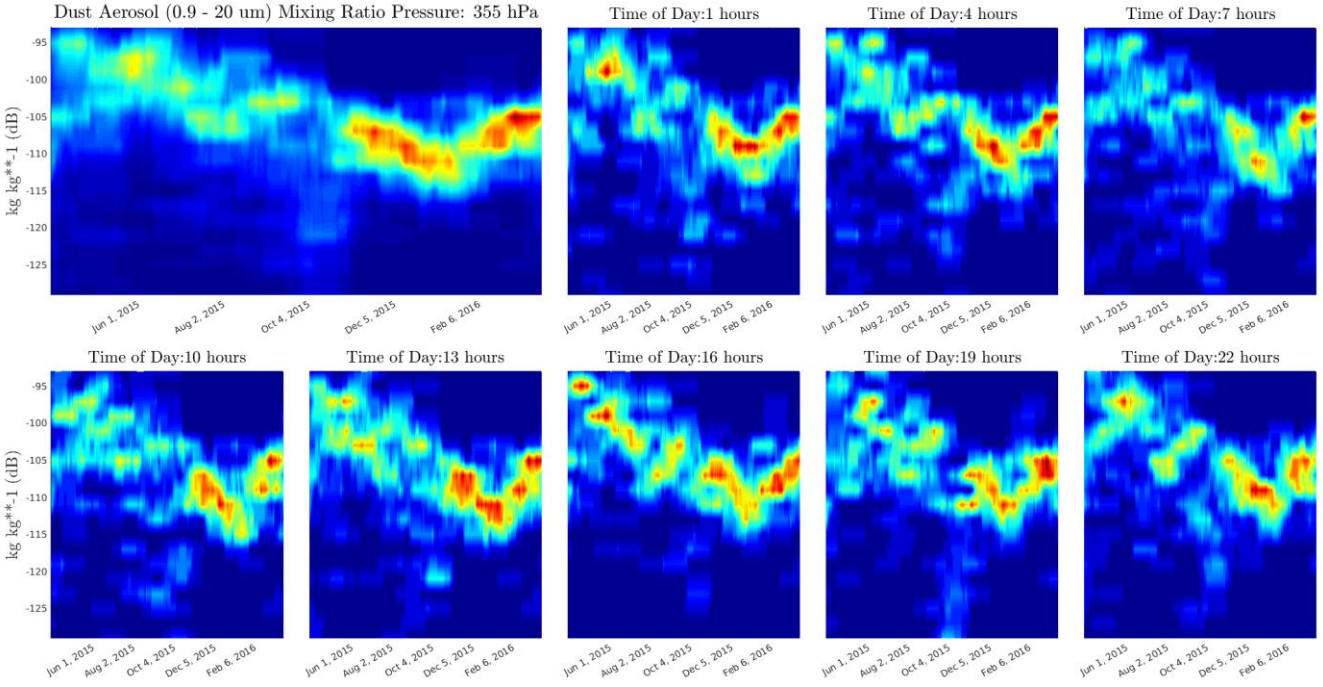

Figure 64: Moving distribution, mid-high layers - Dust aerosol (large)

For mid-low altitudes, Figure 65 shows that from the maximum concentration in April 2015, the mean of the distribution decreases in a sustained manner. However, from January to March 2016 there is a sudden increase, the falls back to continue the decreasing trend.

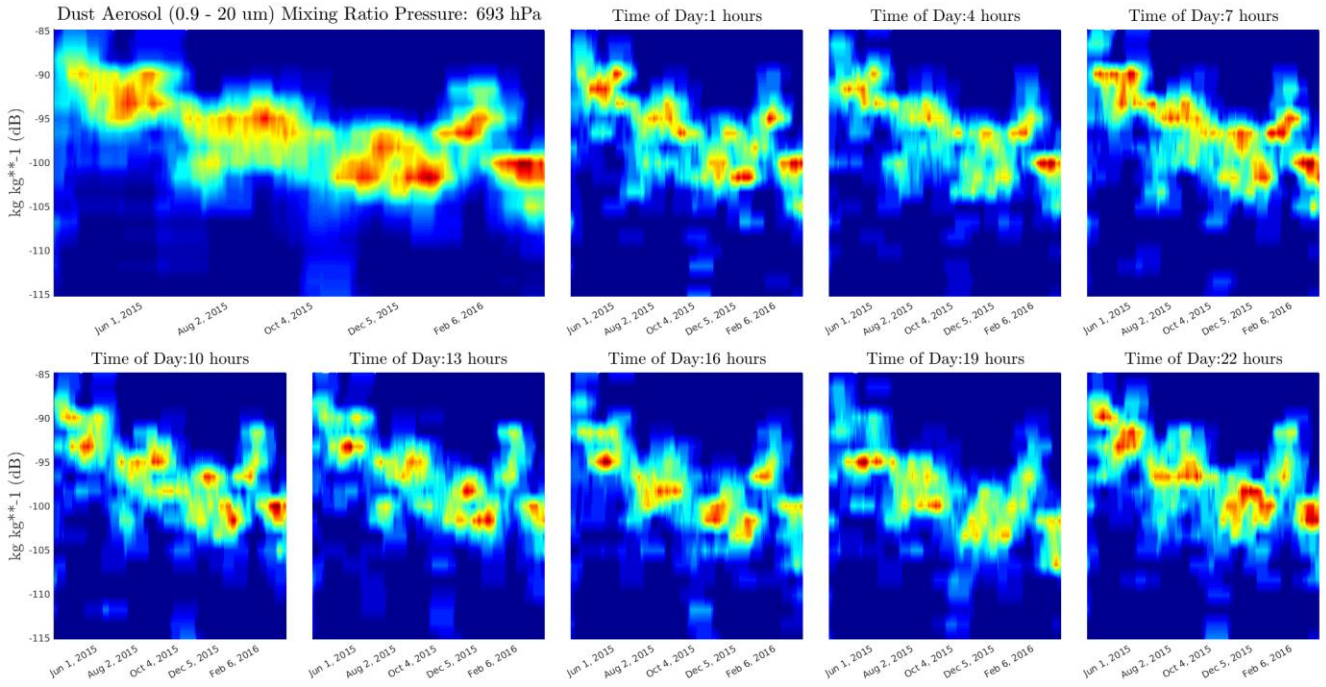

Figure 65: Moving distribution, mid-low layers - Dust aerosol (large)

Figure 66 shows the moving histogram plot for large dust aerosol at surface level. For this case, the hour of day has a high impact on the shape of the distribution. From 1 am to 7 am, values are notably than the rest of the plots, with data points very dispersed in a 25-dB range with no evident trend. For the cases from 10 am to 10 pm, the shape of the distributions resembles that of Figure 65 (for mid-low altitudes), with a monotonically decreasing behavior, except for a sudden peak present around January/February 2016.

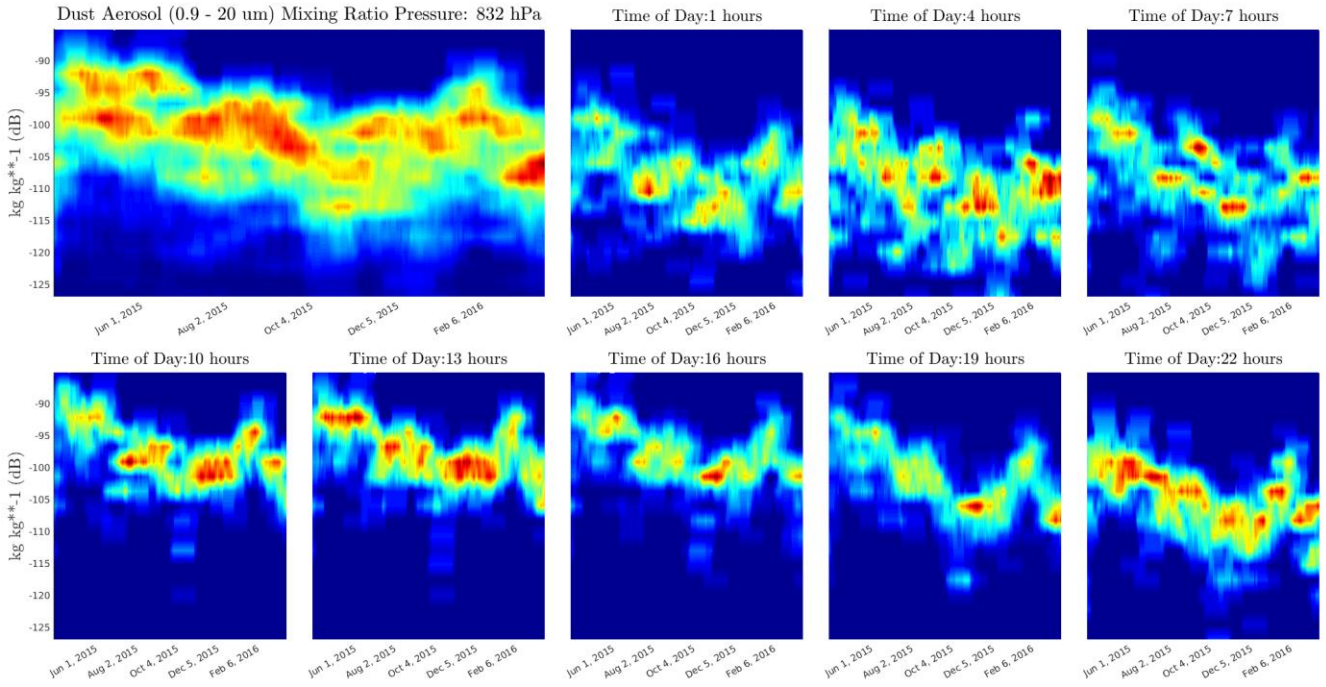

Figure 66: Moving distribution, low layers - Dust aerosol (large)

12. SULPHATE AEROSOL MIXING RATIO

The time and frequency plot for the mixing ratio of sulphate aerosol is shown in Figure 67. Most of the information is contained between surface and mid-high altitudes (approx. 300 hPa to 900 hPa). The time plot shows that an important concentration event was detected between January and May 2016. From the frequency plot, it can be seen that the range 700 – 900 hPa is characterized by low frequency components (yearly cycle), with secondary peaks corresponding with the quarterly and monthly cycles. The surface layer also presents a visible daily cycle component. Also, the mid-high layers (300-700 hPa) are characterized solely by low frequency components.

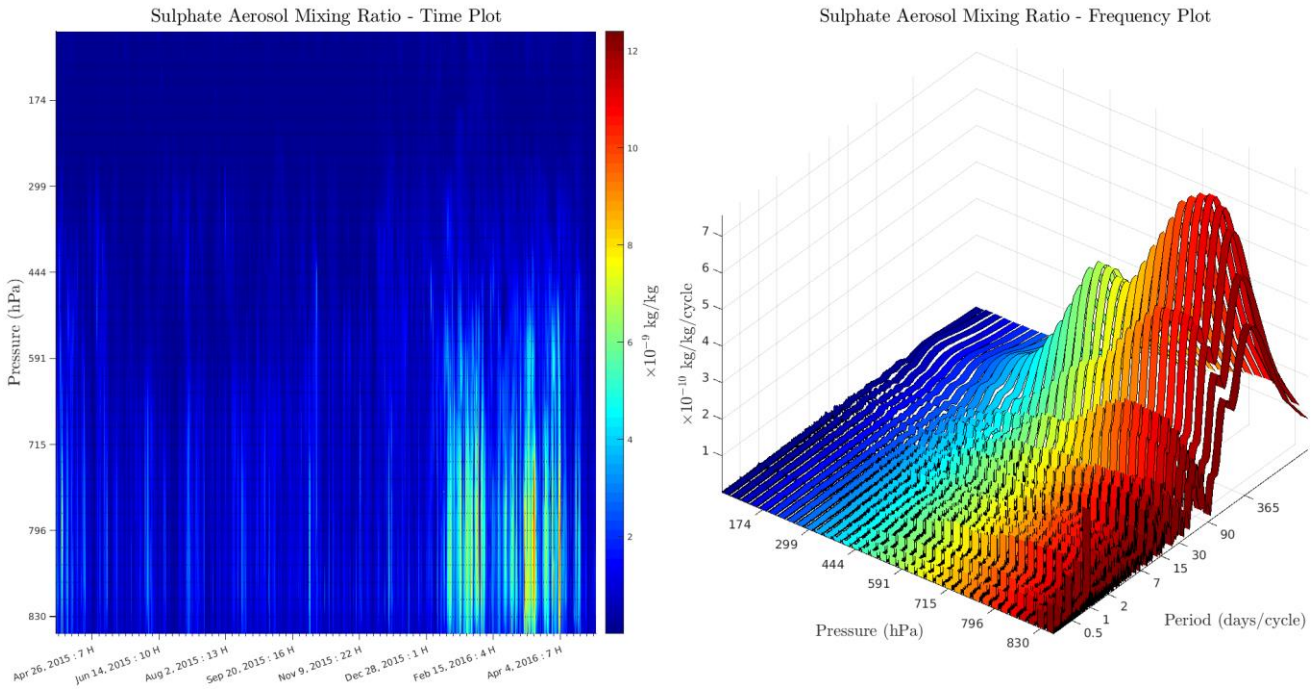

Figure 67: Time and frequency plot for sulphate aerosol.

Figure 68 shows the day cycle scatter plot for sulphate aerosol mixing ratio. For high altitudes, there is no clear distribution for the variable concentration in neither month of year or time of day; there some isolated singular values dispersed over different months. For mid-high altitudes (355 hPa), there are peaks of high values between December and April, and data seems independent of hour of day. Low and mid-low altitudes present significantly higher values of concentration between January and April. However, mid-low layers appear to be independent of hour of day, whereas surface level shows increased values between 10 am and 10 pm.

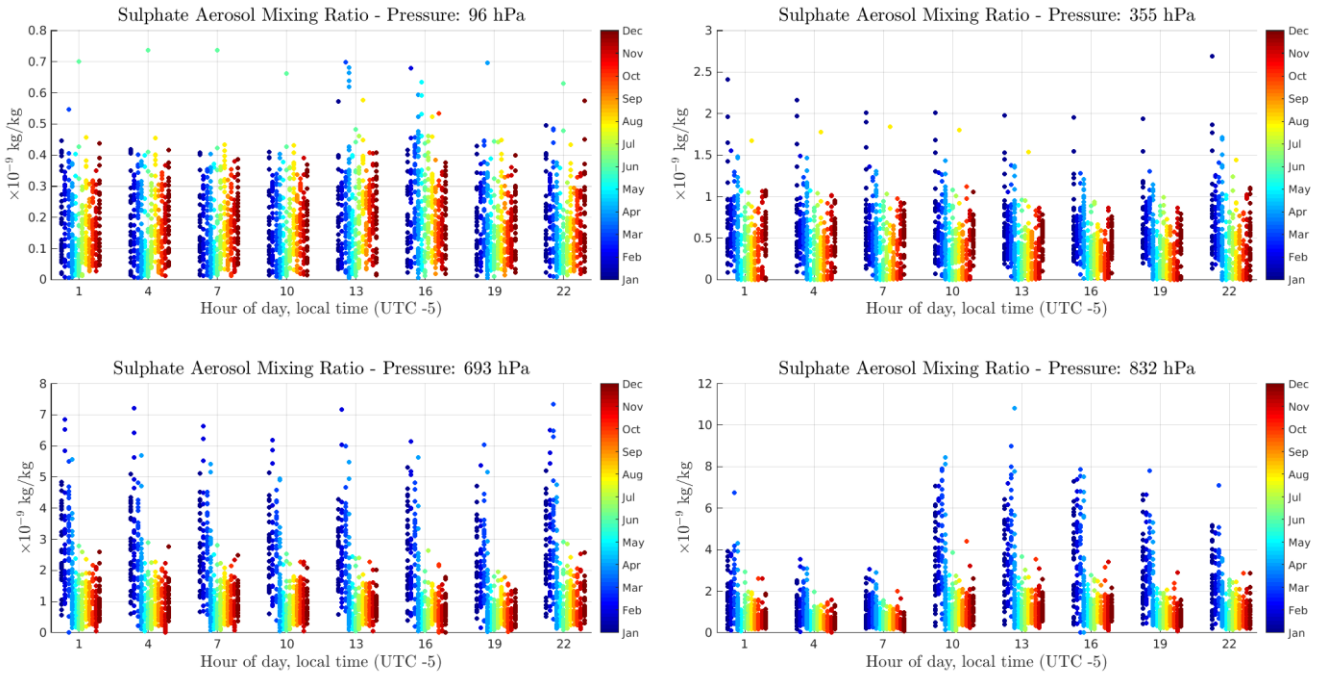

Figure 68: Day cycle plot - sulphate aerosol

The moving histogram plot for high altitude concentrations of sulphate aerosol is shown in Figure 69. The lower concentration values are found between April and June 2015. After this period, the distribution of data does not vary noticeably.

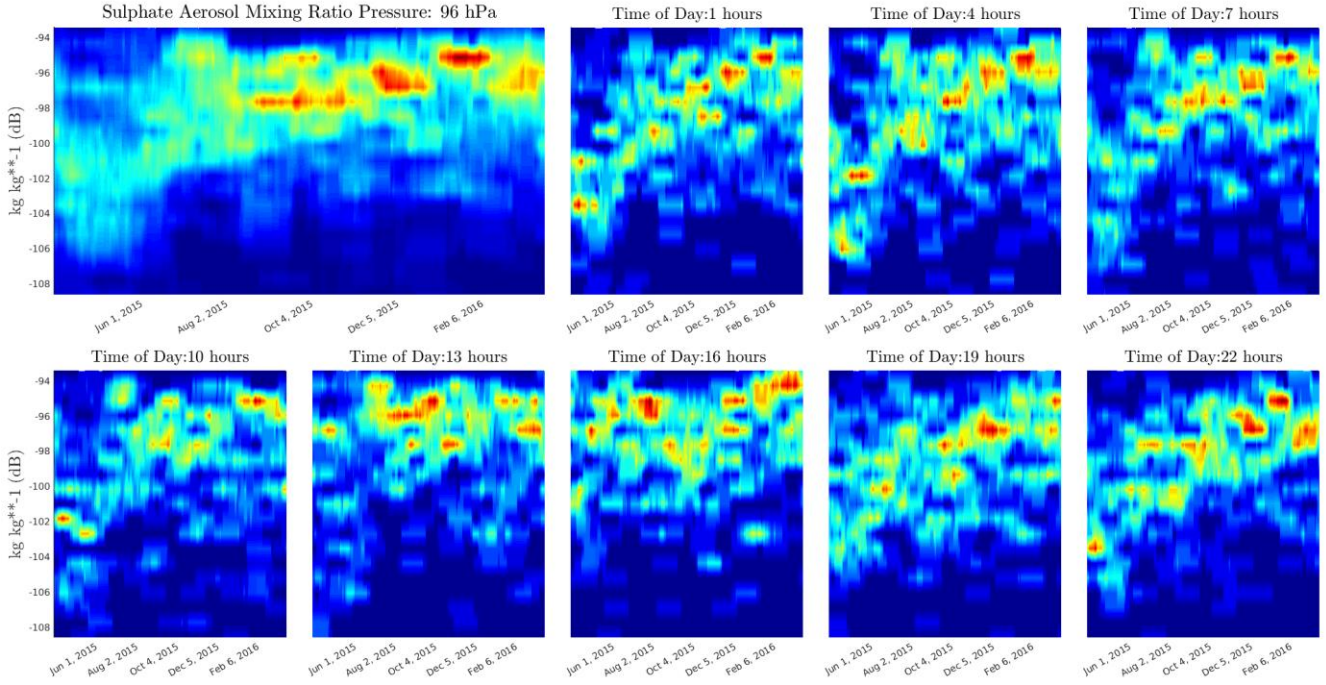

Figure 69: Moving distribution, high layers - Sulphate aerosol

The concentration distribution for mid-high layers (Figure 70) shows that the region of maximum probability is constant throughout the year. However, the period from April to December 2015 presents a higher deviation, and there exist probability to obtain low concentration values. After December 2015, data dispersion is significantly reduced, and all data points are found in a region of high concentrations.

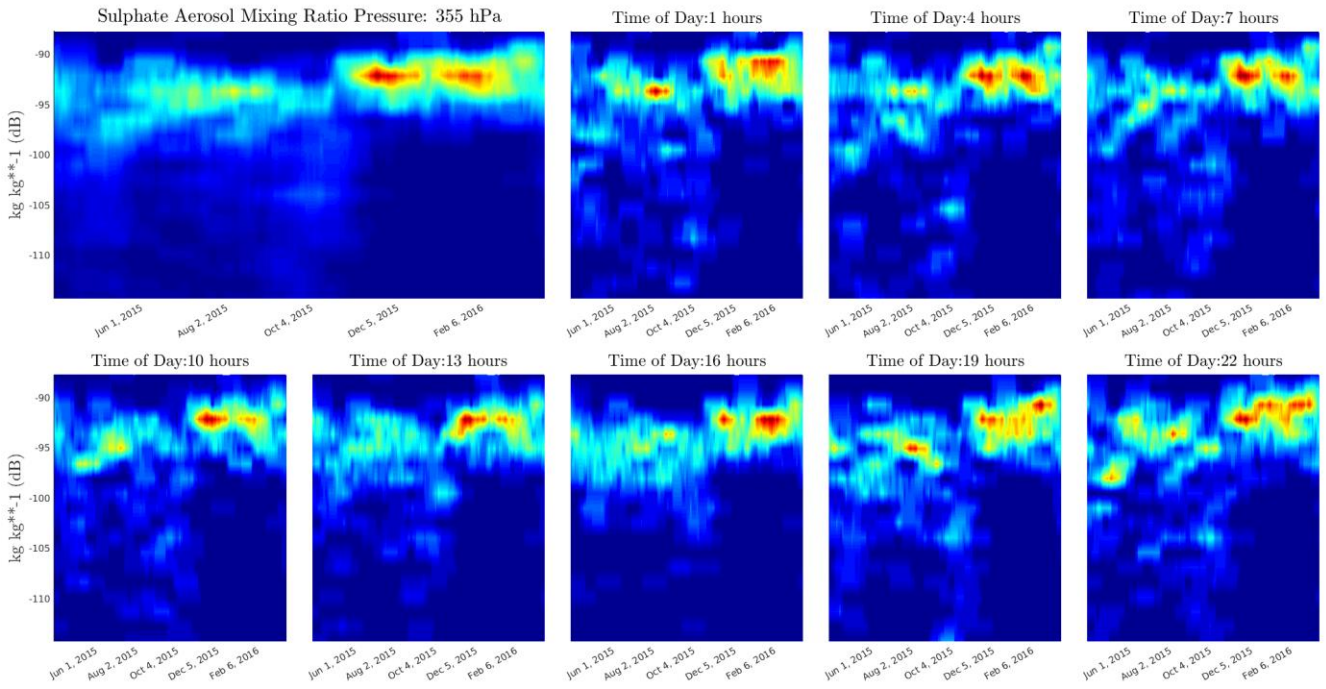

Figure 70: Moving distribution, mid-high layers - Sulphate aerosol

The moving histogram plots for mid-low and surface levels (Figures 71 and 72) share the same distribution shapes. There is a sudden increase in the values of concentration after December 2015. For surface level (Figure 72), the different hours of day present the same distribution, albeit with different mean values.

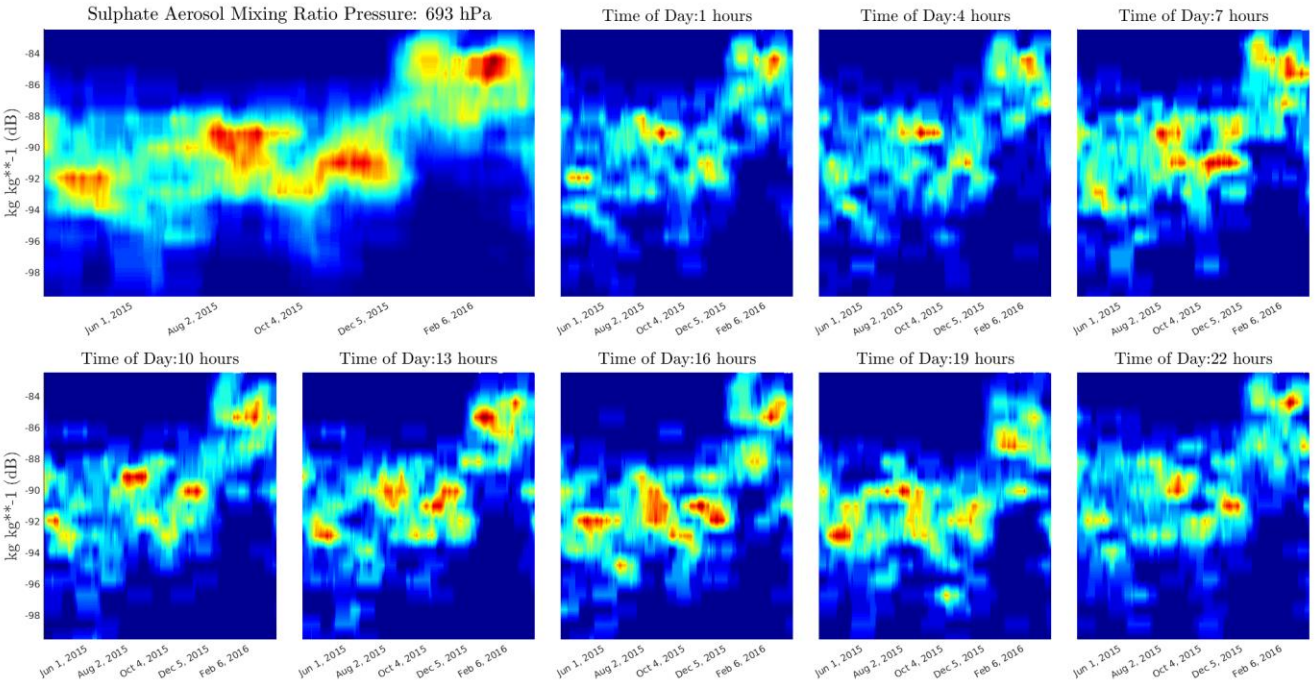

Figure 71: Moving distribution, mid-low layers - Sulphate aerosol

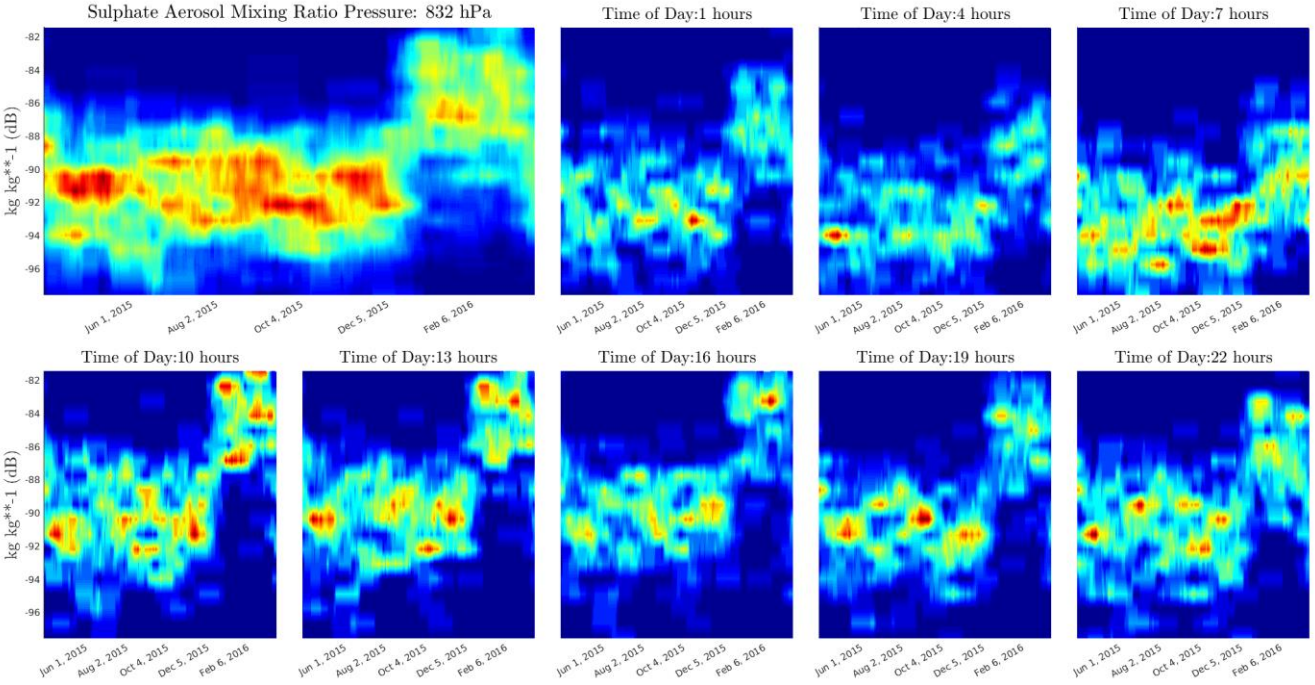

Figure 72: Moving distribution, low layers - Sulphate aerosol

13. HYDROPHOBIC ORGANIC MATTER MIXING RATIO

As seen in Figure 73, most of the information for hydrophobic organic matter aerosol mixing ratio is contained between low and mid altitude layers (approx. 500 – 900 hPa). The time plot shows a high concentration event between March and April 2016. The frequency plot shows that this variable is mainly characterized by low frequencies.

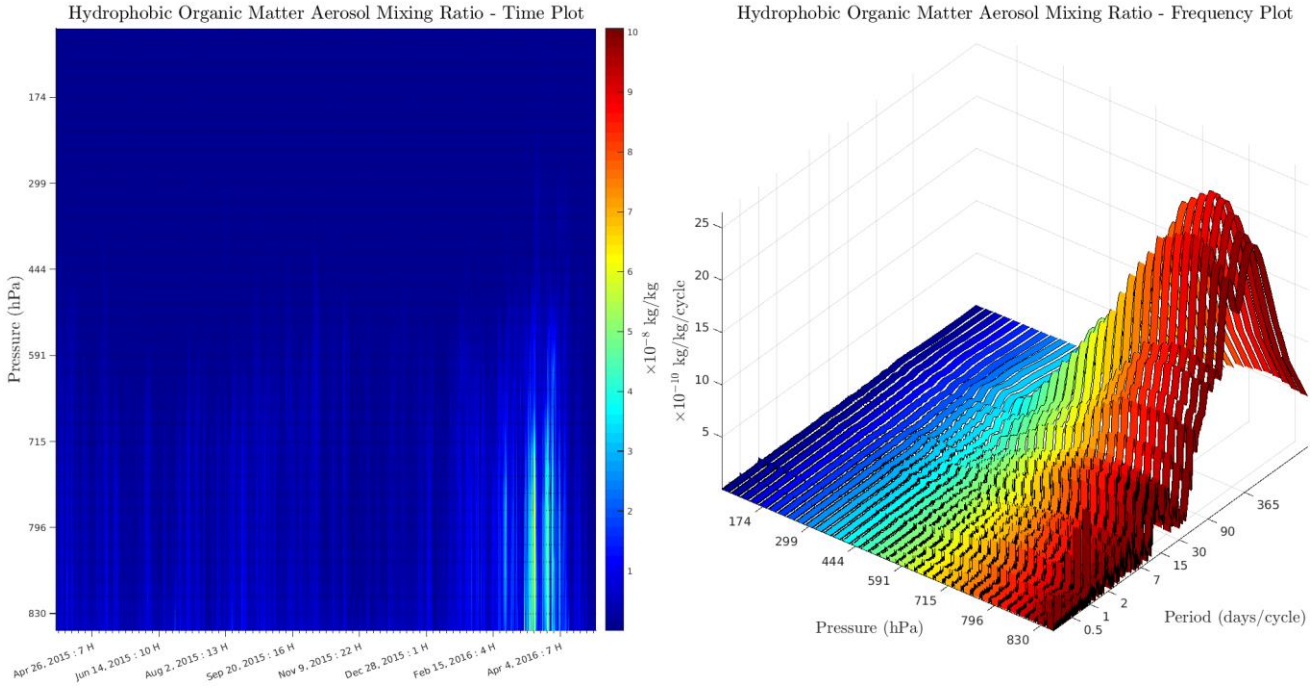

Figure 73: Time and frequency plot for hydrophobic organic matter aerosol

The day cycle plots in Figure 74 show that for all pressures, the highest peak values where obtained between March and May. At high altitudes, it is shown that the variable has a day cycle dependence, as higher values are present from 1 pm to 7 pm. For the remaining pressure levels (300-900 hPa), the structure of the plots is similar, showing little influence by the hour of day.

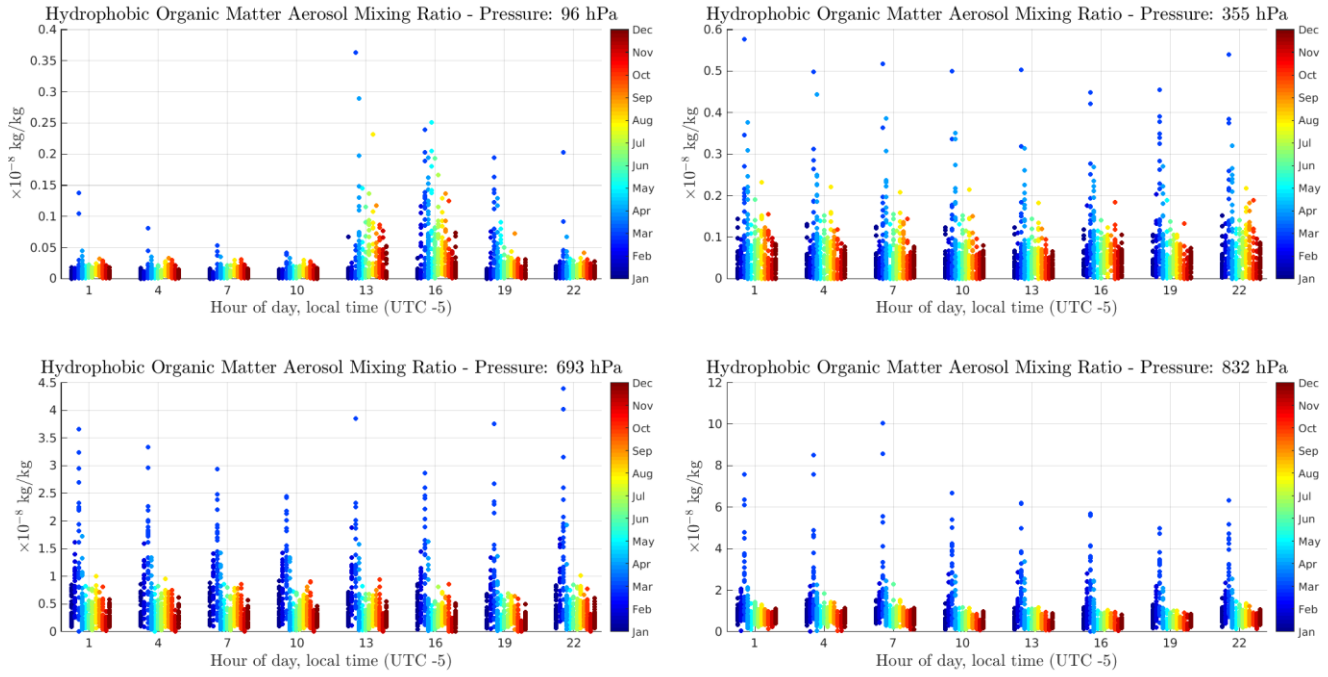

Figure 74: Day cycle plot - hydrophobic organic matter aerosol

Figure 75 shows that for high altitudes, two minimum peaks found at May 2015 and January 2016 are found. Also, the highest concentration values distribution is found at 4 pm.

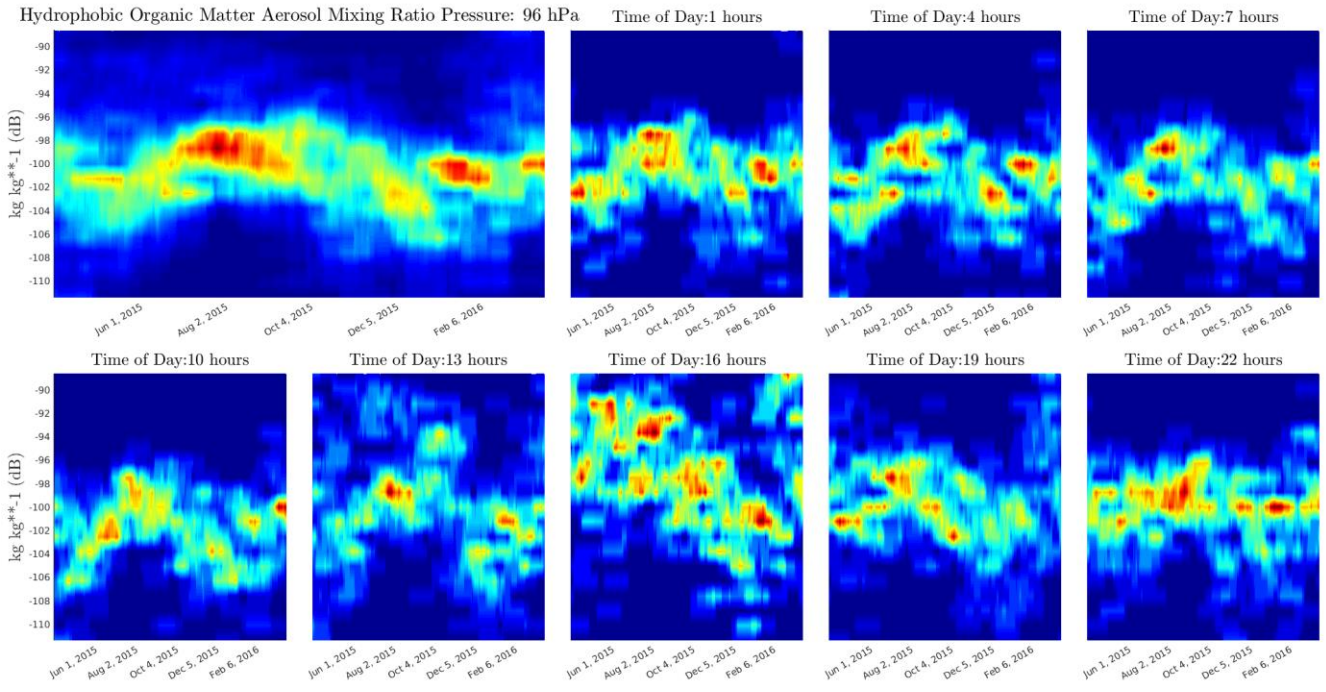

Figure 75: Moving distribution, high layers - Hydrophobic organic matter aerosol

Figures 76 through 78 for pressure layers between 300 and 900 hPa are similar. All of them present minimum peaks at May and October 2015, and a sudden maximum peak at February 2016.

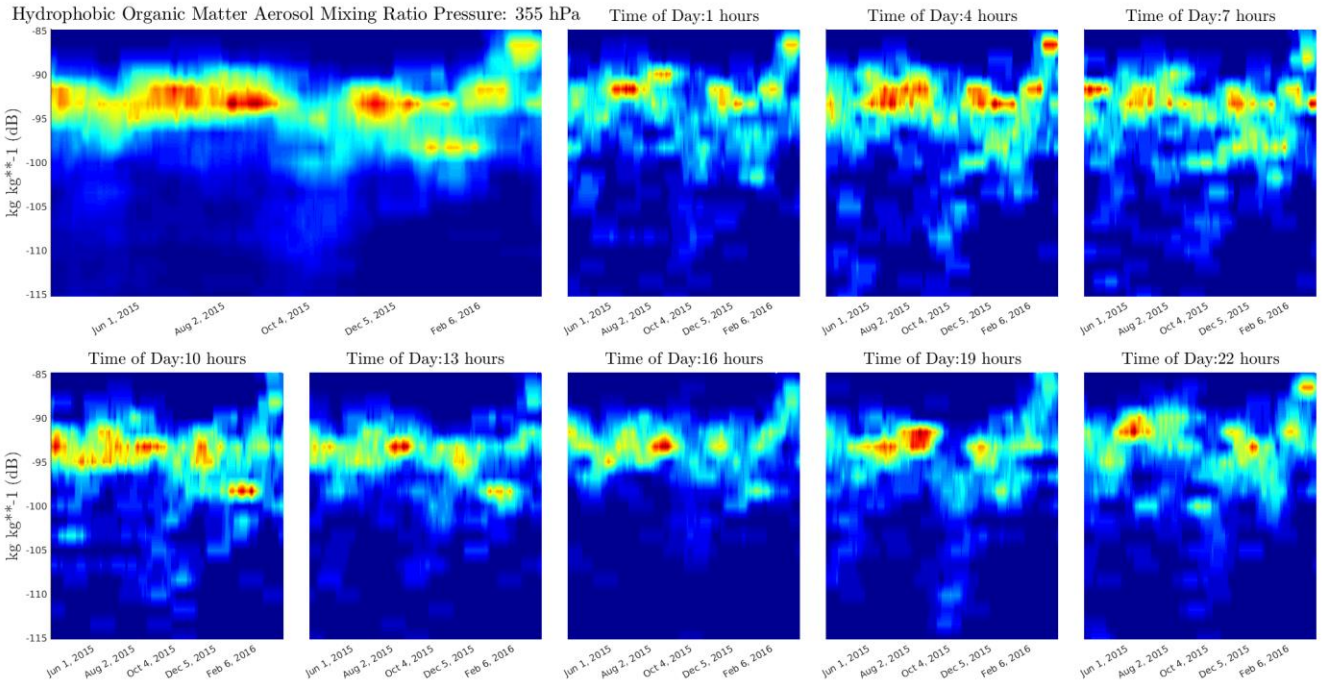

Figure 76: Moving distribution, mid-high layers - Hydrophobic Organic matter aerosol

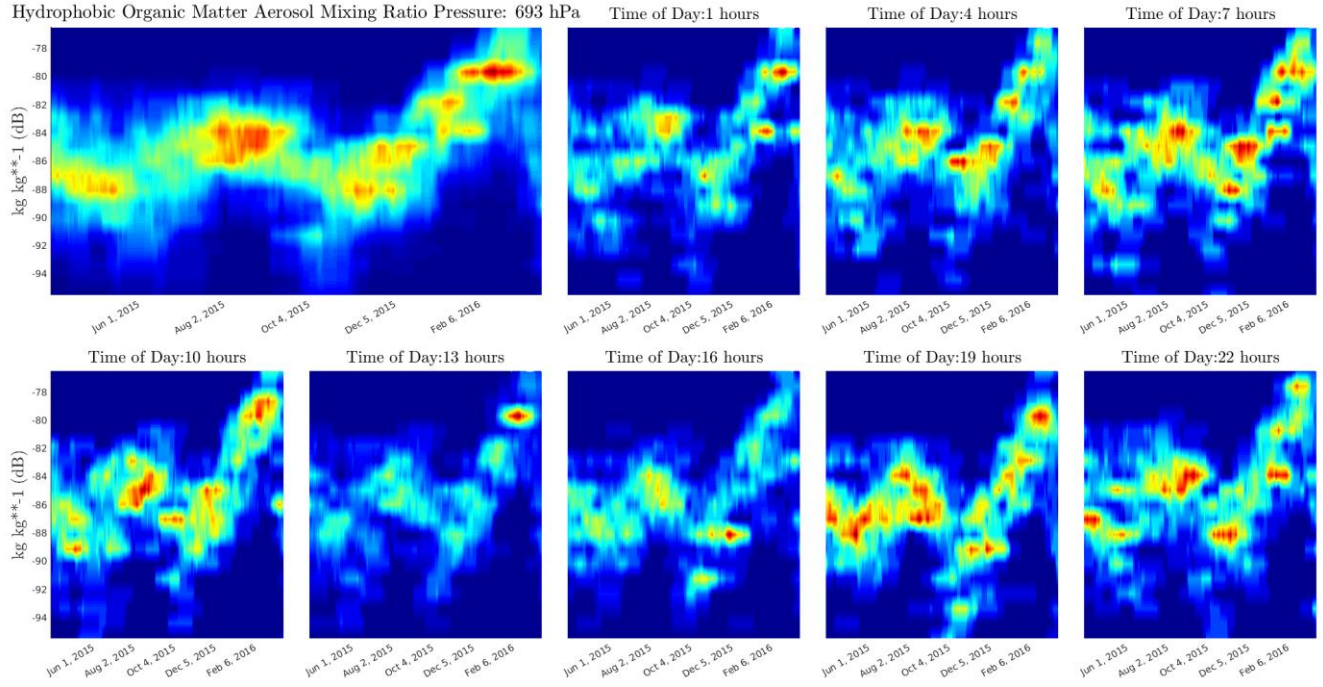

Figure 77: Moving distribution, mid-low layers - Hydrophobic organic matter aerosol

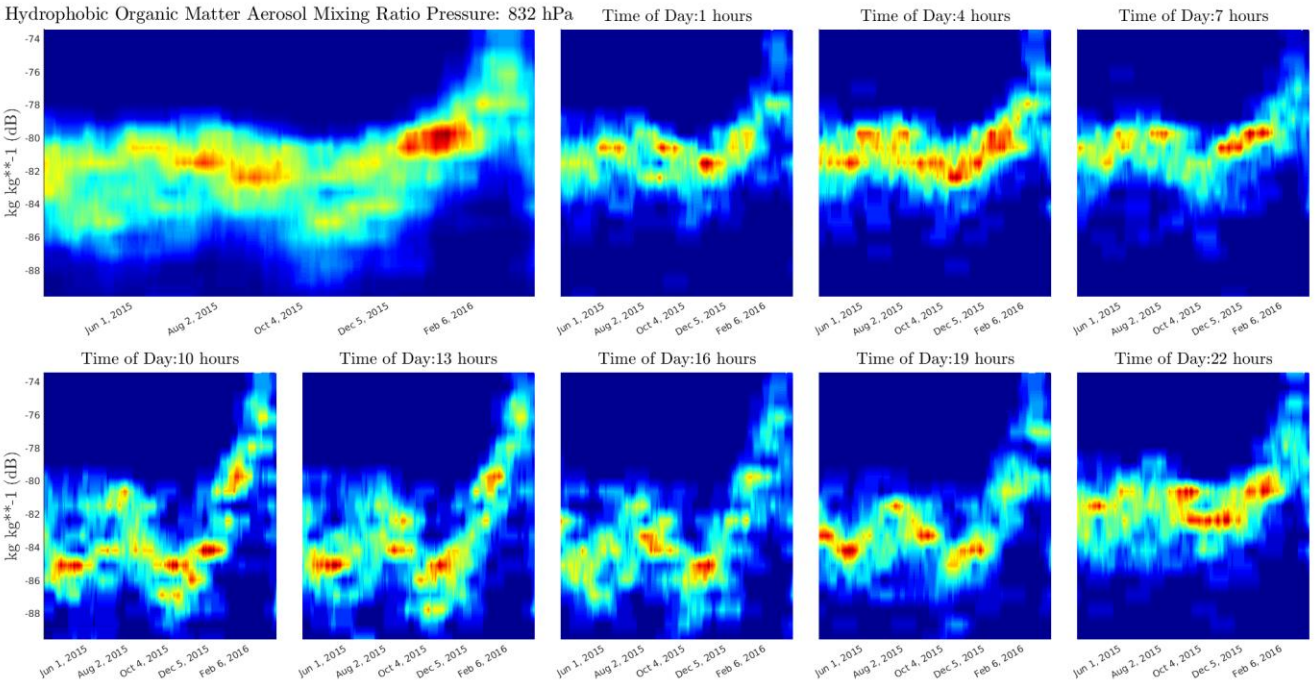

Figure 78: Moving distribution, low layers - Hydrophobic organic matter aerosol

14. HYDROPHILIC ORGANIC MATTER AEROSOL MIXING RATIO

The time and frequency plots for hydrophilic organic matter in Figure 79 show that the most of the information is contained between low and mid-low altitudes (600 – 900 hPa). Surface layers are characterized by daily frequencies with secondary low frequency components (yearly). Mid-low altitudes lack the daily components and are mainly characterized by yearly and lower frequencies.

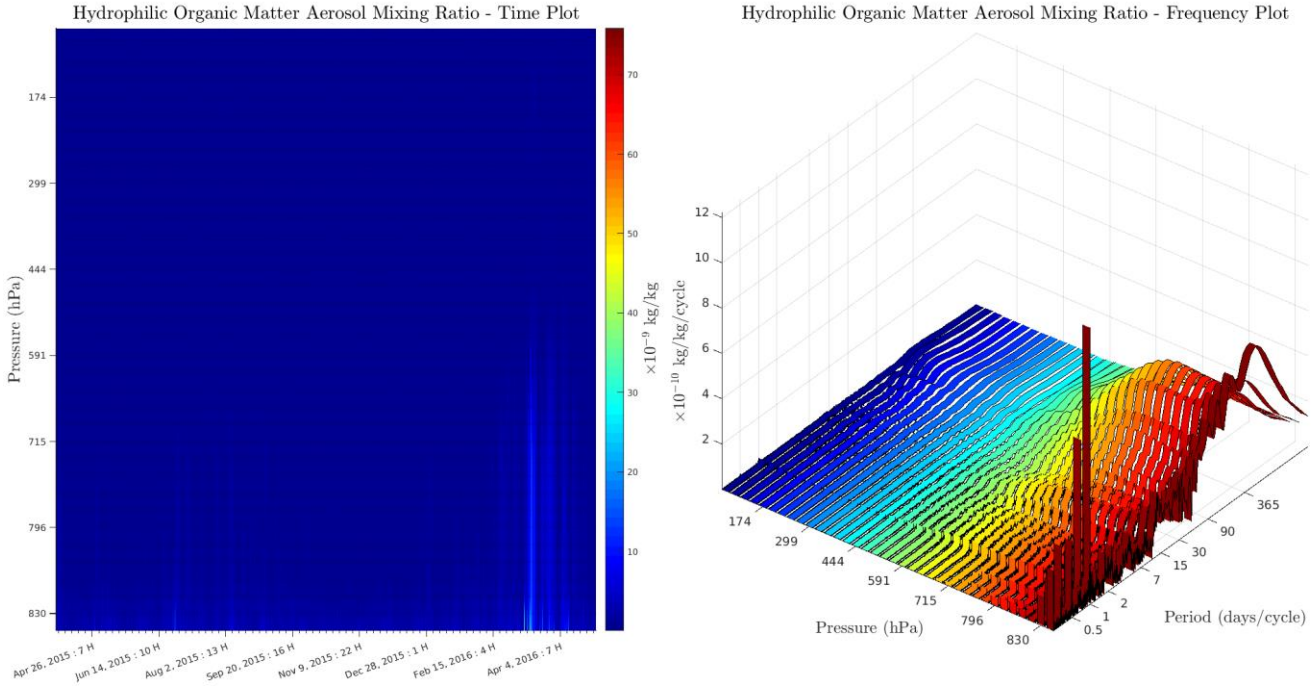

Figure 79: Time and frequency plot for hydrophilic organic matter aerosol.

Figure 80 shows the scatter plots for hydrophilic organic matter. For high altitudes, the higher concentration values are registered between May and August, specially between 1 pm and 10 pm; however, isolated asymptotically high cases are presented in March and April. This behavior is also seen for mid-high layers, albeit without the hour of day dependence.

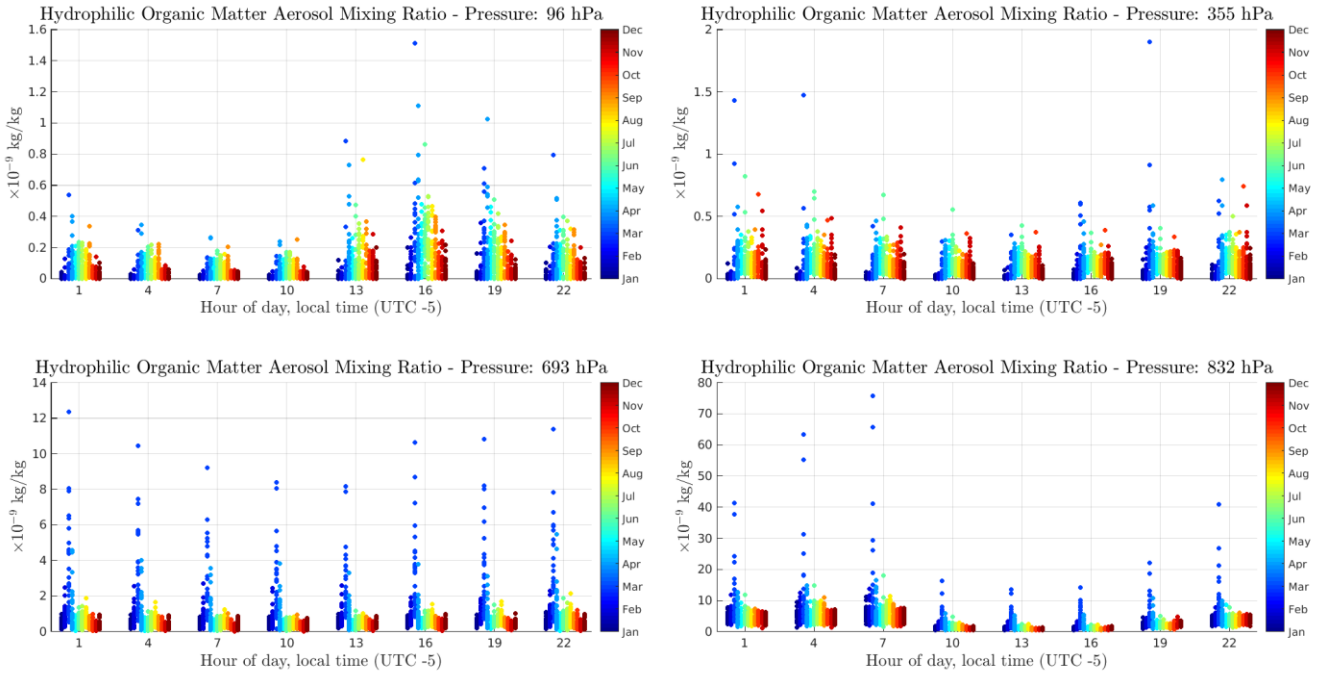

Figure 80: Day cycle plot - hydrophilic organic matter aerosol.

For low and mid-low altitudes, maximums are located between February and April, with especially high values during March. Surface layer shows hour of day dependence, with higher concentrations during night time (7 pm to 7 am).

The moving histogram plots for high and mid-high altitudes (Figures 81 and 82) have a similar behavior: from April 2015 until November 2015 there is a seemingly constant data distribution throughout time. However, after November 2015, the distribution is monotonically decreasing until it reaches a minimum at February 2016. Afterwards, the distribution begins to increase until it reaches its normal mean value after January 2016.

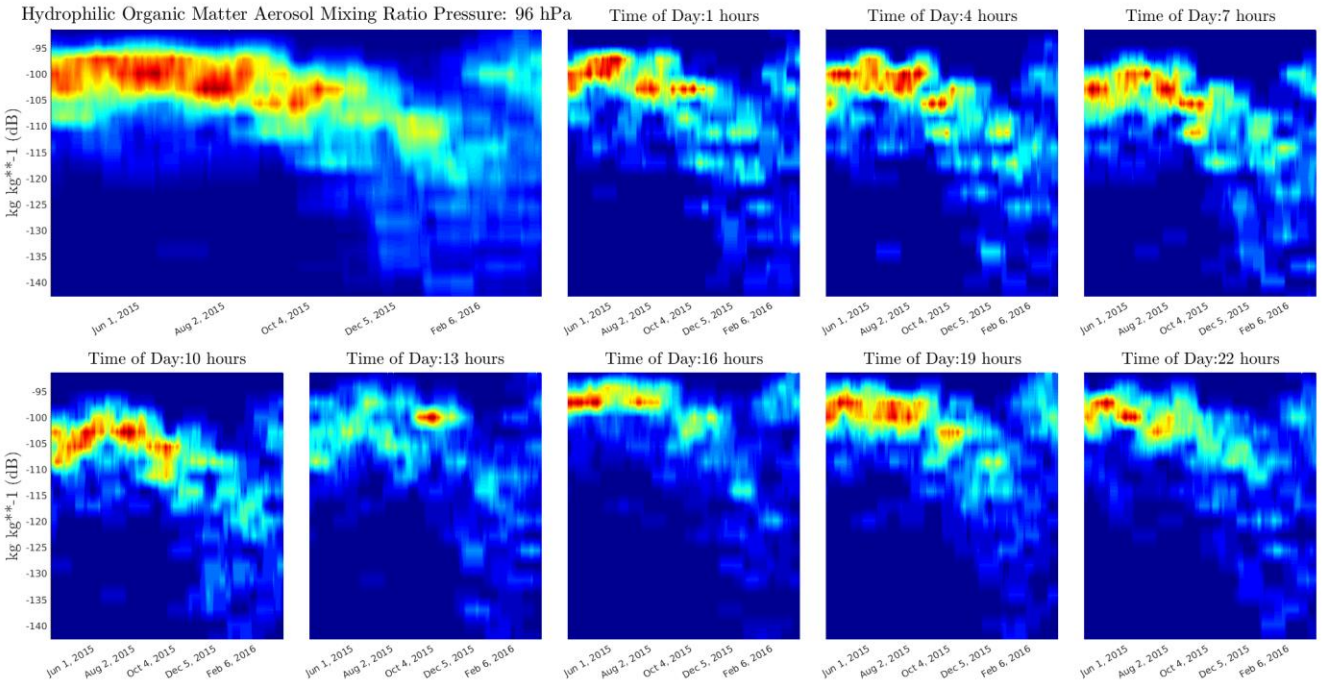

Figure 81: Moving distribution, high layers - Hydrophilic organic matter aerosol

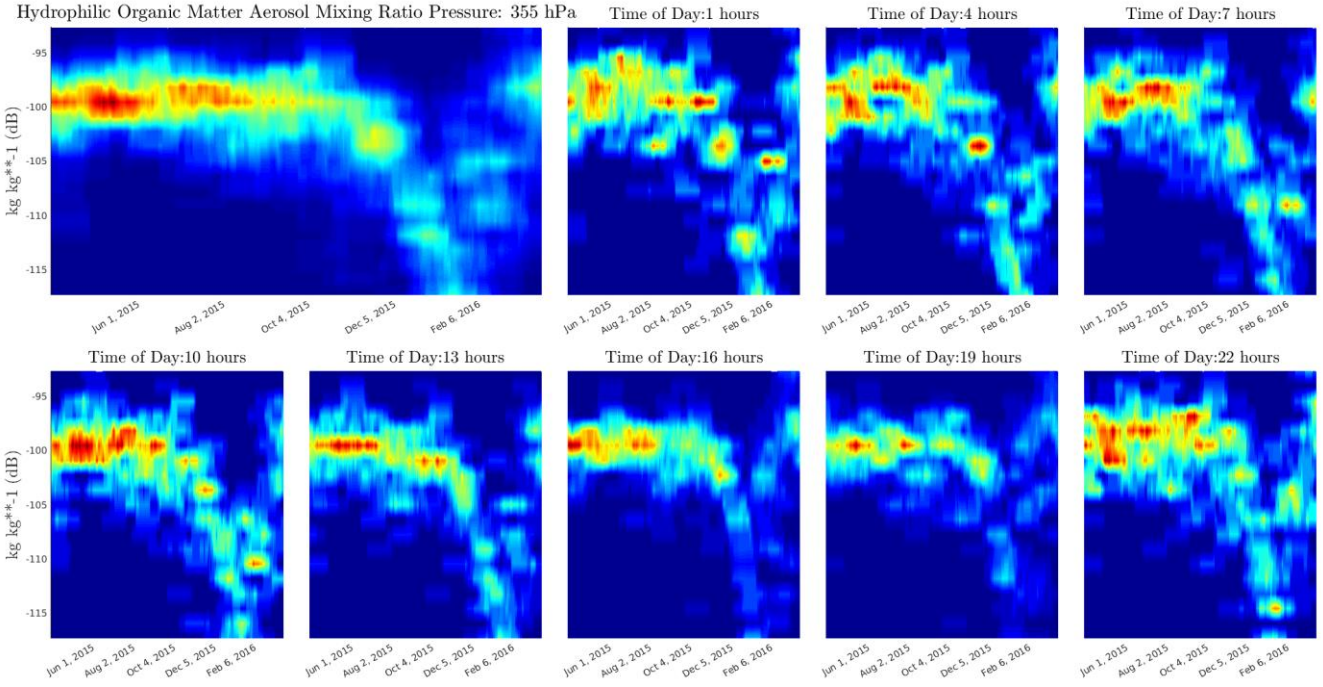

Figure 82: Moving distribution, mid-high layers - Hydrophilic Organic matter aerosol

The behavior of hydrophilic organic matter for mid-low altitudes (Figure 83) is drastically different from the previous cases. The period from April 2015 to December 2015 contains a small maximum during August. After December 2015, the distribution begins to increase rapidly, until it reaches an absolute peak at January 2016.

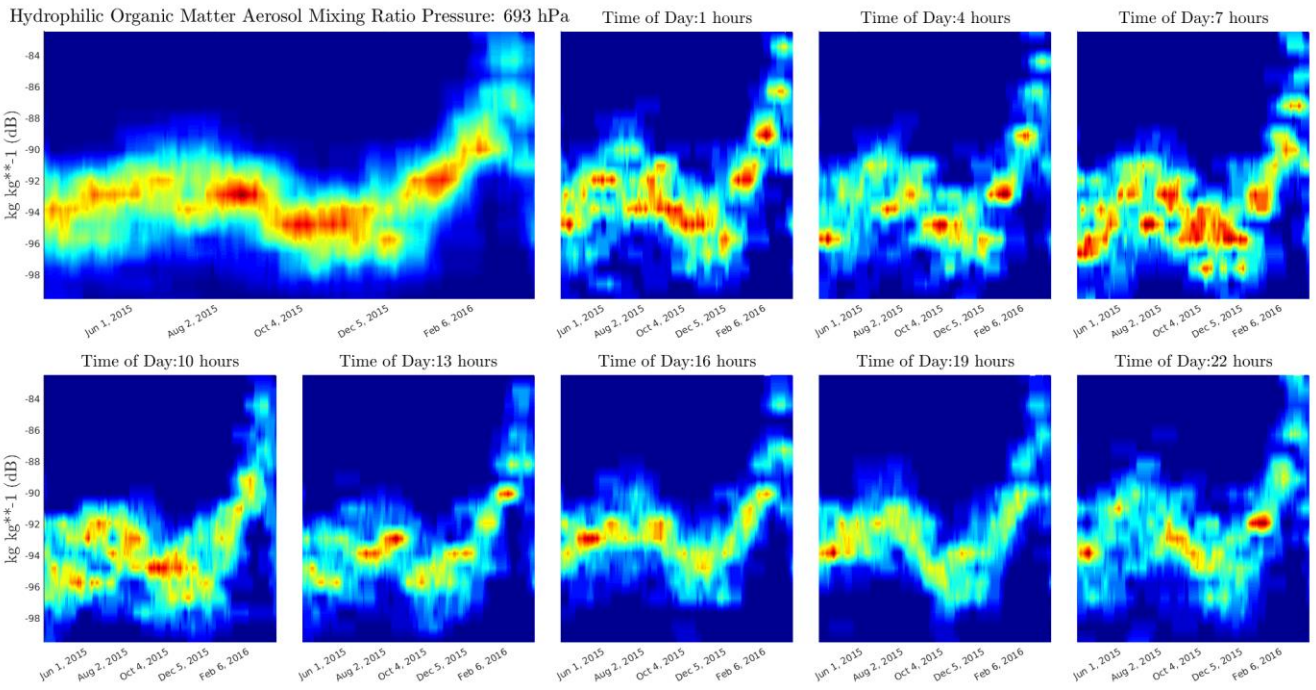

Figure 83: Moving distribution, mid-low layers - Hydrophilic organic aerosol

Figure 84 shows a clear daily-cycle behavior for the surface layer. From 7 pm to 7 am, the distributions are constant throughout the year, with higher values shown from 1 am to 7 am. From 10 am to 4 pm, concentration mean value is lower and follows the same behavior described for mid-low altitudes (Figure 83).

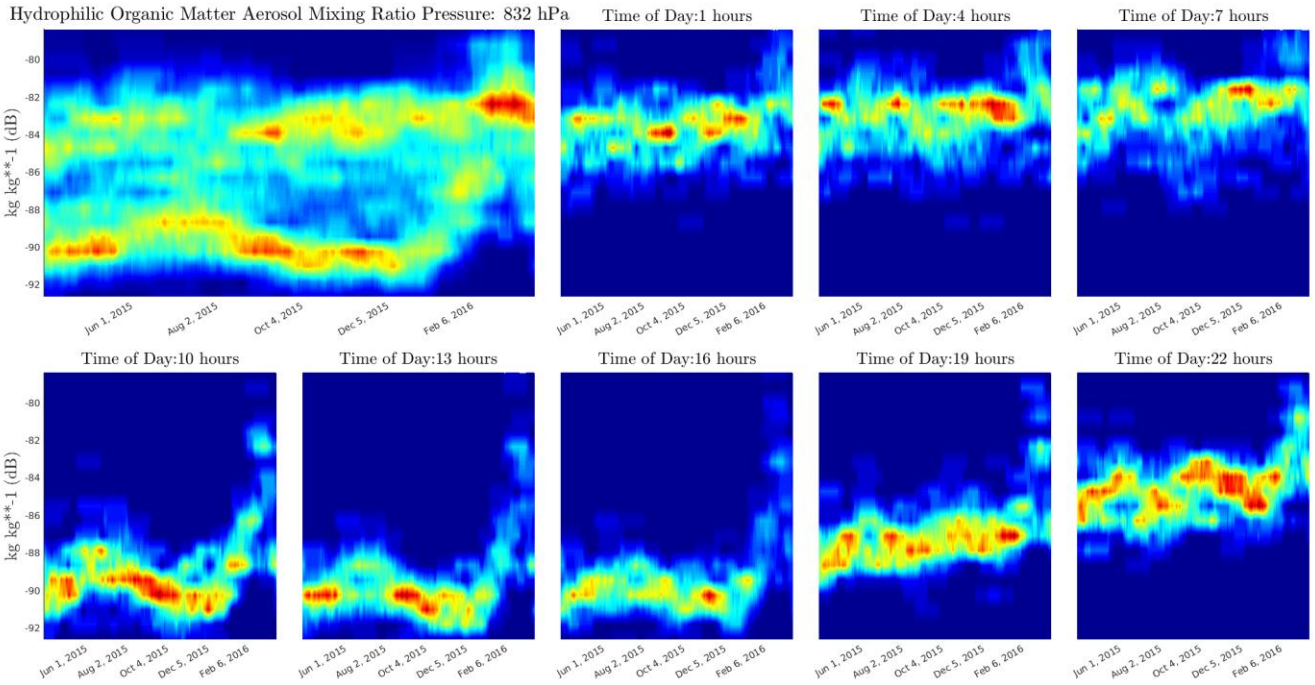

Figure 84: Moving distribution, low layers - hydrophilic organic matter

15. HYDROPHOBIC BLACK CARBON AEROSOL MIXING RATIO

Figure 85 for hydrophobic black carbon shows that most of the information is contained between 500 and 900 hPa approximately. The frequency plot presents that this variable is characterized by low frequencies for this range. It is shown in the time plot that a high concentration event was registered from February 2016 to April 2016.

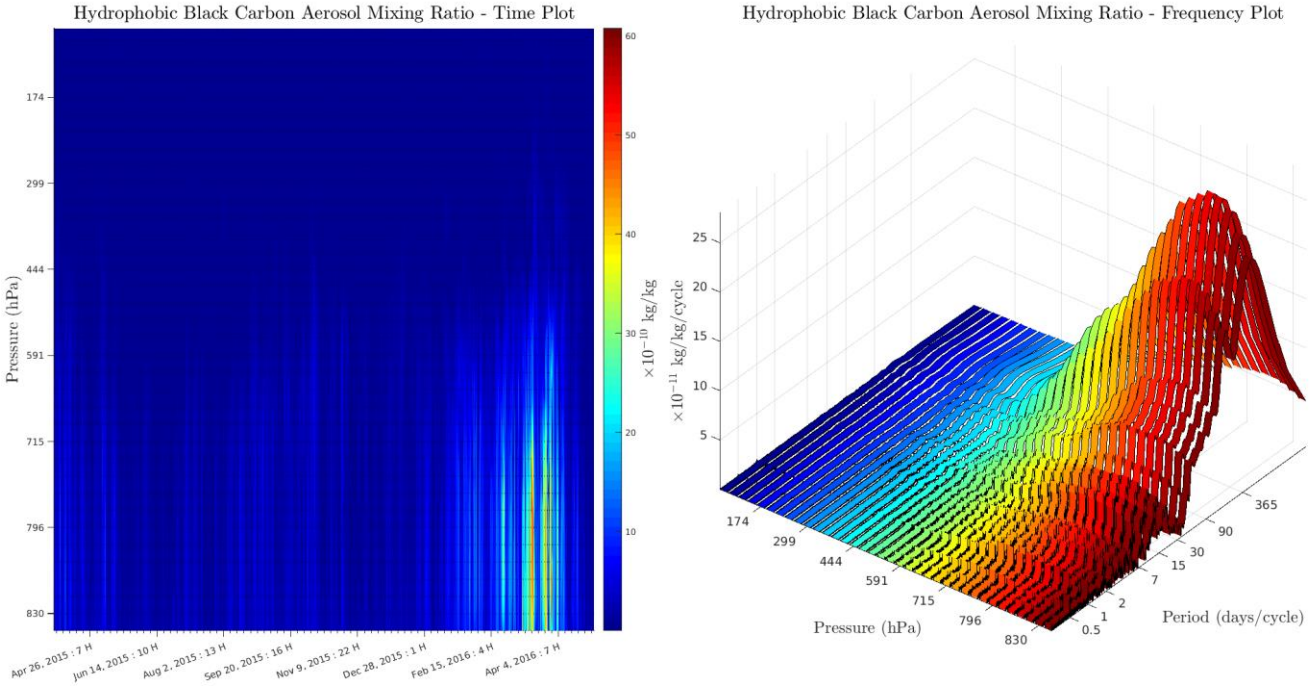

Figure 85: : Time and frequency plot for hydrophobic black carbon aerosol.

The daily cycle plots in Figure 86 shows that low, mid-low and mid-high altitudes (300 – 900 hPa) share the same structure: concentration peaks are found between January and April, with no dependence on the hour of day. In contrast, for high altitudes (100 hPa), the daily-cycle is evidenced as higher concentrations are recorded between 1 pm and 10 pm, with maximum peaks between March and May.

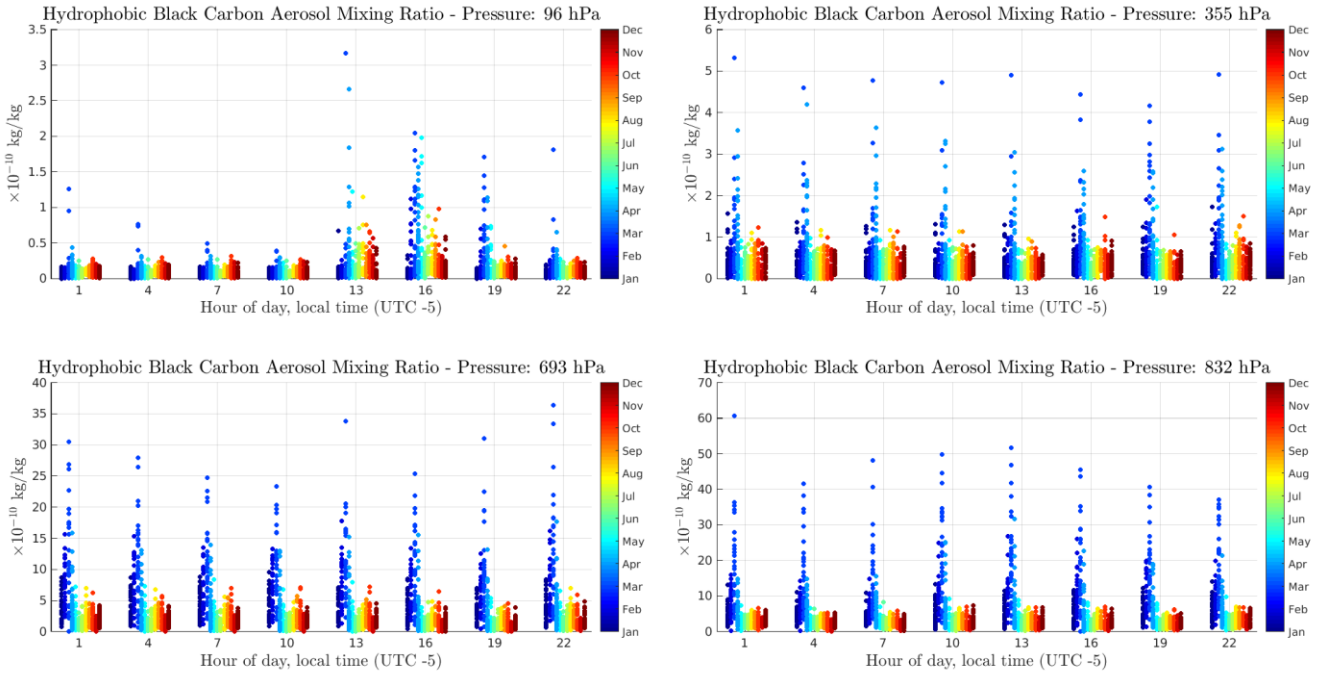

Figure 86: Day cycle plot - hydrophobic black carbon aerosol.

The histogram plot in Figure 87 for high altitudes show that data distribution presents two minimum peaks located at June 2015 and January 2016. Also, at 1 pm and 4 pm, values present a larger dispersion, so higher values are detected in comparison with other hours of day.

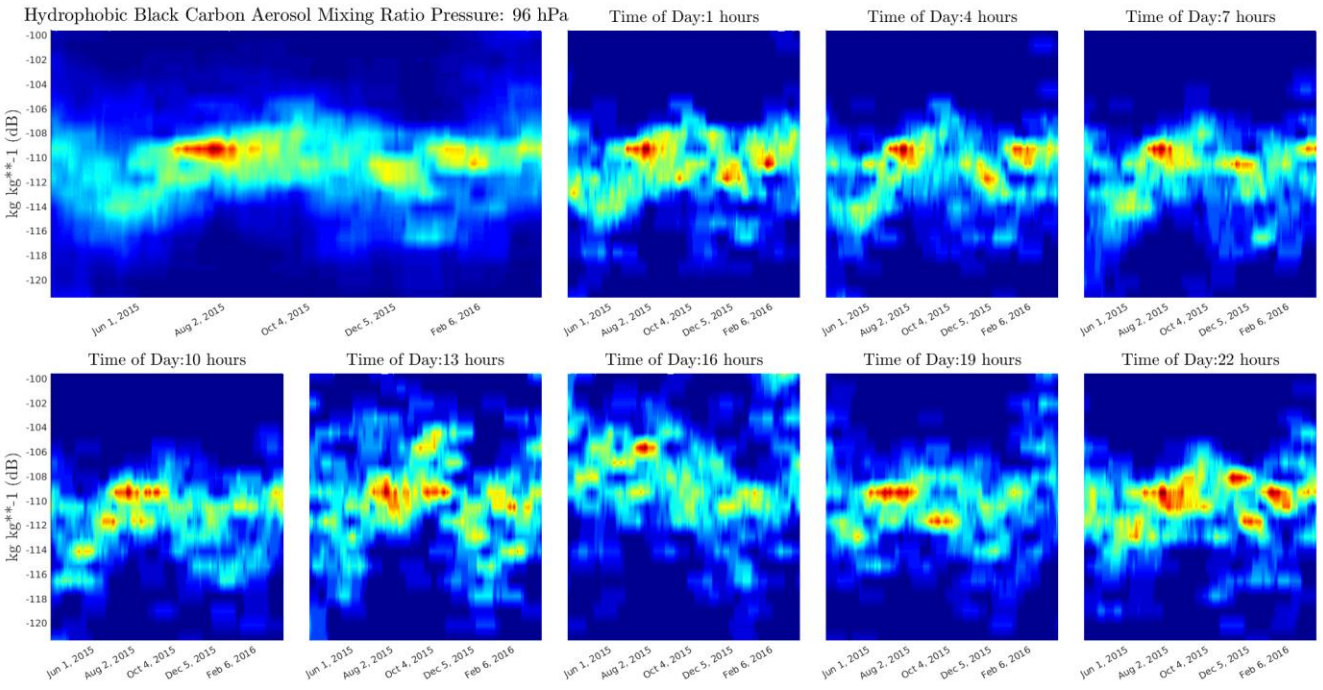

Figure 87: Moving distribution, high layers - Hydrophobic Black carbon aerosol

Figures 88 through 89 present a similar behavior: from April 2015 to December 2015, there are two minimum peaks located at June and November, and a maximum is found during September. From December 2015 onwards, the distribution increases rapidly until it reaches and absolute maximum at March 2016.

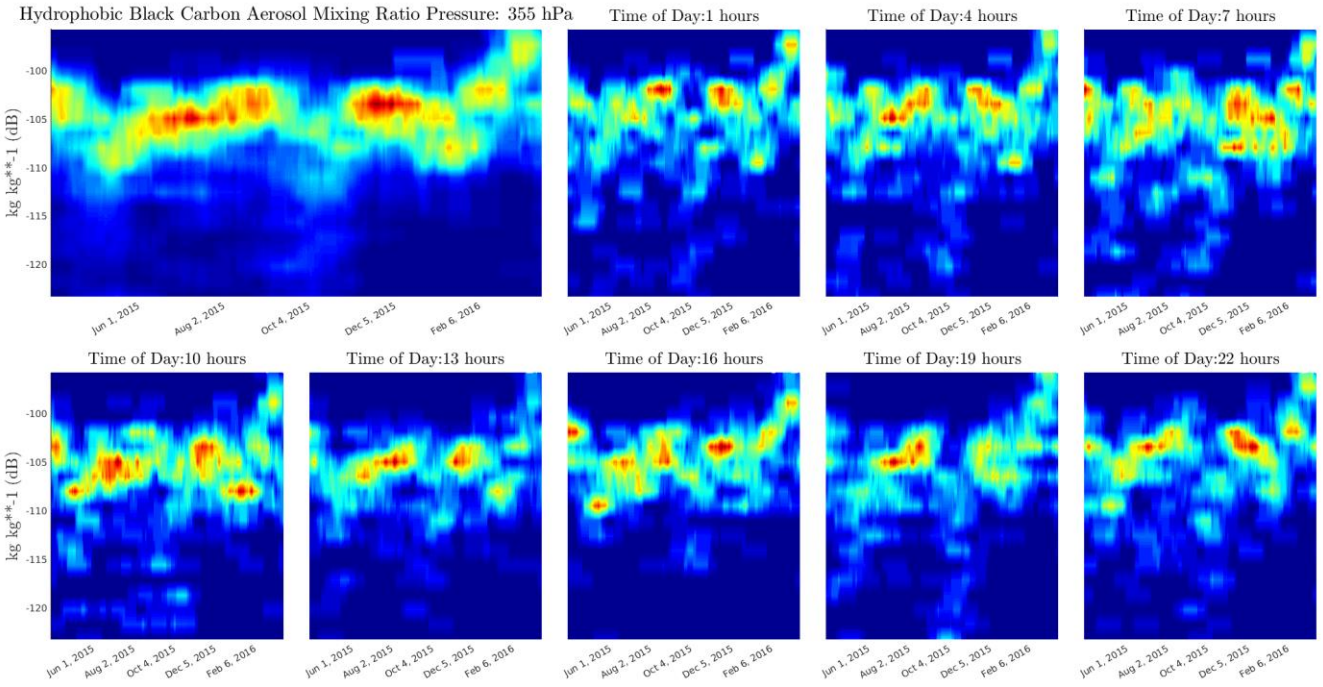

Figure 88: Moving distribution, mid-high layers - Hydrophobic Black Carbon aerosol

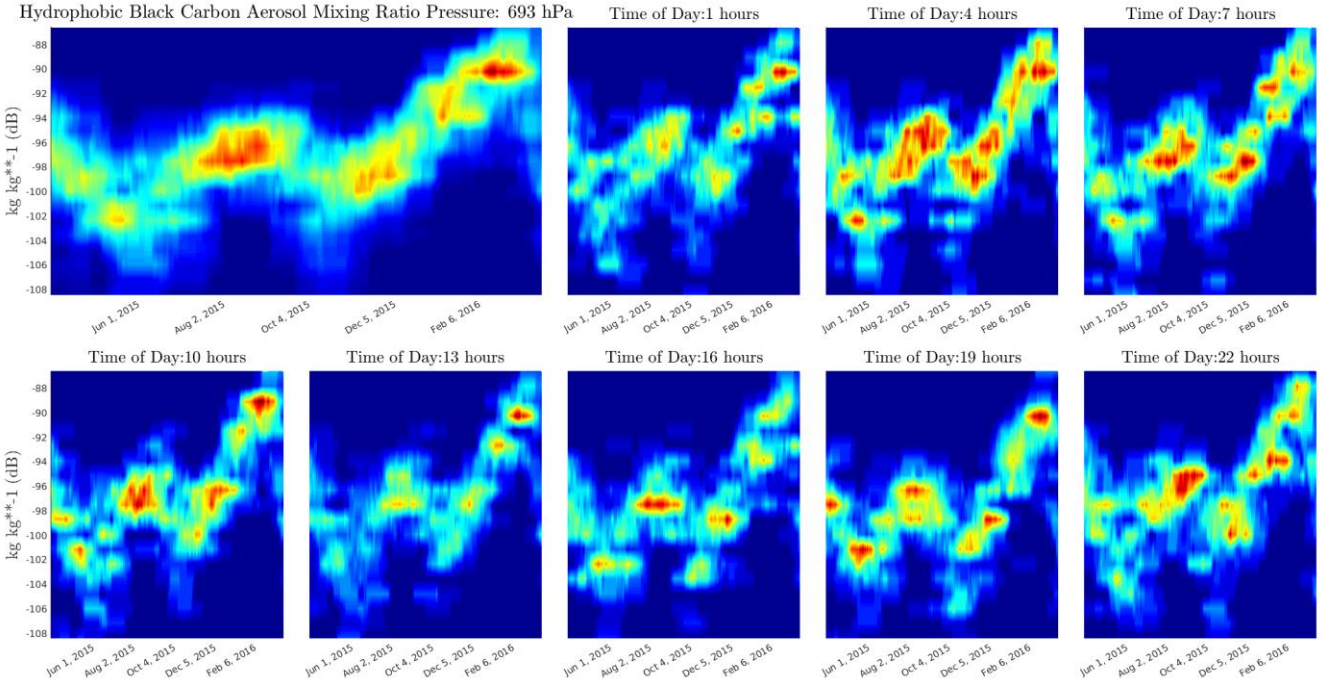

Figure 89: Moving distribution, mid-low layers - Hydrophobic black carbon aerosol

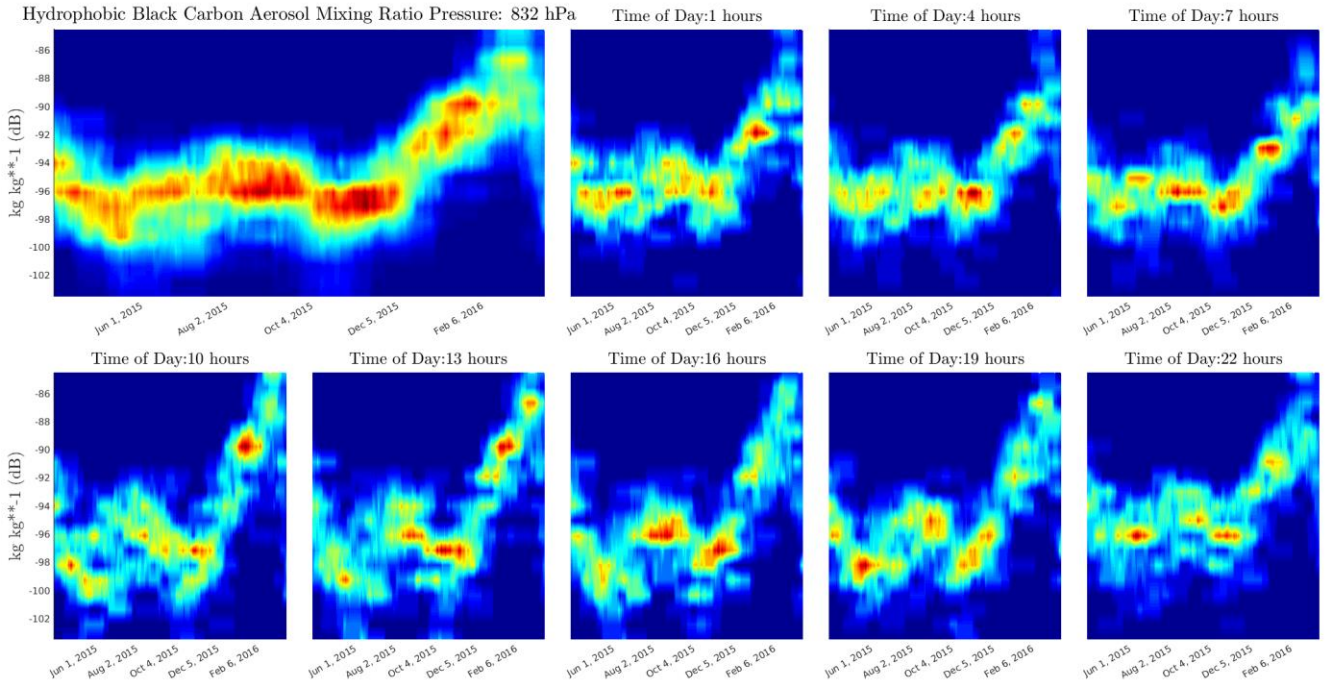

Figure 90: Moving distribution, low layers - Hydrophobic Black carbon aerosol

16. HYDROPHILIC BLACK CARBON AEROSOL MIXING RATIO

The results hydrophilic black carbon are very similar for those described in section 14 for hydrophilic organic matter. For the analysis description, read the discussion in the mentioned section

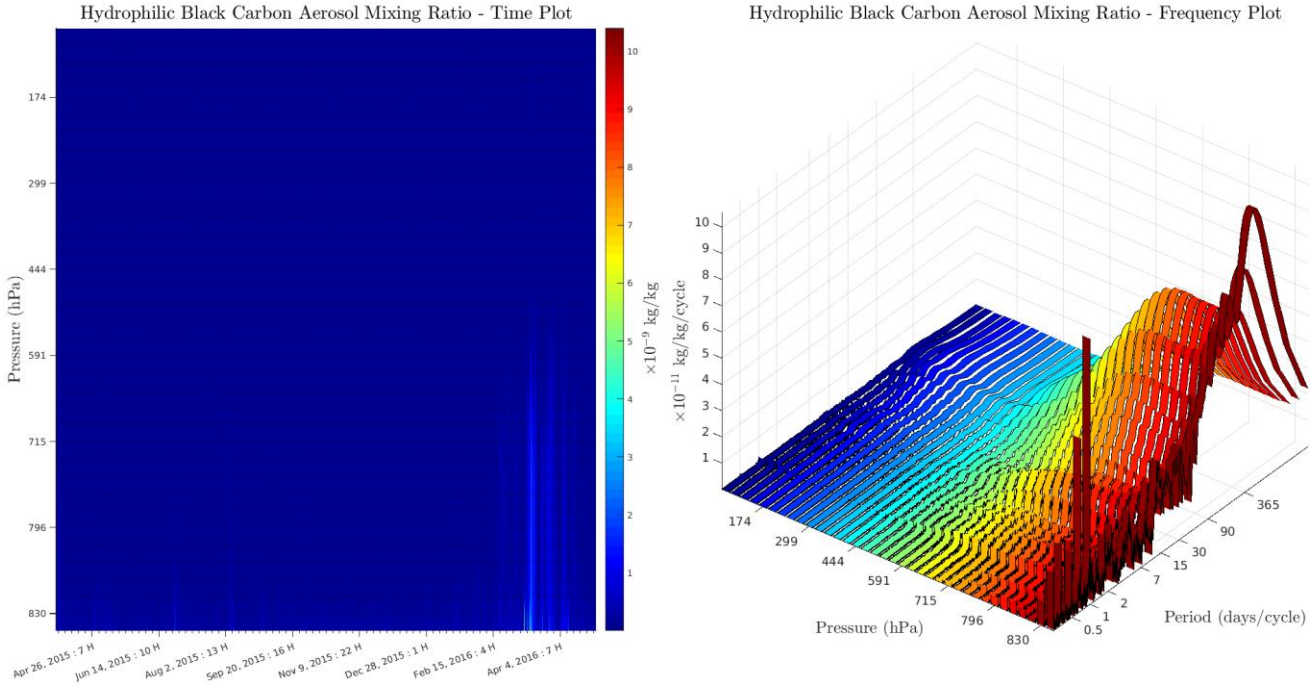

Figure 91: Time and frequency plot for hydrophilic black carbon aerosol.

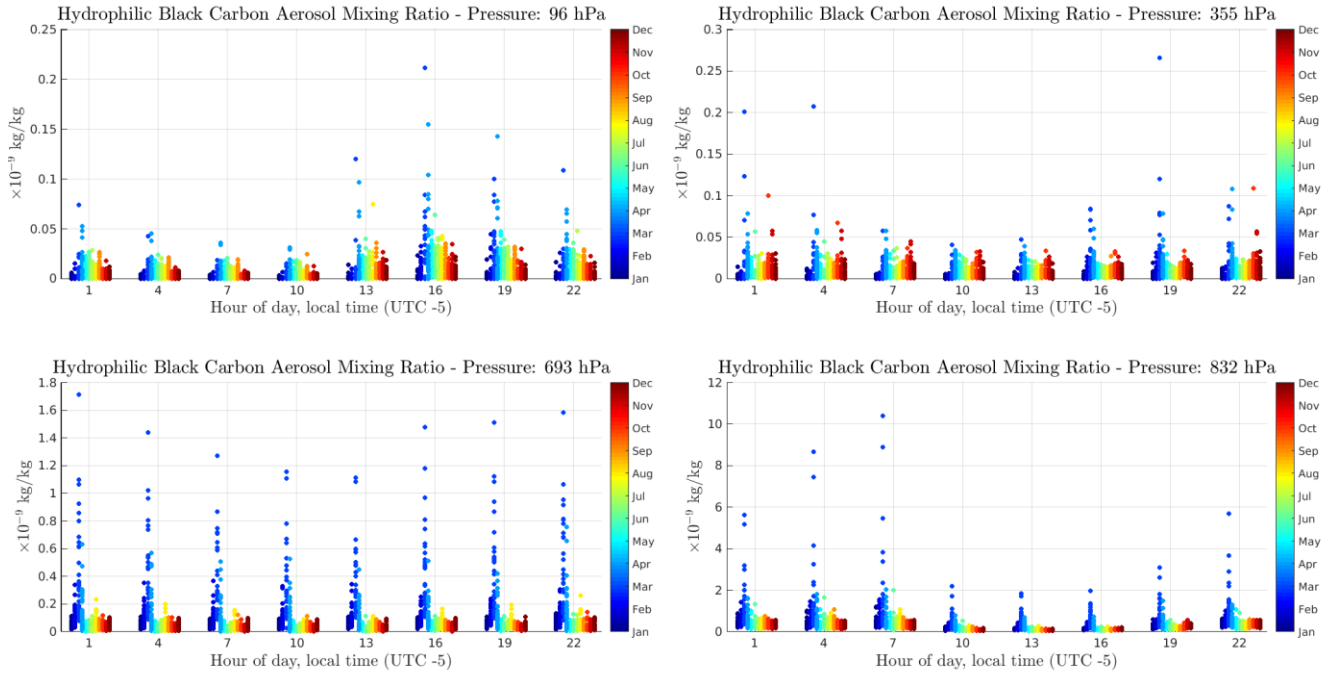

Figure 92: Day cycle plot - hydrophilic black carbon aerosol.

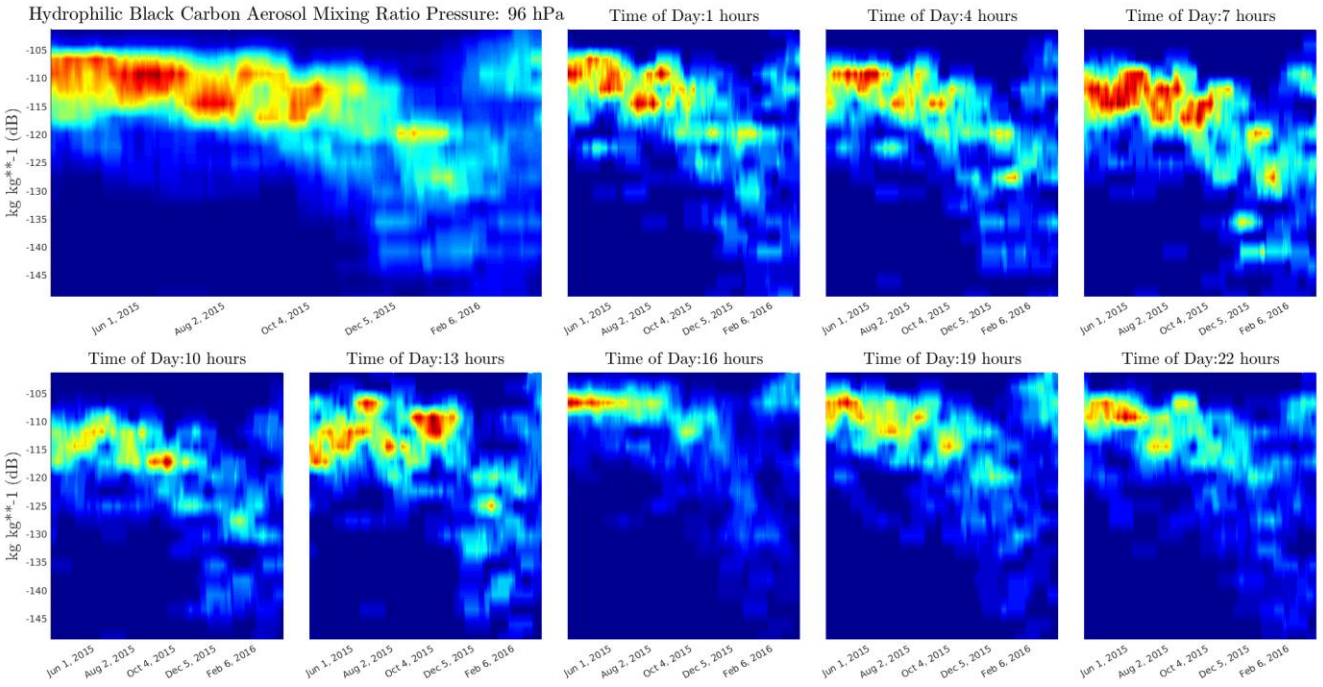

Figure 93: Hydrophilic black carbon aerosol

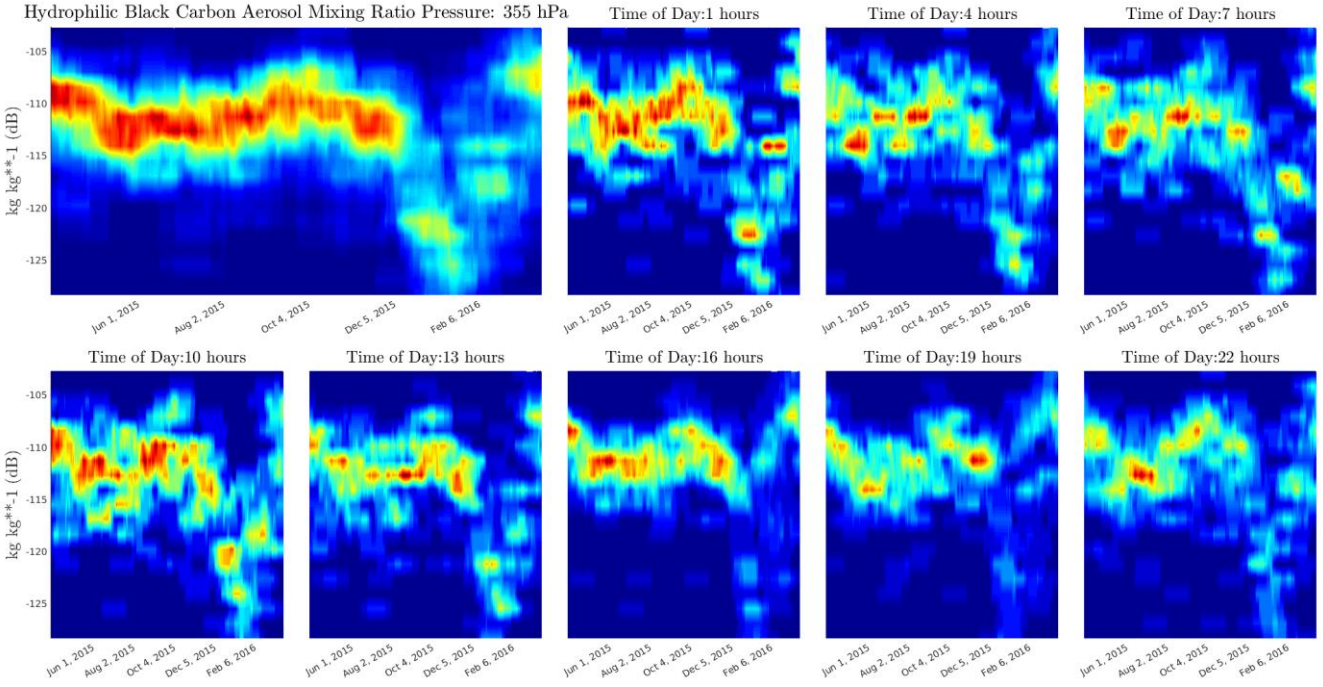

Figure 94: Moving distribution, mid-high layers - Hydrophilic Black carbon

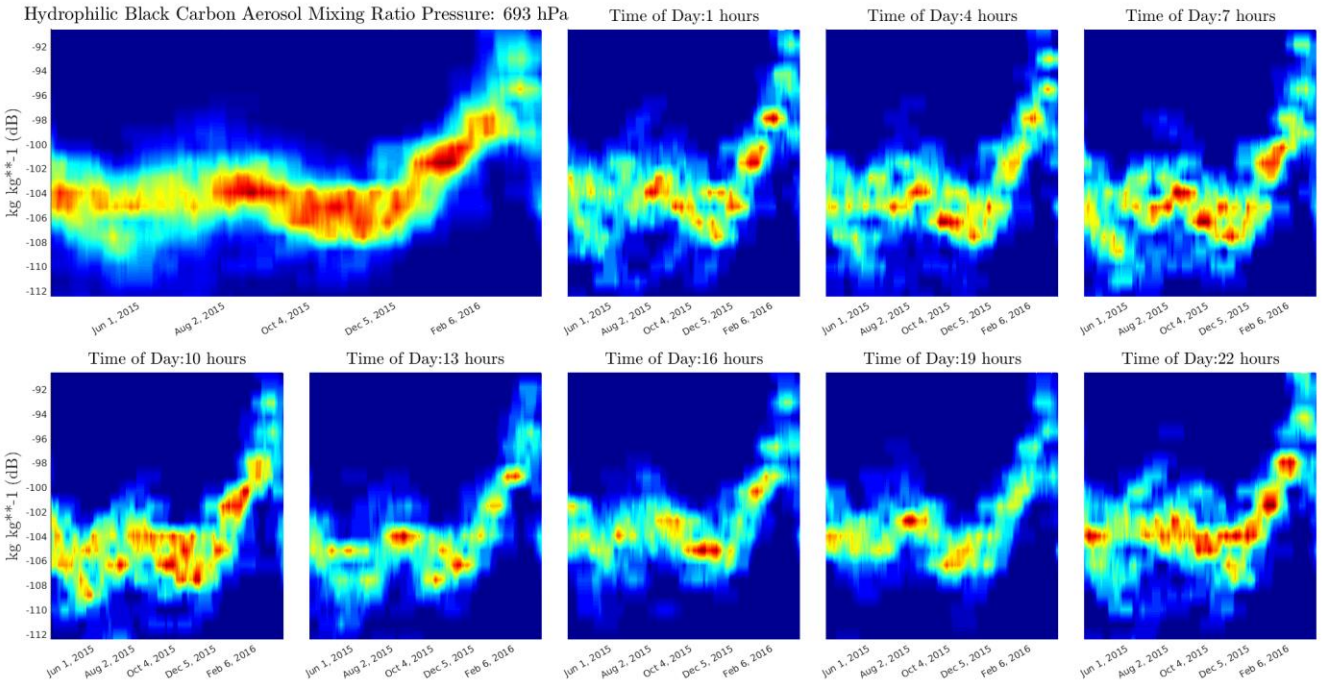

Figure 95: Moving distribution, mid-low layers - Hydrophilic black carbon aerosol

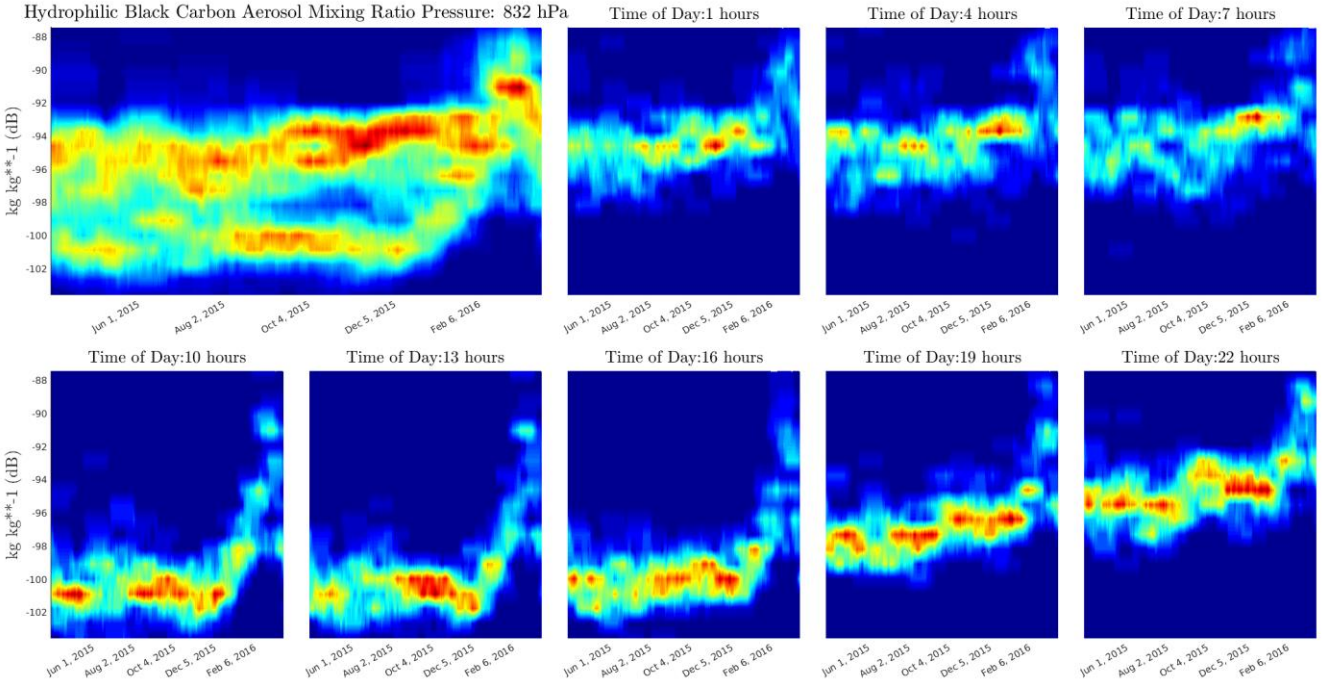

Figure 96: Moving distribution, low layers - Hydrophilic black carbon aerosol